Optimising the dissolution of U/Al in alkaline solutions and subsequent dissolution of the generated uranium residue in nitric acid

PP Morebantwa

orcid.org/0000-0002-2175-9820

Dissertation submitted in fulfilment of the requirements for the degree *Masters of Science in Applied Radiation Science* at the North-West University

Supervisor: Prof VM Tshivhase
Co-supervisor: Dr L Stassen

Graduation: October 2019
Student number: 23971630

Declaration

I hereby declare that this MSc dissertation titled "Optimising the dissolution of U/Al in alkaline solutions and subsequent dissolution of the generated uranium residue in nitric acid" was carried out by me under the guidance and supervision of Prof Victor Tshivhase and Dr Lize Stassen from the North-West University and South African Nuclear Energy Corporation, respectively. The interpretations are based on my reading and comprehension of the original texts and they are not published anywhere in the form of books, monographs or articles. I further declare that the contributions from other sources have been acknowledged by the indicated references.

Signature: R Ravhuanzwa Date: 13 September 2019

Acknowledgments

I would like to firstly, give praise to the Almighty God for always granting me strength through times when giving up looked like the better option. Modimo o ke sa mo direleng sepe.

Professor Makondelele Tshivhase, who I will forever be grateful to for introducing me to the nuclear field and for always reminding me that after every storm there is calm, that all the late nights at the lab will pay off.

To a great radiochemistry scientist, Dr Lize Stassen, who granted me the opportunity to work with her at the South African Nuclear Energy Corporation (Necsa), thank you for imparting all the knowledge that you have unto me. The past two years have been nothing but full of learning experiences that have certainly made me a better researcher.

Dr Thulani Dlamini, Mr Sam Thaga and the colleagues at CARST that were determined to get me through the finish line at all costs, thank you for never giving up and growing impatient when things made no sense to me.

A word of thanks to the North-West University and Necsa for providing me with the workspace, financial support and opportunity to complete this study. I would like to acknowledge the financial support we received from the National Research Foundation (NRF). Opinions expressed and conclusions arrived at, are those of the author and are not necessarily to be attributed to the NRF.

To Kgosiemang and Mokomedi, I give thanks to God for blessing me with parents that gave me everything and the freedom to make my academic choices without any limits or time constraints. I am eternally grateful for the daily reminder that when the going got tough, the tough had to get going. To my siblings (Boitshwarelo, Tshepo and Tumisang) and friends, thank you for always being by my side and reminding me of my ultimate goal on a daily basis. My sanity has been kept at bay by your calmness and positive messages throughout this journey.

Abstract

SAFARI-1 reactor is a "tank-in-pool" high flux reactor that is situated in Pelindaba, South Africa. The SAFARI-1 is a material testing reactor that uses LEU target plates, containing 19% uranium enrichment. When producing the target plate (TP), aluminium alloy of nuclear grade (grade 6061 Al sheets) is used. In order to produce the target assembly, a picture-frame method of target assembly is used to produce the target plate by using two aluminium sheets that sandwich another sheet, which has uranium aluminide in it. The uranium aluminide and aluminium powders are amalgamated and compressed to reach the required 2.17 g/cm^3 of the LEU fuel density (Ali et al., 2013).

During the process of U/Al target plate production; a lot of scrap material is generated containing uranium that may be recovered, purified and recycled into the target plate manufacturing process. Necsa has followed a process of dissolving the target plate scrap using potassium hydroxide; however, the process has not been optimised.

The aim of this study was to determine the optimum dissolution medium for the U/Al scrap material in either NaOH or KOH. Another objective was to evaluate the U recovery process from the residue remaining after alkaline dissolution of the scrap material, and determine if traces of aluminium remaining after dissolving uranium residue in nitric acid had any impact on the recovery of uranium using solvent extraction, and also to assess ion exchange as an alternative purification method. Alkali media concentrations were optimised for both NaOH and KOH, and the optimum concentration, based on the dissolution rate and re-precipitation time, was 6.0 M with a 3.0 M excess alkali concentration required for stoichiometric dissolution of the aluminium. Parameters including stirring rate, temperature and the addition of $NaNO_3$ were also optimised. A combination of all parameters revealed that the optimum dissolution parameters for pure aluminium were an alkaline medium of NaOH at 6.0 M with 3.0 M excess concentration and 3.5 M $NaNO_3$ and stirring the solution at 1000 rpm. This optimisation was based on the effect each parameter had on both the dissolution rate and re-precipitation time.

The optimised parameters were implemented on unirradiated UChem aluminium alloy samples. The optimised dissolution method was an improvement from the previously used method at Necsa. The optimised parameters were further used to dissolve target plates containing depleted uranium (DU). Dissolution kinetics of the DU target plate showed that the dissolution rate of the TP in only sodium hydroxide was higher (0.5328 g/min) when compared to the reaction with the inclusion of sodium nitrate at 3.0 M concentration (0.1488 g/min).

The uranium residue, from previous dissolutions on site at Necsa was used for optimising dissolution of uranium with varied HNO_3 concentrations and temperatures. The optimum dissolution parameters for uranium when favouring a higher dissolution rate were 6.0 M HNO_3 at 50°C. Otherwise, when uranium dissolution efficiency is the priority, a lower concentration of 1.0 M HNO_3 and lowered temperature of 25°C are the parameters to follow. Therefore, for this study, a 3.0 M HNO_3 concentration at 25°C were chosen as parameters for dissolution of the uranium to be further processed via solvent extraction to recover uranium. This choice was made because tributyl phosphate (TBP) has a lower solubility at that concentration of acid. Solvent extraction was performed using 30% TBP in kerosene with a ratio of aqueous (uranium residue dissolved in nitric acid) to organic being 1:1. Different amounts of aluminium were added to the uranium solutions to determine the effect the Al concentration has on uranium extraction. Adding Al to uranium solutions had a small effect on extraction; at 1.25% Al (m/m U), the highest extraction of 98.8% was observed and adding any more than that had a negative effect on extraction. Uranium stripping was also investigated by optimising the $(NH_4)_2CO_3$ concentration between 0.5 M and a higher concentration of 1.0 M. Results showed that at a higher $(NH_4)_2CO_3$ concentration, uranium stripping was increased from an average of 23.89% to 83.90%.

An alternative uranium recovery method using ion exchange resin was evaluated. Three resins, Amberlite IRC747, Amberlite IRC748 and BioRad AG50W-X4, were tested to determine the one that would recover more uranium. The evaluation was done by comparing the distribution coefficient of uranium on each resin. Uranium had the highest K_D of 4461.9 ml/dry g with the use of Amberlite IRC747. Amberlite IRC747 was further tested in a column experiment for uranium recovery with a uranium feed concentration of 480 ppm. With the flow rate set to 1.65 ml/min, uranium breakthrough was observed at 60.69 bed volumes, equivalent to a breakthrough capacity of 29.11 g U/L resin. Comparing both recovery methods, solvent extraction (SX) recovered 86.27% of uranium in the solution, while an ion exchange resin recovered 82.08% uranium. In terms of purification of the uranium, solvent extraction also performed better, since aluminium was removed to below its detection limit, while in the column run no separation of aluminium from uranium was observed.

Keywords: Aluminium, dissolution, uranium

Dedication

To my father, Kgosiemang Morebantwa and my mother, Mokomedi Morebantwa

"O belegwe ke batho ba ba fetotseng matlhabisaditlhong go nna phenyo." – Unknown author

Table of contents

List of figures

List of tables

List of abbreviations

BV	Bed volume
CNEA	Comisión Nactional de Energía Atómica
CP-1	Chicago Pile-1
DU	Depleted Uranium
FCC	Face-centered cubic
FTIR	Fourier Transform Infrared spectroscopy
HEU	High Enriched Uranium
HFR	High Flux Reactors
IAEA	International Atomic Energy Agency
IRE	Institut National des radioelements
LEU	Low Enriched Uranium
MNSR	Miniature neutron source reactor
MTR	Material Testing Reactor
NECSA	South African Nuclear Energy Corporation
PAL	Pelindaba Analytical Laboratories
PUREX	Plutonium Uranium Redox Extraction
TRIGA	Training, Research, Isotopes, General Atomics
RR	Research reactor
RRDB	Research Reactor Data Base
SAFARI-1	South African Fundamental Atomic Research Installation
SNF	Spent nuclear fuel
SUR	Siemens Unterrichtsreaktor
SX	Solvent extraction
TBP	Tributyl phosphate
TP	Target plate
U/Alx	Uranium/Aluminium clad
UChem	Uranium Chemistry Section of Necsa
UT	Ultrasonic Testing
UV/Vis	Ultraviolet/visual spectroscopy
XRD	X-ray Diffraction

Chapter 1: Introduction

1.1 Theoretical background

Research reactors (RRs) are crucial tools for education and training on reactor operation for use in basic and applied research in a wide range of scientific areas, like radioisotope production and the radiation resistance of new materials (such as nuclear fuel) in their prototype stages. RRs may be used either for irradiation purposes or for training and education. When used for irradiation purposes, one would follow a process of inserting specimens (for testing) in the core or near the core of the reactor (which is where the highest neutron flux is experienced) in order to prompt the effects of radioactivity; isotope production; or to test radiation damage that a material can undergo. In terms of using RRs for education and training, this is a good way to expose operators of a power plant to the technicalities as well as provide hands-on experience on learning about the reactor systems that one may encounter when operating a power plant. The education provided by RRs may be formal – for radiological technicians and engineers, and informal when educating the general public and students (National Academies of Sciences and Medicine, 2016).

The primary objectives of an RR are the production of isotopes required in the medical and industrial field, neutron activation analysis, and neutron scattering studies, amongst others. These reactors are also employed to test/study the effects that will be observed when irradiating materials that may further be used for power production reactors (Farrell, 2012).

The International Atomic Energy Agency (IAEA) Nuclear Research Reactor Data Base (RRDB) gives information on more than 270 operating RRs around the world with a range from zero to several hundred MW of thermal power (International Atomic Energy Agency, 2000). There are different types of reactors, such as the Siemens Unterrichtsreaktor (SUR), Argonaught reactor, Slowpoke Reactor, the miniature neutron source reactor (MNSR), TRIGA reactors, High Flux Reactors (HFR), and Material Testing Reactors (MTR) (Böck and Villa, 2001).

The SUR produces power between 100 mW to 10 W by using U_3O_8 fuel material that has been mixed with polyethylene powder. The fuel used to power the reactor is ^{235}U is been enriched by about 20% and packaged in fuel disks. The SUR also produces a maximum neutron flux of 6×10^6 $cm^{-2}.s^{-1}$ (Böck and Villa, 2001).

The Argonaught reactors operate between 2 Watts and 300 kW but most of these reactors are rated to operate up to 100 kW. The fuel used in the core is U-Al where the uranium can either be highly enriched or low enriched and rolled into sheets where the uranium (fuel meat) is compressed

between two sheets of aluminium and cut into plates. This reactor uses graphite as a neutron reflector, utilises light water as both a moderator and a coolant. The maximum neutron flux is 2×10^{12} $cm^{-2}.s^{-1}$ (Böck and Villa, 2001).

A Material Testing Reactor (MTR), which is a type of research reactor and is normally a pool-type reactor, uses plate-type fuel that is shaped in a rectangular form which normally encases highly enriched fuel (Böck and Villa, 2001), but in this study presented the targets plates that are of concern house low enriched uranium fuel.

MTRs are smaller in size compared to power producing reactors. Their purpose is to conduct research on materials which have been proposed to be used in the near future, and utilize the neutrons for diffraction studies on materials. The main purpose of an MTR is for the intense neutron irradiation on materials to further study changes that may occur over a period of time post irradiation. These tests are done under strict and specified conditions in which the material will be used; and safety precautions are a high priority, due to the massive amounts of heat and high doses of radiation which are emitted as a result of the fission reaction. Generally, the MTR is a water-cooled reactor system that uses normal water as a moderator as well as a coolant for the heated core of the reactor. It employs beryllium as a neutron deflector to all those neutrons that may escape the core during the process of fission (Iracane, 2006).

The core of a power-generating reactor contains fuel assemblies which are in long zircaloy clad cylindrical tubes that contain ceramic UO_2 fuel pellets. The fuel rods are typically 60 mm in height and they are placed in a vertical position. The fuel pellets contain ^{235}U which has been enriched to a low percentage, typically below 5% (Iracane, 2006).

The type of fuel that an MTR uses is low-enriched uranium (LEU), which is below 20% enrichment; although in the past MTRs have also utilized high-enriched uranium (HEU), at up to 50% enrichment. With the change from 50% to below 20% enrichment, to maintain the longevity and reactivity of the reactor core there was a need to increase the loading of uranium in the fuel plates. Normally, for an MTR to be functional it will employ a typical aluminium-clad UAl_x or U_3Si_2 alloy fuel type. This is because the fuel has been enriched to a higher level compared to a power supplying reactor. The MTR has the ability to provide radiation at high dose rates by producing isotopes with higher specific activity than those that would be available from other sources. The burn up of the fission material from an MTR is so high that the structure of an MTR must be able to withstand high amounts of heat that will be dissipated (World Nuclear Association, Updated April 2017).

On the 5th of September 1959, the South African Cabinet formally agreed and approved the acquisition of a research reactor, where their choice fell on a material testing reactor with a capacity of 6.66 MW which was a type that was originally built at Oak Ridge National Laboratory. The MTR located in South Africa, Pelindaba in the North West province called the SAFARI-1 (South African Fundamental Atomic Research Installation) had small additions to increase its power capacity from 6.66 MW to 20 MW (Nothnagel, 2015). SAFARI-1 is the first "tank-in-pool" high flux reactor in South Africa (NTP Radioisotopes SOC, 2017)- with an 8×9 grid, housing 28 fuel assemblies, 5 control rods, a regulating rod, in-core irradiation facilities and the reflector elements (Ball et al., 1995). The SAFARI-1 has been profiled as one of the main materials testing reactors in Africa and has been in commission since March 1965 (NTP Radioisotopes SOC, 2017). SAFARI-1 is one of the most highly utilised MTRs commercially in the world, producing around a fourth of important medical radioisotopes; being ^{99}Mo, ^{131}I and ^{177}Lu needed by the world (NTP Radioisotopes SOC, 2017).

The MTR's fuel element uses an assembly of fuel plates, which are common around the world. The typical fuel assembly, consisting of regularly spaced plates found in an MTR is a set of aluminium fuel plates. The spaces in the assembly, allow for cooling water (used as coolant and serving simultaneously as a moderator), to flow in between the plates ensuring that the fuel plates do not overheat resulting in an uncontrolled nuclear reaction. Numerous RRs around the globe use MTR type fuel elements where the fuel plates are fabricated by a world recognized and reputable method in assembling a core which has the fuel meat (fissile material), a frame plate and two aluminium cladding plates (figure 1.1), with subsequent deformation by hot and cold technique (Saliba-Silva et al., 2011).

There are two types of uranium alloys used in MTRs:

1. Uranium aluminide
2. Uranium silicide.

When producing fuel plates for an MTR using uranium aluminide, materials that will be essential to its production are uranium and aluminium. In the case of uranium, it has to, initially, be mined, milled and fabricated to ultimately be placed in fuel pellets and fuel plates. During fuel fabrication of uranium, the uranium ore is treated chemically and physically into a uranium alloy with powdered purified aluminium. To accompany the above-mentioned constituents, for fuel plate production, aluminium sheets of a certain nuclear grade are required (e.g. grade 6061 Al sheets). The aluminium sheets go through a series of processes such as manufacturing, inspection, and crucial quality control procedures that will, at the end, produce MTR fuel plates. Refer to Figure 1.1 (Elseaidy and Ghoneim, 2010).

Figure 1.1: U/Alx Target plate that is used in the production of ^{99}Mo (Kaminski and Goldberg, 2002).

The meat (figure 1.1) is encapsulated in an aluminium alloy cladding (blue material) that provides a barrier to the release of fission products and transfers heat from the meat to the reactor coolant. Targets are manufactured to meet suppliers' particular size specifications (National Academies of Sciences, Engineering and Medicine, 2016). All plates are hot rolled in order to guarantee the metallurgical bond between the plates and the pressed meat, and also serve as a protective cladding layer (Kaminski and Goldberg, 2002).

Aluminium and its alloys have low densities amounting to 2.7 g/cm^3 when compared to steel which has a density of 7.83 g/cm^3 (Davis, 2001). These alloys also exhibit high electrical and thermal conductivities with a resistance to corrosion in a variety of conditions; including ambient atmosphere. These alloys can be formed due to its characterized ductility. This is observed in pure aluminium having the ability to be rolled into thin sheets of Al foil. Aluminium's ductility provides strength even at low temperatures as it exists in a face-centred cubic (FCC) crystal structure. The primary restriction that aluminium has is that it has a low melting point of 660°C which restrains its usage at maximum temperatures. Albeit the low temperatures restrict the usage of pure aluminium in works that may involve high temperatures, its mechanical strength can be enhanced by cold work and alloying. However, these processes have their own disadvantages as they lower the corrosion resistance of aluminium. Elements that are constituents in the alloying process include copper, manganese, magnesium, zinc and silicon (Davis, 2001).

Aluminium is found to be non-toxic and therefore can be recycled with a fraction of energy (5%) that is needed to produce alumina (Al_2O_3) – this is a main motivation for the importance of recycling aluminium. Aluminium readily reacts with oxygen producing a thin aluminium-oxide layer on the surface of the aluminium which serves to protect the metal against harsh conditions that may lead to corrosion (Davis, 2001).

1.2 Problem statement

Necsa's SAFARI-1 reactor provides the country with supplies of ^{99}Mo that will decay further to produce ^{99m}Tc which is used in medical diagnostics. The characteristics of the SAFARI-1 reactor situated at Pelindaba, South Africa are listed in Table 1.1. The reactor uses 19% low enriched uranium fuel, and UAl_x target plates for ^{99}Mo production that in the past contained highly enriched (46%) U, but in recent years the process is being converted to a completely LEU-based process.

The fission process happens when the uranium nucleus absorbs thermal neutrons that will cause the nucleus to become unstable thus fissioning either into two or three lower mass fragments. In these fission fragments, only a small percentage of them are molybdenum-99 (^{99}Mo) atoms. For this kind of fission reaction, the nuclear reactor serves as a good thermal neutron producer aiding in the production of the desired ^{99}Mo.

Table 1.1: Characteristics of SAFARI-1 reactor.

Name	Thermal power (MW)	Thermal neutron flux ($n/s/cm^2$)	Fuel type	^{99}Mo production Target type	Maximum annual operation (days)	Typical share of worldwide production (%)
SAFARI-1	20	2.4×10^{14}	U_3Si_2 (LEU-19% enriched)	UAl_x (both HEU = 46% and LEU = 19%)	315	10 - 15

During the production of ^{99}Mo, the production rate is dependent on the irradiation time, the thermal neutron fission cross section of ^{235}U, thermal neutron flux on the target material, the mass of ^{235}U in the target plate, and the half-life of ^{99}Mo. In the typical case of an MTR, the neutron fluxes are in the order of 1×10^{14} neutrons per square centimetre per second ($n/cm^2/s$), while an irradiation time of about 5-7 days is usually required to obtain a near-maximum ^{99}Mo production in the target plates.

To extract ^{99}Mo from irradiated target plates, they are dissolved in alkaline solution. While the process of dissolution takes place, the uranium and many of the fission products are precipitated to form a residue that is comprised of mixed hydrated oxides. The residue is then stored in stainless steel drums in a hot cell at the ^{99}Mo production facility. These drums are stored at the facility either awaiting final disposal or plans of separating and purifying the contents for further use in the future, that may include reusing the uranium as target plates for the production of medical isotopes.

During the production of the U/Al target plates at the UChem plant at Necsa, a lot of scrap is generated that contains U/Al alloy, and due to the high value of the uranium, it needs to be recovered from this scrap, purified and recycled back into the target plate manufacturing process. Currently a dissolution route in KOH is being followed, whereby aluminium is dissolved and a

uranium residue is generated, which is then dissolved in HNO_3 and purified through solvent extraction in TBP. This process has not been optimized in terms of dissolution parameters of the alloy scrap in alkali, and the residue in HNO_3. The effect of traces of aluminium remaining behind after dissolution of the scrap in alkali on subsequent dissolution of the residue in HNO_3 and the solvent extraction purification step thereafter, has also never been ascertained. The possibility of using an alternative method for uranium purification, such as ion exchange, has also never been pursued.

1.3 Aim and objectives

The aim of this study was to determine the optimum dissolution medium for the U/Al scrap material in either NaOH or KOH, and evaluating ion exchange as an alternative purification technology.

The objectives of this study were to:

1. find the most effective alkaline solution to dissolve aluminium and its requirement for excess solution in order to keep Al stable in solution, by comparing kinetics of dissolution in NaOH and KOH,
2. optimize all dissolution parameters in the chosen alkali, i.e. temperature, stirring rate, NaOH or KOH concentration, influence of added $NaNO_3$ on dissolution rate and solution stability,
3. test validity of optimised parameters on aluminium samples provided by UChem
4. test the optimized parameters on aluminium containing depleted uranium (DU),
5. determine the optimum dissolution parameters (optimum HNO_3 concentration and temperature) for U residue in nitric acid,
6. determine the effect of various amounts of Al added to the dissolved uranyl nitrate, on the efficiency of extraction with TBP and
7. determine the possibility of resin technology for U purification from generated solution with added Al on chelating resins such as Amberlite IRC747 and IRC748, or cationic exchange resins such as BioRad AG50W-X4.

Chapter 2: Theoretical background and literature review

2.1 Use of aluminium in the nuclear industry

Aluminium is a metal that is used widely in the industrial sector. This is because of its observed characteristics, such as high strength to mass ratio, durability and high corrosion resistance amongst others. Because of the fact that aluminium is hardly used in its purest form, an alloy is manufactured, which includes the addition of copper, magnesium or silicon which have proven to be the optimum elements to form an alloy with aluminium. Aluminium metal is important in the nuclear engineering field because of its low neutron absorption characteristics. The passage of neutrons is not restricted, which is vital in the case of a continuous nuclear reaction of uranium fuel in power production plants or research reactors. Furthermore, aluminium is an effective material with regards to the intensive usage in a reactor core with a low temperature that needs to be continuously maintained (Mindrisz et al., 2013).

Aluminium has been at the forefront of the development of nuclear technology, due to its use as a non-fissile metal amongst other properties. It was used in the first continuously operating nuclear reactor called the X-10 Graphite Reactor situated in Oak Ridge, Tennessee, which went critical in 1943. It was used in the Graphite Reactor as a clad, protecting the encased highly chemically reactive uranium from being contaminated by the air and graphite during the prolonged times of irradiation and also providing protection from corrosion by water throughout the stages of nuclear decay whilst in an underwater storage facility. Additionally, the aluminium can be employed in entrapping the radiation products that may be volatile and in abundance due to the long irradiation periods (Farrell, 2012).

In the industry, pure aluminium is regarded to be unsuitable due to its temperature restrictions which prevent it from being used in industrial applications where its low melting point characteristic would make it unsuitable. Therefore, the use of aluminium in the nuclear industry is limited in terms of electricity production processes that include high temperatures, or marine (turbine) propulsion. However, in conditions where the temperature is less than 100°C, aluminium is permitted to be in use for a lot of research reactors; of which many are water cooled reactors. The use of aluminium alloys has contributed to the longevity of the reactors (Farrell, 2012). The fact that aluminium has the capacity to remove heat as well as limit the generation of heat has made it widely exceptional in research reactors. During the fission reaction, the energy that is dissipated during the decay process is in the form of heat. Most of the heat that is released (about 80%) would be from the fuel that is undergoing fission reactions, whilst some (5-20%) of the energy would be produced

by the bombardment of the released daughter nuclides and other particles against the target and the non-fissile material surrounding the core of the reactor (Farrell, 2012).

Characteristics that make aluminium such an attractive metal in the nuclear industry are that it is found in abundance, inexpensive and it is light in weight. Generally, aluminium is malleable and can be shaped to any form through conventional processes of rolling, forging, and extrusion. (Farrell, 2012). When aluminium has been exposed to air or aqueous solutions, a thin oxide layer is formed which serves to further protect the aluminium from oxidation; except if it is exposed to conditions that will destroy the protective layer on the aluminium (Noor, 2009).

Aluminium's tensile strength is not high; therefore, it can be strengthened through cold work, solid solution hardening, and precipitation treatments. Aluminium exhibits an FCC structure and has no crystallographic phase changes. The fact that it is isotropic, guarantees that it will not undergo thermal expansion which will cause damage to its structure and also radiation growth similar to what graphite goes through and other metals like magnesium and zinc (Farrell, 2012).

2.2 MTR fuel and targets plates

The National Research Council of the National Academies of the USA (2009) states that in order to successfully migrate from HEU targets to LEU targets, an increase of ^{235}U in the target is required and this can be achieved by altering the composition of the target meat. Existing reactors that mostly produce ^{99}Mo utilise HEU uranium-aluminium alloy targets that contain about 1.6 g U/cm3. Therefore, in order to maintain an equal amount of ^{235}U inside an LEU target of the same size as that of an HEU target, the fuel loading would have to be increased to a density of 8 g U/cm^3. The LEU targets that contain high density uranium loading may be manufactured using several materials which include: uranium metal targets, uranium–aluminium dispersion targets, uranium silicide targets, and uranium-molybdenum targets (National Research Council of the National Academies of the USA, 2009).

For uranium metal targets, the Argonne National Laboratory with the assistance of numerous organizations have established uranium metal-foil targets that comprises of a LEU metal foil that has been rolled to the thickness of about 100 to 150 microns, that is wrapped in an aluminium (or nickel) foil and then encapsulated in a cylinder-shaped aluminium clad. The aluminium barrier functions as a recoil obstacle as well as inhibits the uranium foil from bonding with the aluminium cladding. Amongst other advantages that encourage the use of the cylindrical targets, the use of uranium foil was said to be potentially compatible with the alkaline and acidic dissolution process that are currently employed by large scale producers. (National Research Council of the National Academies of the USA, 2009).

High-density low-enriched Uranium-aluminium dispersion targets have been developed and are produced by the Comisión Nactional de Energía Atómica of Argentina (CNEA) for the production of ^{99}Mo aimed at the domestic market (Kohut et al., 2000; Cestau et al., 2008). For this type of target, the fuel meat has the uranium density of 2.9 g U/cm^3 obtained by increasing the ratio of uranium aluminide to aluminium in the target's fuel meat, with the aluminium in the target assisting in binding to the target meat. These uranium-aluminium dispersion targets are suitable for use with the alkaline dissolution method that are presently used by companies that produce ^{99}Mo on a large scale. However, due to the mass of ^{235}U in the targets, they are not able to produce the same amount of molybdenum that is produced by the current HEU targets (National Research Council of the National Academies of the USA, 2009).

Uranium silicide targets were primarily developed as a replacement for the LEU targets utilised in RRs. An advantage to implementing U_3Si_2 was that they were able to hold a higher density of 4.8 g U/cm^3 fuel compared to uranium-aluminium dispersion targets with a maximum of 2.9 g U/cm^3. However, when using this target it proved to be difficult to dissolve using the conventional dissolution process of alkaline or acidic media (National Research Council of the National Academies of the USA, 2009).

The production of uranium-molybdenum targets is being developed and the aim is to use a higher density of uranium load by using uranium-molybdenum alloys. The density expected is in the range of 7 g U/cm^3 to 9 g U/cm^3, enough to directly substitute the use of HEU targets. The problem of using uranium-molybdenum alloys for producing ^{99}Mo is that there are high amounts of ^{98}Mo in the alloy that will dilute the needed ^{99}Mo during irradiation, as a consequence the specific activity of ^{99}Mo will be reduced rendering it unusable (National Research Council of the National Academies of the USA, 2009).

Fabricating of LEU MTR-type targets for operating a RR requires that there be an increase in the amount of uranium that will be loaded in the fuel core plates. With a higher density loading of uranium (4.20 g U/cm^3); it leads to an increase in the core thickness of the fuel plate. A higher load of uranium could potentially lead to problems with the cladding of the plates. Each type of MTR uses a fuel type that is compatible with the reactor itself. Besides reactor specificity, the manufacturing process of these plates must be in accordance with the scope that has been set down along with general conditions, manufacturing method, inspection requirements and the accepted criteria (Elseaidy and Ghoneim, 2010).

Even so, the manufacturers do not always use a consistent formula in producing the target plates. The ratio between Al and U is never constant and the Al alloy may (at times) contain contaminants

which may render the target faulty or useless (i.e. power generated by the reaction is lower than the expected, leading to the reactor not performing to its optimised power output).
With time, the raw material constituents of MTR fuel types are changed with new ones. Therefore, the change that comes about has an effect that could influence the quality of the plates. Therefore, when that is done, a process of re-qualification is undergone to ensure the usability of the targets (Elseaidy and Ghoneim, 2010).

Currently, the target plates used for the production of ^{99}Mo are normally Al-clad; which are miniature aluminium-clad target plates (Fallais et al., 1978) or Al-clad fuel pins (Jones, 1982), and consist of uranium-aluminium alloy (or U/Al_x) dispersion. Mushtaq (2011), conducted various tests on the targets prior to them being inserted in the reactor core; the tests included both destructive and non-destructive testing. These tests were done in order to determine the maximum power of the targets, their maximum uranium content along with the uniformity requirements for their loading. For destructive tests, blister annealing tests, bend tests for the adjusted plate cladding and microscopic examinations were performed. Non-destructive analysis (for fuel meat location and density) involved ultrasonic testing (UT) and radiography (Mushtaq, 2011).

2.2.1 Uranium Silicide

In a study conducted by Srinivasan et al. (2004), it is stated that the LEU uranium silicide fuel was aimed at replacing the uranium aluminide with regards to dissolution process utilized by the Institut National des radioelements (IRE) in Fluerus, Belgium and the Atomic Energy Corporation of South Africa; to name a few (Srinivasan et al., 2004). When replacing the UAl_x with U_3Si_2 targets, it would be required that there be an advancement in the type of dissolution method. The method would have to be more aggressive because U_3Si_2 targets do not readily dissolve in basic solutions. The problem with dissolving U_3Si_2 targets in acid is that the silica will undergo precipitation leaving the ^{99}Mo to be irrecoverable from that solution (Burrill and Harrison, 1987).

Nampira, (2000) elaborated that dissolving uranium silicide fuel plates in HNO_3 cannot be achieved due to the presence of an aluminium oxide layer on the aluminium cladding used. However, HNO_3 is able to penetrate through the two gaps on either sides of the (fuel element) aluminium plate - used in that study - thereby dissolving the uranium fuel. A set back to this kind of mechanism is that HNO_3 is not able to dissolve the uranium silicide fuel used in the target plate. To counter the disadvantage of HNO_3, $Hg(HNO_3)_2$-HNO_3 solution is used to dissolve the uranium silicide composition while the nitrate dissolves the uranium. The rate of dissolution is in direct proportion with the concentration of $[Hg^+]$ (Nampira, 2000). The dissolution efficiency of uranium is conditioned by the presence of Hg^+. It was found that the optimum concentration of Hg^+ for the dissolution process was 250 ppm in concentrated HNO_3 (Nampira, 2000).

2.2.2 Uranium Aluminide

Two technologies are available in producing LEU targets. One of them being based on a uranium-aluminium intermediate compound (UAl_x) which is spread into an aluminium matrix, called dispersion targets and another one which is based on thin metallic uranium foils. The dispersion targets are manufactured by using a long-familiar technology called the picture-frame technique with certain specifications depending on the company producing them (Cunningham and Boyle, 1955; Durazzo et al., 2007; Conturbia & Durazzo, 2017). When using this kind of technology, the fissile meat with a dispersion of UAl_x and Al is cladded in an aluminium structure and then rolled until the specified thickness is reached. In the UAl_x compound x is the value that will vary and depend on the fabrication parameters that will be followed, such as the temperature setting during hot rolling along with thermal treatment process. Sim et al. (2013) lists the different candidate alloys along with the compounds that range from UAl_x to pure uranium. The UAl_x denotes the mixture of uranium aluminides subsequent from melting and casting of a uranium-aluminium binary system (Sim et al., 2013). In the research conducted by Conturbia and Durazzo, (2017), UAl_2 was utilised as the initial material, where during the processes of rolling and thermal treatment, the uranium dialuminide reacted with aluminium contained in the matrix therefore forming higher aluminides (UAl_3 and UAl_4). Sim et al. (2013) further explain that 50% particle loading of uranium is deemed to be the practical limit when using dispersion meats fabricated by roll bonding. Furthermore, the uranium density of dispersion plates can differ from 2.3 g U/cm^3 to 9.5 g U/cm^3 conditional to the variability of alloys and compounds used in the fuel meat (Sim et al., 2013).
Kaminski and Goldberg, (2002) corroborate this by mentioning that most of the U-Al dispersion fuels are made of powder intermetallic uranium aluminide (UAl_x) which may be in the form of UAl_2, UAl_3, and UAl_4 in aluminium being clad with aluminium. Whenever the targets undergo irradiation, the aluminide (UAl_4) is the most stable and plentiful in the fuel (Kaminski and Goldberg, 2002). In this study, aluminide fuels were considered high priority because of the presented volume inventory by the United States' Department of Energy, their high enrichment along with their metallurgical similarity to the final alloy form from the melt-dilute process (Adams et al., 1999).

2.3 Chemistry of aluminium

Aluminium exists in the following oxidation states: Al^+ (e.g. AlH), Al^{2+} (e.g. AlO) and Al^{3+} (e.g. Al_2O_3). Al^{3+} is the most common oxidation state. The ionic radii of Al allows for the octahedral coordination with other compounds/elements with Al^{3+} at the center of the octahedron and six closely packed compounds/elements (Goldberg et al., 1996).

When aluminium reacts with hydroxides, the behaviour observed between Al^{3+} and the OH^- ions can be explained by the dependency of aluminium hydroxides' solubility on pH. Since the OH^- molecule and the O^{2-} ions are very similar in physical dimensions, they can easily replace each other in some crystal structures (Goldberg et al., 1996). Goldberg et al. (1996) differentiated the behaviour that was observed from the formation of different crystals formed by using information that was known about the surface structure of hydroxides. Data currently available is that of aluminium's surface chemical behaviour which stems from the study of crystalline hydroxide in the form of gibbsite [α-$Al(OH)_3$] or a synthetic oxide γ-Al_2O_3. Available information on other phases is limited. Goldberg et al. (1996) also looked at the different phases of crystal formation and other ways in which the behaviour of surface chemistry determines the precipitate that is formed in the final stage of aluminium interacting with hydroxides (Goldberg et al., 1996). Whenever the aluminium metal is dry, the top layer will only consist of oxide ions, which are arranged over the aluminium ions in octahedral positions on the lower layer. Alumina (Al ions along with oxide ions) chemisorbs a monolayer of water when exposed to moisture, therefore forming hydroxyl ions (Tóth, 2002). A surface functional group that is found abundantly and is chemically reactive (in soil clays), which would be found unprotected on the outer periphery of a mineral is the hydroxyl group (Sposito, 1984). This chemical compound formation stoichiometrically corresponds to the reaction of the oxide ions layer and aluminium ion along with water to form $Al_2O_3 \cdot H_2O$. The presence of hydroxyl groups arranged in different ways with the Al ions contribute to the reactive functional group of alumina surfaces; this is based on stereochemical reasoning (Goldberg et al., 1996). More than one kind of surface hydroxyl groups may be present on a metal (or mineral), where the different groups may be differentiated by their properties such as their infrared absorption spectra which would distinguish them from those that are in the bulk of the metal arrangement (Sposito, 1984). The amount and nature of hydroxide groups is determined by the preferential crystal planes that are exposed along with the distribution of aluminium ions that are present at the surface (Tóth, 2002).

2.4 Dissolution chemistry of aluminium and targets

Compton et al. (1993) mentions that reactions between solids and liquids include a joint sequence of mass transportation, adsorption/desorption phenomena, heterogeneous reaction, chemical conversion of intermediates at a fundamental level, whose identification, separation and kinetic quantification are important if the mechanism of the process is to be thoroughly understood and described (Compton et al., 1993).

In the field of chemistry, particularly that of analytical chemistry, the process of dissolution can be one which poses a lot of challenges (EPA, 2004). This is because a lot of samples contain impurities

which may be unknown. These impurities have characteristics which vary from the element of study. Therefore, to overcome such challenges, the investigator will have to consider a few factors such as the analytical instruments employed, the sample medium, any surface contamination that may be present, if the dissolution technique that will be used will be effective, the loss of analyte, interference caused by reagents in the subsequent analysis, and so forth (EPA, 2004).

2.4.1 Dissolution of metals

The process of dissolution, since the early ages, has generated interest in characteristics which have proven to be important in the chemistry of acids (and bases). This is due to the evolution of hydrogen gas during the reaction of acids and bases with metals. Therefore, dissolution reactions have been widely studied. Before 1931, many investigations focused on impure/heterogeneous metals. Bronsted and Kane (1931) have mentioned that when intending to elucidate the kinetics of reactions between acids (and bases) and metals one is compelled to using homogeneous metals only, as to avoid any impurities contributing to the inconsistency of kinetics that will be observed (Bronsted & Kane, 1931).

Aluminium in various environments has been an interesting subject of study to scientists, simply because of the many applications in which aluminium is used. In normal conditions, aluminium relies on its own defense mechanism, which happens to be the production of a somewhat compact, adherently passive oxide film which aids in the inability for corrosion to occur in different environments. The film on the surface of the aluminium piece is amphoteric; which can be explained as a metal that can react both as an acid and as a base - therefore it dissolves significantly when it is exposed to highly concentrated acidic or basic solutions. During the process of dissolution, once the oxide film has corroded away, exposing the bare surface of the metal, the solution used as a corrodant begins to dissolve the metal. This is a sequence of electrochemical processes that follows after the dissolution of the oxide film (Oguzie, 2007).

The study conducted by Mindrisz et al. (2013) was mainly directed to determine any significant changes during the dissolution of different types of aluminium alloys that may be present or used in the manufacture of target plates (Mindrisz et al., 2013). In the investigation of dissolving aluminium scraps UAl_x-Al were used with the expectation of understanding the reaction through hot dissolution studies. It is mentioned that for this experiment conducted by Mindrisz et al. (2013), the dissolution time and amount of gas evolved would be of interest in evaluating the results, due to the importance of these parameters to the development of the process. In the study of Mindrisz et al. (2013) the solution that was used for dissolution was externally heated up to 85°C. The solution was a 3.0 M NaOH and with the addition of 2.0 M or 4.0 M $NaNO_3$. Following that, the aluminium

scrap was placed in the heated alkaline solutions. In this reaction, a water bath to regulate temperature had not been used (Mindrisz et al., 2013).

2.4.2 Caustic aluminium dissolution

Teams from Hanford and Oak Ridge have studied the dissolution of the uranium-aluminium alloy in basic solutions, with the purpose of designing a continuous alloy dissolver to be operated in conjunction with a reactor. Dissolving the aforementioned alloys can be achieved in two ways; either with the aid of sodium nitrate or without it. The purpose of $NaNO_3$ addition is to mainly restrict the evolution of hydrogen gas, which can pose a great explosive threat. To better understand the chemistry behind these reactions, the reactions are illustrated as equation (1) and (2) (Snyder and Davis, 1956)

Without sodium nitrate

$$2Al + 2NaOH + 2H_2O \rightarrow 2NaAlO_2 + 3H_2 \uparrow \quad (1)$$

The addition of sodium nitrate yields

$$8Al + 5NaOH + 3NaNO_3 + 2H_2O \rightarrow 8NaAlO_2 + 3NH_3 \quad (2)$$

Aleksandrov et al. (2003) studied the reaction of Al foil and powder with dilute aqueous NaOH (Aleksandrov et al., 2003). The reaction of aluminium and dilute NaOH readily occurs at room temperature yielding H_2 gas and sodium aluminate. In the case of a dilute solution, species of aluminium which are found to be stable are monomeric tetrahedral aluminate ions $[Al(OH)_4]^-$. Their dimers can reach stability when cations are present in the solution. Aleksandrov et al. (2003) observed that the reaction of Al with aqueous NaOH is a topochemical reaction; meaning that the reaction involves introduction of a guest species into the host (aluminium), which will result in a significant structural modification of the aluminium. This modification may be a breakage of bonds. The alkaline reaction with the aluminium powder typically gives S-shaped curves with the reaction rate (W) being at a maximum of approximately 20 wt% conversion of the Al (Aleksandrov et al., 2003). The same reaction with Al foil is a multistage reaction. The reaction rate increases until 0.02-0.2 wt% has reacted, depending on the reaction. After some time, the reaction rate steadily decreases to a steady state level. The period up to the steady state being reached is called the induction period (the time needed by the solution to destruct the oxide film found on a metal and begin the dissolution of the metal) (Aleksandrov et al., 2003).

Studies performed by (Alwitt, et al., 1974; Foley, 1986) were conducted on the protection against/inhibition of the acids and/or bases which work by attacking the oxide film on aluminium metals. Alkaline solutions degrade the protective layer on the aluminium at a rapid rate; this is

possibly due to the presence of OH^- ions which are positively absorbed (Evans, 1981). This is further explained by (Pyun and Moon, 2000).

For a system that includes aluminium-alkaline solution, there is a requirement to determine the dissociation of the aluminium hydroxide phase that will be needed in determining the solubility of the aluminium in that solution. Reports have been made that the dissolution process is a function of the aluminium hydroxide in the solid phase (Zhang et al., 2009).

In the case of electrochemical dissolution of metals, the usage of sodium hydroxide as a media of corrosion is known to proceed by the action of local cells; where aluminium will be used as an electrode, thus leading to a loss of metal (aluminium) along with electrical power. In an electrochemical dissolution setup, there is a partial anodic reaction and a partial cathodic reaction occurring simultaneously on the metal surface (Deepa & Padmalatha, 2017).

The corrosion mechanism (3) - (4) of aluminium in basic solution is as follows:

Cathodic reaction is the reduction of water to hydrogen:

$$H_2O + e^- \rightarrow \frac{1}{2}H_2 + OH^- \quad (3)$$

Anodic reaction for dissolving aluminium in an alkaline solution is:

$$Al + 4OH^- \rightarrow Al(OH)_4^- + 3e^- \quad (4)$$

And the overall reaction (5) will be:

$$Al + 3H_2O + OH^- \rightarrow Al(OH)_4^- + \frac{3}{2}H_2 \uparrow \quad (5)$$

(Armstrong and Braham, 1996; Adhikari, 2008; Boukerche et al., 2014)

The behaviour of aluminium in alkaline solutions

The process of Al dissolution can be considered as a single step process. This is so because the reaction requires two conjugated transfer reactions, where there will be one from Al to Al^{3+} and another between H_2O and H_2. This kind of dissolution reaction depends on several factors which include the hydroxide ion [OH^-] concentrations and the amount of aluminate ion [$Al(OH)^-_4$] present in the electrolyte (Emregül & Aksüt, 2000; Pyun & Moon, 2000). Pyun and Moon, (2000) mentioned that the transportation of OH^- and $Al(OH)_4^-$ ions in the solution to and away from the metal/solution interface, respectively is anticipated to have an effect on the anodic dissolution process of the aluminium metal (Pyun and Moon, 2000).

Structure and behaviour of aluminate ions in solution

Eremin et al. (1974) stated that the structure of aluminate ions present in solution has proven to be one of the most important problems regarding the chemistry of aluminium and the production of alumina through alkali techniques. The underlying nature of the solutions, either being colloidal or true solutions was once a disputed study. The dispute, in general, had been on the nature and

structure of the aluminate ions in solution, due to the complexity of their behaviour along with the inconsistency of the numerous test results from previous investigations. The composition and structure of the aluminate ions in the solutions which contain different concentrations and varying pH levels was still unresolved then (Eremin et al., 1974).

Aluminium hydroxide phase

In a case where there is a reaction between aluminium and an alkaline solution, there is a need to determine the dissociation of aluminium hydroxide in the solid phase along with determining the solubility of the aluminium in the solution. In the studies of aluminium's solubility, specifically when using the metal in chemical separations (Zhang et al., 2009) and the chemistry of it in waste solution has been investigated in different contexts (Addai-Mensah et al., 2004; Peterson et al., 2007). In the liquid phase the Eh-pH relationship of solvated aluminium species have been studied by Wesolowski, (1992) and Addai-Mensah et al., (2004) forming multiple equilibria in strong alkaline solutions to strong acidic solutions. The aforementioned literature stated that, in caustic solutions, aluminium hydroxide forms a tetrahedral $[Al(OH)_4^-]$ species which equilibrates gibbsite $Al(OH)_{3(s)}$. In the caustic solution, the aluminate species form ion pairs with the sodium therefore producing electrically neutral species of $NaAl(OH)_{4\,(aq)}$ (McFarlane et al., 2015).

It has been reported that the dissolution process is a function of aluminium hydroxide in the solid phase (Goldberg et al., 1996; Zhang et al., 2009). The aluminium hydroxide formed will have no distinct form, existing as one of the three crystalline forms as gibbsite, bayerite or nordstandite (McFarlane et al., 2015).

Zhang et al. (2009) made predictions that aluminium's solubility in an alkaline solution determined by the dissolution reaction of aluminium hydroxide, where the equilibrium of the reaction will be a function of the aluminium hydroxide phase:

$$Al(OH)_3 = Al^{3+} + 3OH^- \tag{6}$$

Calculating the thermodynamic solubility product (K_{sp}) as

$$K_{sp} = [Al^{3+}][OH^-]^3, \tag{7}$$

given that

$$K_w = [H^+][OH^-], \tag{8}$$

substitute K_w into K_{sp}

giving:

$$K_{sp} = [Al^{3+}] \times \left(\frac{K_w}{[H^+]}\right)^3. \tag{9}$$

The concentration of aluminium can be calculated as

$$[Al^{3+}] = \frac{K_{sp}\,[H^+]^3}{K_w} \tag{10}$$

Where the equilibrium constant is represented by K_w

Usually, in alkaline or acidic solutions, aluminium can be found in different states: Al^{3+}, $Al(OH)_4^-$, $AlOH^{2+}$, $Al(OH)_2^+$ and $Al(OH)_3^0$. Zhang et al. (2009) go on to express the total solubility of aluminium as:

$$\sum Al_{(aq)} = [Al^{3+}] + [Al(OH)^{2+}] + [Al(OH)_2^{3+}] + [Al(OH)_3^0] + [Al(OH)_4^-] \quad (11)$$

The cumulative complexation reactions are further explained by using the concentration of Al-OH complex and relating it to Al^{3+}. The results show that in an alkaline solution (NaOH or KOH), the main hydroxide form that is present is $Al(OH)_4^-$ while the aluminium ions present in solution are not stable (Zhang et al., 2009).

2.4.3 Acidic aluminium dissolution

The corrosion mechanism of aluminium in acid solution is as follows:

$$Al + H_2O \rightarrow AlOH_{(ads)} + H^+ + e^- \quad (12)$$

$$AlOH_{(ads)} + 5H_2O + H^+ \rightarrow Al^{3+} + 6H_2O + 2e^- \quad (13)$$

$$Al^{3+} + H_2O \rightarrow [AlOH]^{2+} + H^+ \quad (14)$$

$$[AlOH]^{2+} + X^+ \rightarrow [AlOHX]^+ \quad (15)$$

Therefore, the soluble $[AlOHX]^+$ complex ion leads to the dissolution of the metal of investigation (Deepa & Padmalatha, 2017).

2.4.4 Comparison of aluminium dissolution in acid and alkaline solutions

An investigation conducted by Garcia-Garcia et al. (2012) possibly evaluated the effects of the addition of nickel to the reaction of Al of an AA1050 grade in HCl and NaOH solution, which is used in the lithographic industry. The results obtained showed that the addition of nickel improved the dissolution rate for both solutions. On the other hand, a study by Boukerche et al. (2014) reported that the dissolution rate in NaOH was greater than that in HCl. Furthermore, this dissolution study was focused on the kinetics of aluminium dissolution in HCl, H_2SO_4, HNO_3 and NaOH under the same conditions (Boukerche et al., 2014). The experiments were conducted by contacting an aluminium disc with mass of 0.75 g with 200 mL of the desired solution (HCl, H_2SO_4, HNO_3 and NaOH). The chemical equation for the dissolution of aluminium in an acidic and basic media is shown by equation (16) and (17):

$$Al + e^- \rightarrow Al^{3+} \quad (16)$$

$$Al + 4OH^- \rightarrow Al(OH)_4^- + 3e^- \quad (17)$$

With the overall equation for equation (16) and (17) being

$$Al + 3H_2O + OH^- \rightarrow Al(OH)_4^- + {}^3/_2 H_2 \uparrow \quad (18)$$

The volume of 200 mL was chosen to avoid any saturation that may take place in the solution. The data presented for this experiment had two test replicates with an error of 5%. The dissolved aluminium was calculated in terms of the weight-loss using the equation (19);

$$\text{Aluminium dissolved} = \frac{C \times V \times M}{A} \ (mg/cm^2) \quad (19)$$

where C is concentration of the Al^{3+} analysed in the solution (mol/L),

V is volume of the solution (0.2 L),

M is molar mass of aluminium (26.982 g/mol), and

A is surface area of the aluminium disc (0.927 cm^2).

The concentrations of the solutions that would dissolve the disc varied from 0.5 M to 4.0 M, with the temperature varying from 40°C to 80°C while stirring at 350 rpm. When dissolving aluminium in a solution, the solvent must be in excess to prevent precipitation/saturation (Boukerche et al., 2014). In alkaline solutions (NaOH) of concentrations of 0.5, 1.0 and 2.0 M, there would be higher amounts of Al dissolved compared to the acidic (HCl) solutions of the same concentrations. Comparing NaOH and HCl, it was found that the induction period in HCl was slower than that of NaOH. Normally, the process of dissolving metal occurs through a heterogeneous reaction; this involving the transfer of chemicals and reactants (Boukerche et al., 2014).

In the case of dissolving plates containing metallic uranium, it is important to note that uranium in elemental form is very reactive when compared to magnesium in terms of dissolution characteristics. When the metal, which may be in the form of turnings or fine powder, reacts with hydrochloric acid and nitric acid, the surface is oxidized in air. This powder becomes extremely hazardous because it is pyrophoric (ignition by spontaneous reaction with air); which may be caused by mechanical friction, minute addition of water or acid, or simply spontaneously in air; ultimately leading to radioactive contamination (Larsen, 1959).

Due to the lack of literature on the corrosion of 6063 aluminium, Deepa & Padmalatha (2017) studied the dissolution of aluminium and aluminium alloys in phosphoric acid and sodium hydroxide. This investigation focused on a few parameters, including different temperatures and concentration of solutions. Analysis was performed by electrochemical methods using the Tafel polarization technique, accompanied by electrical impedance spectroscopy (EIS) (Deepa & Padmalatha, 2017). The morphology of the aluminium's surface was studied using a scanning electron microscope (SEM) with an energy-dispersive X-ray spectroscopy (EDX). It was found that the major corrosion of 6063 aluminium alloy occurred in a sodium hydroxide (NaOH) solution, compared to phosphoric acid solution (H_3PO_4). Deepa and Padmalatha, (2017) determined that the rate of corrosion was directly proportional to increasing temperature and concentration of both acid and alkali solutions. Using the transition state and Arrhenius theories, thermodynamic and kinetic

parameters were calculated and an appropriate mechanism was proposed when corroding 6063 aluminium alloys in H_3PO_4 and NaOH media (Deepa & Padmalatha, 2017).

In another paper by Boukerche et al. (2014) the ability for aluminium to degrade in acidic and alkaline solution was tested in both static (absence of stirring) and agitated media. While only one type of alkaline solution, i.e. sodium hydroxide (NaOH) was used, three different acidic solutions were used, namely; hydrochloric acid (HCl), nitric acid (HNO_3) and sulphuric acid (H_2SO_4). Solutions with concentrations of 0.5 M, 1.0 M and 2.0 M were prepared for all the acidic and basic media. In this experiment a huge quantity of NaOH was used in excess in order to prevent the precipitation of aluminium. It was noted that the rate of aluminium released from the reaction was directly proportional to the concentration of the solution; except for the reaction in HNO_3. The highest reported release of the Al was from NaOH, comparable to HCl at all three concentrations. When comparing the reaction rates in H_2SO_4 and HNO_3, they were notably slower than in NaOH and HCl. In case of the agitated media reactions, only four solutions had been prepared at a concentration of 2.0 M. The solutions were heated prior to the commencement of the reaction to temperatures from 40 to 80°C. Boukerche et al. (2014) found out that NaOH dissolved the aluminium faster at lower temperatures (40 to 50°C) when compared to HCl. However, it was also reported that at higher temperatures (70 to 80°C), NaOH seemed to have a slower rate in dissolving the aluminium than HCl. The rate constants in both NaOH and HCl were calculated. In HCl it was 0.0141 and 0.0214 min^{-1} at 70 and 80°C, respectively. In NaOH the rate constants at 70°C were 0.0069 min^{-1} and 0.0106 min^{-1} at 80°C. The data showed that HCl had double the rate constant compared to NaOH. Boukerche et al. (2014) calculated the activation energies for aluminium dissolution in HCl and NaOH, as 86.5 and 52.4 kJ/mol, respectively (Boukerche et al., 2014).

2.4.5 Target dissolution

In an investigation by Cols et al. (1997) uranium silicide (mini-plates) was the selected material to undergo testing because U_3Si_2 has a uranium mass per volume unit, therefore allowing for the reduction of uranium enrichment to 20%. Mini-plates that contained natural uranium and clad with aluminium were utilised to conduct the experiment. Sodium hydroxide was used to dissolve the target plates and an oxidizing agent, H_2O_2 was added in order to ensure complete dissolution of the silicide. When considering dissolving uranium silicide, neither NaOH nor H_2O_2 can completely dissolve it independently. Therefore, the ratio of NaOH to H_2O_2 in solution is vital in achieving thorough dissolution. Cols et al. (1997) used 97 ml of 3.0 M NaOH along with 5 ml of H_2O_2 for 100 vol. per gram of the target. The experiment was said to be promising regarding the results obtained from the dissolution process, recovery and purification of ^{99}Mo (Cols et al., 1997).

Conner et al. (1997) established the practicality of dissolving aluminium-clad LEU UO_2/Al dispersion targets in alkaline solutions. This is because alkaline dissolution of the targets has a number of advantages i.e. it is well-matched with the present (uranium-aluminide) dissolution process, it isolates iodine from fission noble gases, and uranium along with activation and numerous fission products are insoluble in alkaline media (Conner et al., 1997).

2.5 Separation methods

When planning an effective separation process to be implemented on nuclear fuel, one has to fully comprehend the various physical and chemical concepts that encompass the process. Processes that can be used in separation methods are precipitation, separation techniques coupled with redox reactions, solvent extraction, ion exchange, etc. In order for one to predict the outcome of a given separation process, a thorough understanding of the chemistry of the elements being separated is valuable.

2.5.1 Separation and recovery of uranium

The two major classifications of nuclear fuel are 1) aqueous and 2) non-aqueous reprocessing. Where the aqueous reprocessing can be carried out by one of the two approaches either being solvent extraction or precipitation. The main focus is on the aqueous reprocessing method. In the process of actually separating elements that are constituted in the nuclear fuel, there is a process that ultimately separates these constituents by a method called the plutonium and uranium redox extraction (PUREX); or in other cases, a modified version of the PUREX process (Peterson & Wymer, 1963). This process is undergone because of the need to completely separate and possibly purify actinides and other elements (krypton, carbon-14) that have been used in the fuel and those that form during the process of fission reactions, such as uranium, plutonium, etc. Briefly, PUREX is a process in which fuel elements are dissolved in concentrated nitric acid, and uranium and plutonium are separated by solvent extraction (Norbash et al., 2010). It is also a process in which the separation process is achieved by transferring the uranium and/or plutonium from the aqueous phase to the organic phase and then recovering the uranium and/or plutonium by using the back-extraction or stripping process into an aqueous phase (Hough, 1997).

After the uranium-aluminium alloy has been irradiated, uranium must be isolated and recovered from the rods, plates or slugs that were used as fuel. This is done because the uranium can be re-used. Gile, (1965) mentioned that the recovery process is important because the fuel contain enriched ^{235}U which is a valuable nuclear fuel element. Another area where recovery of U from fuel or target plates is important is in the manufacturing process of the plates. The plates that will be used to fuel the reactor may be flawed due to impurities that will hinder the process of a controlled nuclear reaction. Therefore, the components of the used alloy and the uranium itself must be

recovered. Gile, (1965) stated that the most preferred method of separating the uranium from the uranium-aluminium alloy is through the dissolution of the alloy. For example, by utilizing a mixture of sodium nitrate and sodium hydroxide solutions, where a speedy dissolution will be advantageous. When using solutions of $NaOH/NaNO_3$ during the recovery of uranium from the plates, the aluminium converts to aluminate ions whilst the uranium precipitates as an oxide. Gile, (1965) found it difficult to adjust the quantities of the sodium hydroxide and sodium nitrate to optimise the dissolution conditions. He reported that a high concentration of NaOH was ideal for the rapid dissolution period, but the disadvantage is that there is a higher percentage loss of uranium to the solution, during the process of separating precipitated uranium from the aluminate solution.

An investigation piloted by Stassen & Suthiram, (2015), reported on characterization of the residue that was recovered after dissolving U/Al target plates, similar in composition to those used in the production of ^{99}Mo, however, they contained unirradiated depleted uranium instead of irradiated enriched uranium as in the real ^{99}Mo production process. Unirradiated DU was mainly used in order to lower the radiation hazard and allow characterization studies outside of a hot cell. The NTP Radioisotopes SOC Ltd (a subsidiary company of Necsa) process was used to dissolve the plates. After dissolution, the residue containing U was recovered, fully dried, and homogenised to a fine powder for future use. Optimization of the dissolution process of the residue in a carbonate medium was performed on a 10 g scale, where a number of parameters were tested i.e. the addition of H_2O_2 at different times, the solid liquid ratio, varying temperatures, diverse concentrations of H_2O_2 and $(NH_4)_2CO_3$, the stirring rate and the reaction time. The samples underwent chemical analysis to deduce the uranium and chemical impurities concentration in the residue. The concentration of uranium in the residue was found to be 71%. The optimised dissolution parameters were tested by using irradiated samples and measuring the recovery of uranium from the samples. The optimized dissolution parameters tested on the irradiated samples, proved to successfully recover all the uranium by employing three successive carbonate/peroxide leaches (Stassen & Suthiram, 2015).

2.6 U dissolution in nitric acid

2.6.1 Dissolution of uranium

Recycling spent nuclear fuel (SNF) has led to several processes, mostly based on hydrometallurgical principles, be developed (Bourgeois, 2000; Marc et al., 2017; Lecomte & Bonin, 2008). One of the hydrometallurgical processes included is the widely used PUREX process mentioned before, that has enabled successful separation and salvage of uranium and plutonium from SNF. This process is based on the dissolution of SNF in nitric acid.

The process of dissolving uranium in acid media (i.e. nitric acid) has been studied widely, where different compounds of uranium were tested. The methodology was similar in many ways differing

in the concentration of the nitric acid and the temperature to which the solution was at. Metal-catalysts with nitric acid have been used by Burns & Holm, (1952); Maher, (2015); Almond et al. 2018, in dissolving aluminium-uranium alloy. The use of a metal catalyst (Hg-II catalyzed nitric acid) was investigated in order to find the optimum mercury concentration that would decrease the dissolution time (Burns and Holm, 1952).

2.6.1.1 UO_2 with HNO_3

Marc et al. (2017) compiled their study on the dissolution of UO_2 in HNO_3 media elaborating that the process produces soluble uranyl nitrate salts ($UO_2(NO_3)_2$). The reaction between uranium dioxide and nitric acid is performed in order to achieve the VI oxidative state from the IV state of uranium, which is much more soluble than U(IV). Nash and Nilsson, (2015) stated that, when performing dissolution on the uranium, the concentration of nitric acid would be adjusted to a moderate level approximately between 2.0 – 4.0 M before the separation stage.

Hermann, (1984); Fournier, (2000); Almond et al. (2018); have illustrated the different stoichiometric equations to describe the reaction of the dissolution of UO_2 in HNO_3. Marc et al. (2017) further illustrated the chemical equations that would take place when reacting uranium dioxide with nitric acid. Literature study has also shown many proposed mechanisms (Shabbir & Robins; 1968 Fournier, 2000) which take place during the oxidation stage (Marc et al., 2017). Some of the summarized reactions (20) – (22) of UO_2 with HNO_3 provided by (Marc et al., 2017) include;

$$UO_2 + \frac{8}{3}HNO_3 \rightarrow UO_2(NO_3)_2 + \frac{2}{3}NO + \frac{4}{3}H_2O \quad (20)$$

$$UO_2 + 4HNO_3 \rightarrow UO_2(NO_3)_2 + 2NO_2 + 2H_2O \quad (21)$$

$$UO_2 + \frac{12}{5}HNO_3 \rightarrow UO_2(NO_3)_2 + \frac{1}{5}N_2 + \frac{6}{5}H_2O \quad (22)$$

2.6.1.2 U/Al with HNO_3

Larsen, (1959) stated that one of the most useful methods of dissolving uranium metal and its alloys is by using nitric acid. It is further explained that the reaction with nitric acid is a complicated one as the by-products given off may be nitrogen dioxide or dissolved ammonia (Larsen, 1959). Another factor brought by the complication presented by dissolution of uranium in nitric acid is that when the powder is finely ground, the reaction has the potential to be explosive. Lacher et al. (1961) stated that when dissolving uranium metal, the dissolution rate depends on the concentration of present impurities and the type of metallurgical treatment the metal underwent. After carrying out experiments, results obtained suggested that reacting uranium with concentrated HNO_3 produced $UO_2(NO_3)_3$ and NO_2 while using a lower concentrated HNO_3 manly produced NO (Lacher et al., 1961).

2.7 U purification using solvent extraction

2.7.1 Solvent extraction

Liquid-liquid extraction, also called solvent extraction (SX), is an extraction method used to separate metals in solution. Solvent extraction refers to the distribution of a solute of interest between immiscible phases/solvents that are in contact with one another; one which is usually water and the other being an organic solvent. Organic solvents used in this technique include benzene, carbon tetrachloride, and chloroform. The SX method may be used for different purposes such as preparation, purification, enrichment, separation and analysis, on different scales of working processes (micro to macro) (Shabbir & Robins, 1968; De, Khopkar & Chalmers, 1970).

Stary & Irving (1964) mentioned that ever since the development of SX in 1957 by Ames Laboratory together with the U.S. Bureau of Mines, it has been considered an exceptional separation method. This method gained popularity and preference amongst other separation techniques mainly through its simplicity, rapidity and its wide scope in separation. Another point that makes SX attractive is the simple apparatus, which includes a separatory funnel with only a few minutes needed to complete extraction of desired element, this is beneficial to a chemist. This kind of separating method is ideal when extricating trace constituents from large quantities of substance. This process is desirable as it is able to extract a very large amount of the desired element through several repetitions of the extraction method. This kind of technique is prevalent in nuclear chemistry and the technology used in separating radioisotopes along with reprocessing of nuclear fuels (Stary & Irving, 1964).

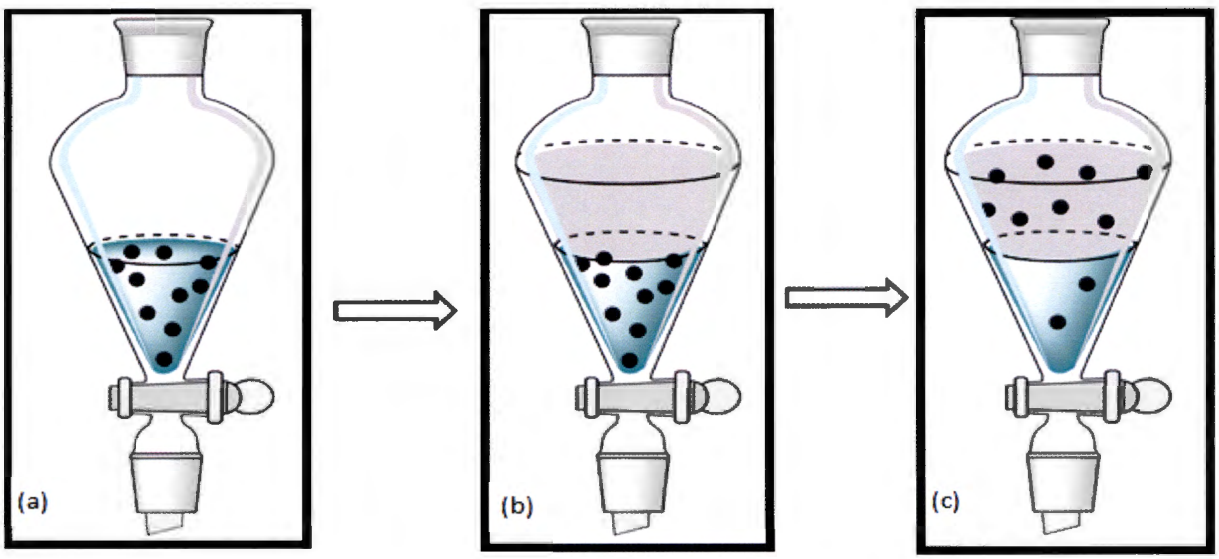

Figure 2.1: Simple illustration showing a separatory funnel with both the organic solvent and aqueous solvent divided by their difference in densities, modified from (LibreTexts, 2019).

(a) Aqueous solution containing uranium, (b) organic extractant (e.g. TBP) added to uranium aqueous phase (bottom), and (c) organic phase (top) containing $UO_2(NO_3)_2 \cdot 2TBP$ complex after agitation and settling.

Solvent extraction has become an integral part of hydrometallurgy in Southern Africa for several years. During the 1950s, the first major usage of SX technology took place commercially. Other successful operations of SX followed suit around the world after copper extraction was proved to be possible (Sole et al., 2005). In Southern Africa, SX has been utilised by Rössing Uranium, situated in Namibia. This is achieved through open-cast uranium mining, producing U_3O_8 (Basson & Greenway, 2004). The mined ore is crushed to smaller rocks to a size of 16 cm where is is further crushed to smaller sizes that are easier to work with. A leaching process by utilizing sulphuric acid is applied and a suitable solid-liquid separation technique is set up. The ion exchange technique is then used to extract the uranium from the acidic solution using a Duolite A101-DU resin. In order to make up a more concentrated uranium solution, the stripping process is facilitated by diluted sulphuric acid. The solution is pumped through to an SX facility where the solution is further concentrated and other impurities eliminated. The Vaal River South Uranium Plant run by AngloAshanti is a plant that was built in order to recover uranium as a by-product of gold mining. This plant also produced uranium in the form of U_3O_8. Ore treatment began with acid leaching, allowing the uranium to dissolve before any gold recovery processes could be performed. The uranium in the uranitite mineral requires oxidation from the tetravalent species to the hexavalent species prior to solubilisation. The sulphuric acid leaching oxidation was attained by means of ferric ions that had been produced by oxidation of iron (II) existing in the blend with manganese dioxide. Further processing using ion exchange (IX) is employed using columns and thereafter further purification using SX (Sole et al., 2005). Generally, the extraction of uranium can be achieved through selective partitioning of ions into either the organic phase or the aqueous phase. The selectivity of the partitioning of ions into the different phases will depend on the chemical complexes formed. The complex formed will depend on the solution medium along with the pH range of the solution.

2.7.2 SX extractants

A number of extractants used to facilitate extraction are commercially available and fall into different categories i.e.

1. Phosphorus-based extractants
2. Sulphur-based extractants
3. Nitrogen-based extractants
4. Other extractants

(Abbasi & Streat, 1998 & Kumar et al., 2011;) further elaborate on the different extractants that may be used for SX.

2.8 U purification using solvent extraction into TBP

In nitric acid media, kerosene (and other various organic diluents) are commonly used when extracting uranium in many industrial applications due to the ability to meet environmental regulations, availability, cost-effectiveness and the low toxicity they present when compared to other diluents (Kumar et al., 2011). Kumar et al. (2011) also mentioned that TBP proved to be the best extractant for uranium. TBP is the most used solvent in the process of liquid-liquid extraction for fuel reprocessing as well as in nuclear chemistry mainly for the recovery of actinides such as Np, Pu, Th and U. Another point to consider in favouring TBP as a solvent for the process of solvent extraction is that, compared to other purification processes, it has a high selectivity for uranium metal therefore providing an outstanding decontamination factor for a lot of impurities. TBP is able to remain stable in environments which may cause degradation during uranium purification. In addition, TBP/kerosene solutions have low vapour pressure this meaning that they may be stored and handled without excessive caution against fires (Schulz & Navratil, 1984; Stas et al., 2005). The challenge with using TBP is that it has similar viscosity and density when compared to water; therefore, it presents a problem when having to separate TBP from water. This challenge is overcome by diluting TBP with a light, saturated hydrocarbon, i.e. kerosene, n-dodecane, normal paraffin hydrocarbon (NPH), etc which ultimately reduces the density value of the TBP and encourages phase separation (Schulz & Navratil, 1984).
A study conducted by Alibrahim & Shlewit (2007) showed that 20% TBP was able to extract 78 g/l uranium in nitric acid solutions.

An extensive study was conducted on TBP-diluent-nitric acid system in detail by Alcock et al. (1956). They investigated the TBP-diluent-water-HNO_3 system and measured TBP and water mutual solubility in the presence of nitric acid along with the presence of a variety of diluents such as benzene, cyclohexane, heptane, hexane, kerosene and toluene. The partitioning of HNO_3 between water and TBP in kerosene measured at different concentrations was also determined. Alcock et al. (1956) also reported on the extraction of HNO_3 in the organic phase; that extraction took place with the formation of a 1:1 compound with TBP. Siddall III et al. (1957) presented their findings after investigating the distribution equilibrium of thorium, uranium and nitric acid with solutions of n-TBP in kerosene, along with the different aqueous solutions encountered in the separation of uranium and plutonium for the recovery of ^{235}U from reactor spent fuel (Siddall III et al., 1957).

Horng (1984) developed an extraction model which was based on the extraction kinetics of $UO_2(NO_3)_2$-TBP-kerosene system in an acidic medium by proposing that the extraction rate of uranyl nitrate is a pseudo first order reaction with regards to its concentration in the aqueous phase in addition to the concentration of free TBP. During the course of reprocessing spent nuclear fuel, an aqueous based method involving the use of TBP is used, therefore forming a $UO_2(NO_3)_2{\cdot}2TBP$. The mechanism proposed by Naito (1960) is presented as equation (23):

$$(UO_2^{2+})_{aq} + 2(NO_3^-)_{aq} + 2(TBP)_{org} \leftrightarrow (UO_2(NO_3)_2 \cdot 2TBP)_{org} \quad (23)$$

In the extraction method, UO_2^{2+} and NO_3^- constitute the aqueous phase, while TBP (with kerosene as a diluent, for example) represents the organic phase, thereby forming $UO_2(NO_3)_2{\cdot}2TBP$ in the organic phase shown by equation (23) (Ye et al., 2010).

The rate of stripping was also found to be pseudo first order with respect to the concentration of tributyl phosphate complexed by uranyl nitrate. The calculated values of $Be^{\Delta H/RT}$ (where B represent the proportional constant times the equilibrium concentration of nitric acid, in the aqueous phase, ΔH the heat of extraction, R the gas constant and T, , the absolute temperature) of 20% TBP in kerosene could be utilised to forecast the equilibrium values of the system of 30% TBP (Horng, 1984). Horng (1984) further stated that the Langmuir model was used to characterise the extraction equilibrium isotherms, where the absolute errors in the correlation coefficients between the experimental data and the projected values were in the ranges from 2.68% and 6.73% (Horng, 1984). A chemical model for extraction of uranyl nitrate with TBP was suggested by (Kopečni & Petković, 1994). This model could use chemical activities of the extracted species in the aqueous phase. The model was developed and centred around the chemical reaction where a neutral extractant would interact with an inorganic salt present in the aqueous phase thus forming a neutral complex that would be extracted into the organic phase. The model appeared to fit effectively with the distribution results over the complete concentration range of the extraction isotherm (Kopečni & Petković, 1994).

2.9 U purification using ion exchange

Adsorption treatment is not to be confused with ion exchange as they are similar in many ways such as their basis of matrix composition, polarity, physical and chemical resistivity, particle size distribution, inner and specific surface areas, density, porosity and the effect of pore size radius on distribution; therefore, the process of ion exchange is a chemical mechanism rather than adsorption (Harland, 2007; Kammerer et al., 2010). With adsorption, it is normally used for purifying or adsorbing atoms, ions, or molecules from a gas, dissolved solid or liquid substance stick to the surface of surface (e.g. activated carbon). Materials utilized for ion exchangers comprise of insoluble constituents that contain weakly bound ions which are able to be easily exchanged with

other ions in solution when they come in contact with each other. The ionic exchange takes place without any physical alteration to the exchange material. The insolubility of ion exchanger material, rendered by insoluble salts present on the beads allows for cations or anions to be removed successfully (Patel, 2016).

The method of ion exchange can be explained as the removal/interchange of an ion in a solution and the replacement of that ion by a different ionic species (Alexandratos, 2008). Mahbub Hasan et al. (2014) further elaborated that it is a process in which ions present in an aqueous solution are transferred to a solid matrix which, in exchange, liberates different type of ions that have the same polarity (Mahbub Hasan et al., 2014). The history behind ion exchanging dates back from the Bible after preparing water to drink from brackish water, this was taken further by agricultural chemists, Thompson (1850); Way (1850), when they discovered that some soils were able to absorb ammonia from fertilizers better than others. Progress in ion exchange occurred during the middle and late eighteenth century when a polystyrene-divinylbenzene-based anion exchanger was able to remove all anions, therefore, making it possible to demineralize water (Kumar & Jain, 2013). Pashalidis & Tsertos (2004) were able to recover uranium from seawater using a cation exchanger, Chelex-100. Recovery was conducted at pH levels below 7 (specifically at 5.3), at that level, the dominating uranium species in the solution are UO_2^{2+} and UO_2OH^+. The percentage recovery of uranium was analysed by spectrophotometry using Arsenazo(III) and found to be $97\pm2\%$. Studies conducted by Ladeira & Morais (2005) utilized ion exchange resins in recovering uranium from synthetic solutions (Ladeira & Morais, 2005). It was reported that the extent to which uranium had absorbed in the resin was influenced by the concentration of uranium in the solution compared to other ions, the pH of the solution along with the relative affinity of the resin for the anionic species (Merritt, 1971a).

In this study, two types of ion exchangers were tested for their ability to effectively recover uranium from a nitric acid solution and purify it from aluminium; i.e. a cation exchange resin BioRad AG50W-X4 and two chelating resins, i.e. Amberlite IRC747 and Amberlite IRC748. Multidentate chelating agents are intentionally made for their specific affinity to desired metal ions from contaminants. These chelating agents use electrostatic and covalent bonds, and in some cases, use steric factors that are combined to produce an anticipated complex strength and selectivity (Nash & Nilsson, 2015).

The AG50W-X4 resin is a strong acid cation exchange resin, composed of sulfonic acid functional groups ($-SO_3H$) attached to a styrene divinylbenzene copolymer lattice. In dilute nitric acid, it has the ability to exchange UO_2^{2+} ions with reasonably high selectivity (Strelow et al., 1965).

A special type of cation exchanger exists, called a chelating resin, which forms a chemical bond with ion to be exchanged. Chelating resins are almost always used to bind cations. They utilize chelating agents covalently attached to a polymer matrix. Chelating resins have the same bead form and polymer matrix as the usual ion exchangers. As chelating groups, various ligands with nitrogen (N), oxygen (O), and/or sulfur (S) donor atoms, are immobilized on the matrix. Common chelating groups are iminodiacetic acid (figure 2.2); used in Amberlite IRC748 and Chelex 100, and aminophosphonic acid (figure 2.3), used in Amberlite IRC747 and Purolite S940.

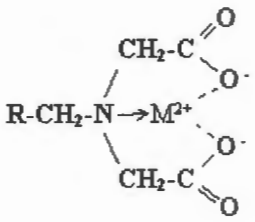

Figure 2.2: Iminodiacetic acid functional group

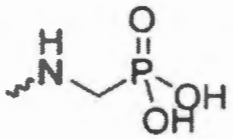

Figure 2.3: Aminophosphonic acid functional group

These functional groups could form a complex with the UO_2^{2+} ion from dilute nitric acid solution, thereby removing it from the feed solution.

2.10 Characterization of the uranium residue generated during alkaline dissolution of U/Al plates

The unirradiated residue along with the chemical impurities were characterised using XRF, ICP-OES, Glow Discharge Mass Spectrometry, neutron activation analysis, combustion analysis and thermogravimetric analysis, by Stassen & Suthiram (2015). It was recorded that the main contributors to impurities were Na and Al; the Na being due to the solvent used in dissolving the ^{99}Mo production process targets and Al (main constituent) from the target plates. In another experiment conducted by Stassen & Suthiram (2015) using X-ray Diffraction (XRD), UV/Vis/NIR and FTIR, the characterised residue revealed that the U was most likely to be present as a mixture of UO_2, UO_3 and $Na_2U_2O_7$. From characterising the residue, the U(IV) – U(VI) ratio had to be determined from two different batches where one had a ratio of 86:12 and another had the ratio of 88:12, respectively. When comparing the measurements, nearest value similarities were observed where U(IV) was present as UO_2 and U(VI) as either UO_3 or $Na_2U_2O_7$. Due to the importance of lower water content in both cases, along with U(VI) being present as UO_3, residual quantity of the sodium hydroxide is required in order to account for the residue's Na content. It is reported that the

results showed a discrepancy of 4% in the total mass, which may have stemmed from the under determination of both U and O in the residue (Stassen & Suthiram, 2015).

Chapter 3: Methods of investigation

For this chapter, the experiments are described which were conducted in order to;

1. Determine the optimum dissolution conditions for pure aluminium.
2. Determine the optimum dissolution conditions for the uranium residue generated from alkaline dissolution of U/Al target plates
3. Determine the optimum conditions for solvent extraction of uranium into TBP, and the effect of Al on extraction
4. Determine if uranium can be successfully purified from the nitric acid solution using ion exchange resins

3.1 Effective alkaline media

Two experiments were conducted to determine the optimum dissolution media. The two media tested were NaOH (≥97.0%) and KOH (≥85.0%) supplied by Sigma-Aldrich of ACS (analytical grade). Dissolution media were tested to determine the optimum concentration along with the requirement for excess alkali to keep the dissolved Al stable in solution, the influence of temperature, stirring rate and the addition of $NaNO_3$ (≥99.0%), supplied by Sigma-Aldrich of ACS (analytical grade), has on the reaction rate.

The test vessel used for Al dissolution is shown in Figure 3.1.

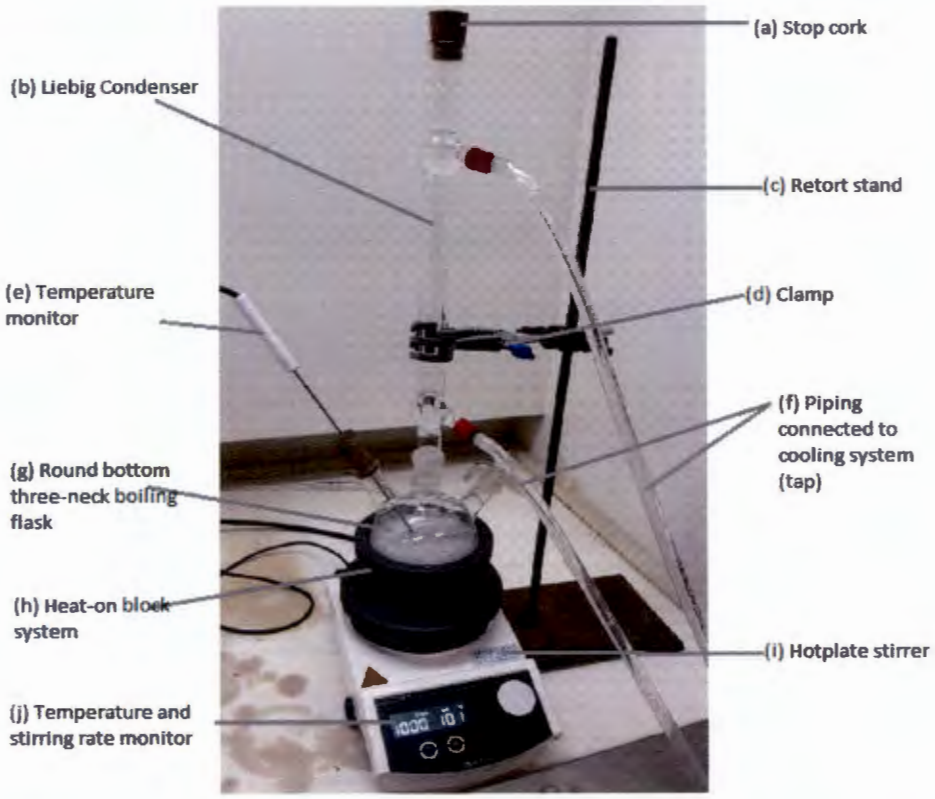

Figure 3.1: Dissolution setup used to conduct experiments in a non-radiation environment.

3.1.1 Experimental procedure

The aluminium sheets (99.0% purity, supplied by Sigma-Aldrich of ACS (analytical)) were cut into 2 cm × 2 cm × 0.3 cm and 1 cm × 1 cm × 0.3 cm pieces. The pieces were then weighed to about 16.2 g for each reaction. The Al sheets were not pretreated in any way prior to dissolution.

To test for the optimum concentration and the requirement of excess alkali, solutions of 6.0 M NaOH and KOH were prepared, and different volumes of these solutions were used to determine the effect of a stoichiometric vs excess amount of NaOH on the dissolution rate.

3.1.1.1 Concentration test

Dissolution of aluminium in sodium hydroxide is represented by equation (24)

$$2Al + 2NaOH + 2H_2O \rightarrow 2NaAlO_2 + 3H_2 \quad (24)$$

From this reaction equation, 2 mol of Al reacts with 2 mol of NaOH to completely dissolve, and it can then be shown that the stoichiometric volume of 6.0 M NaOH required to dissolve 16.2 g of aluminium (the standardized mass chosen for these tests) is 100 ml. A solution of 6.0 M NaOH was prepared in a 1.0 L volumetric flask and used to dissolve 16.2 g ± 0.47 of Al for each experiment. A Radwag PS 750/C/2 ± 3 mg balance was used to weigh out the masses of aluminium. Thereafter 100 ml, 133 ml and 200 ml of the alkali solutions (representing stoichiometric 6.0 M NaOH solution, 1.5 M excess NaOH and 3.0 M excess NaOH) were measured and placed in a three-necked round bottom flask, placed in a heat-on block system that was connected to the temperature monitor. The flask was connected to a Liebig condenser that used tap water (at temperature of 25°C) as a coolant. The solutions were heated to 80°C and stirred at 1000 rpm. The stirring rate and temperature were kept constant so that the variable tested would only be the amount of NaOH (stoichiometric vs excess). The time was recorded until the reaction was complete for all the reactions. The completion of the reaction was noted when no more effervescence was observed; by that observation, it was assumed that all the aluminium had been dissolved. The dissolution rate was calculated using equation (25);

$$Dissolution\ rate = \frac{m_{Al}}{t} \quad (25)$$

where m_{Al} is the mass of aluminium (g)

t is the time taken for aluminium to be dissolved (min)

A stopwatch was used to record the time taken for each reaction to complete. The optimum concentration for both sodium hydroxide and potassium hydroxide was determined to be a stoichiometric volume of 6.0 M NaOH plus 3.0 M excess above the required stoichiometric amount for complete dissolution of the weighed amount of Al discussed below in Section 4.2) and was applied in dissolving Al in order to optimise other dissolution parameters.

3.2 Optimising dissolution parameters

3.2.1 Temperature

The results obtained from concentration optimisation, were applied for optimising the temperature for Al dissolution. A total of 200 ml of 6.0 M alkali solution was used to dissolve 16.2 g Al, representing an excess of 3.0 M alkali above the stoichiometric amount needed for dissolving the mass of Al used. To test for temperature, the solutions were heated at varying temperatures of 30°C, 60°C and 80°C, the stirring rate was kept constant at 1000 rpm. To monitor the temperature of the solution before adding Al, a HeidolphMR Hei-Tec hotplate stirrer with Pt 1000 (P/N 505-30081-00) temperature probe, supplied by Separations, was used. The optimum temperature in terms of dissolution rate and re-precipitation time was selected to be 80°C (discussed in Section 4.2.2).

3.2.2 Stirring rate

For the stirring rate test, 0, 500 and 1000 rpm rates were chosen and implemented on both of the alkali media containing an excess of 3.0 M alkali above the stoichiometric amount needed for dissolving the mass of 16.2 g of Al and heated to 80°C.

3.2.3 $NaNO_3$

Sodium nitrate was added to prevent the production of hydrogen gas that would pose as a threat to the investigator. Dissolving aluminium in sodium hydroxide in the presence of $NaNO_3$ is represented by equation (26)

$$8Al + 5NaOH + 3NaNO_3 + 2H_2O \rightarrow 8NaAlO_2 + 3NH_3 \quad (26)$$

From this reaction equation, 8 mol of Al reacts with 5 mol of NaOH and 3 mol of $NaNO_3$ to completely dissolve, and it can then be shown that the stoichiometric volume of 6.0 M NaOH required to dissolve 16.2 g of aluminium is 62.5 ml. Since the other optimization experiments were all performed with a 3.0 M excess of NaOH above the stoichiometric amount, this was also added in these tests, requiring an additional 62.5 ml, i.e. a total of 125 ml 6.0 M NaOH. The amount of 3.0 M $NaNO_3$ required to stoichiometrically bind all hydrogen as NH_3 in the above reaction, is 75 ml, therefore a total reaction volume of 200 ml. In these tests, the effect of adding additional $NaNO_3$ above the required stoichiometric amount was investigated by adding the same volume of $NaNO_3$ at higher concentrations.

To achieve that, sodium nitrate ACS reagent of ≥99.0% purity supplied by Sigma-Aldrich was prepared in three 500 ml volumetric flasks each containing different concentrations 3.0 M, 3.5 M, and 4.0 M. The experiments were conducted using 125 ml of 6.0 M alkali solution and 75 ml of 3.0 M, 3.5 M and 4.0 M $NaNO_3$ solution that were heated to 80°C and stirred at 1000 rpm.

From the results acquired from the tests, the optimum dissolution medium between NaOH and KOH, was chosen. After optimising the parameters in terms of concentration, temperature, stirring

rate and addition of $NaNO_3$ at different concentrations, they were implemented on the three different types of aluminium pieces used at UChem, and the reaction rates were determined.

3.3 UChem aluminium dissolution

The optimised dissolution parameters being sodium hydroxide at 6.0 M concentration in 3.0 M excess with the presence of 3.5 M $NaNO_3$ heated to 80°C and stirred at 1000 rpm were tested on UChem aluminium. The aluminium was supplied by UChem and were already sheared to square pieces with the dimensions shown in Table 3.1. The dissolution setup shown in figure 3.2 was used.

Table 3.1: UChem samples dimensions.

Sample ID	Length (cm)	Thickness (cm)	Width (cm)	Mass (g)
LP-COC-12/41	1.3	0.66	1.06	4.046
LP-COC-11/238	0.91	0.4	1.1	4.836
LP-COC-14/54	1.12	0.22	0.934	4.738

3.4 Dissolution of DU target plate

The test vessel for TP dissolution is shown in figure 3.2.

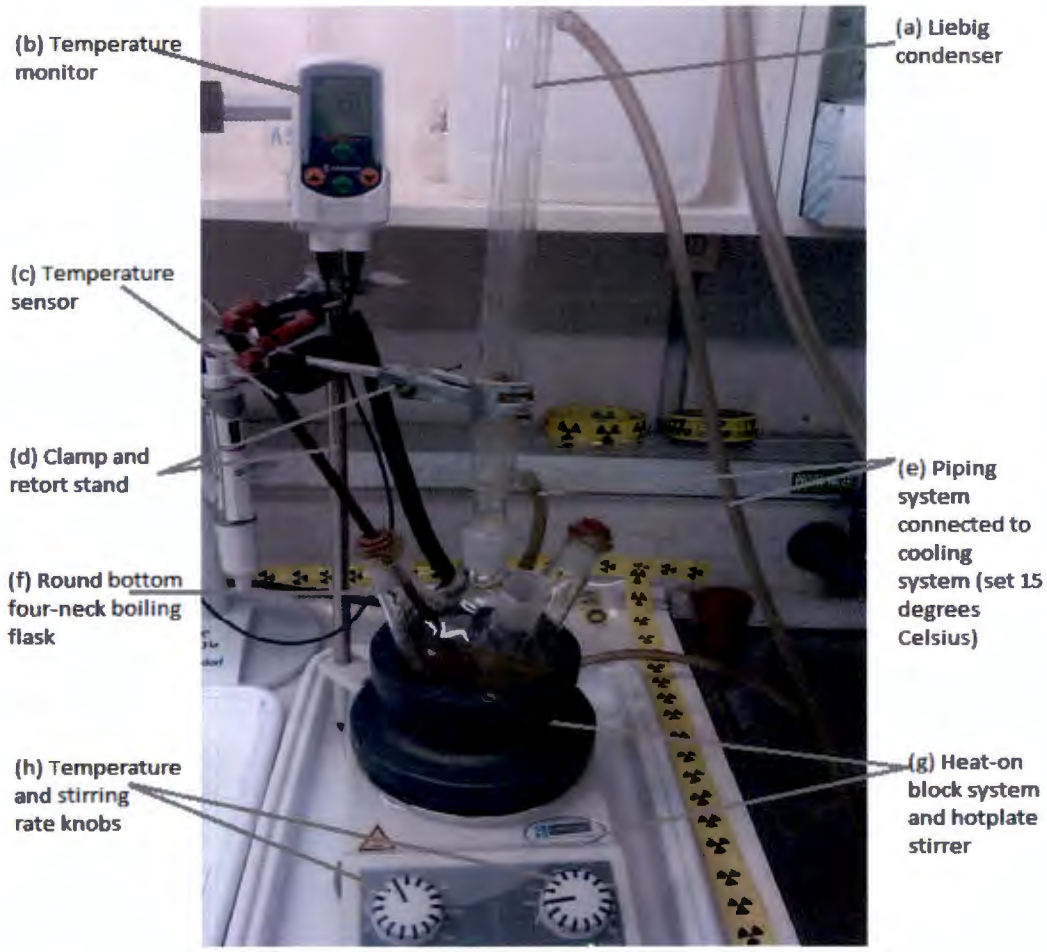

Figure 3.2: Dissolution setup used to conduct TP dissolution experiments in a radiation controlled environment

The optimised factors from section 3.1 and 3.2 were applied to dissolving TP pieces containing depleted uranium (DU). Two dissolution experiments were performed on the TP pieces, where each piece was about a quarter of the target. The pieces were further cut into rectangular pieces (figure 3.3) in order to fit through the neck of the boiling flask. The overall dimensions and chemical specifics are tabulated in Tables 3.2 and 3.3.

Figure 3.3: ¼ of TP that has been sheared further to smaller pieces.

The time for each reaction was recorded using a stop watch with the end point of the reaction noted by the absence of effervescence and lowered temperature shown by the temperature monitor.

Table 3.2: U/Al TP dimensions and volume content of Al and U.

TP dimensions	
Length	20 cm
Width	5 cm
Total thickness	1.585 cm
Typical TP	
Meat length	18 cm
Core alloy mass	24.8 g
Al mass in the core	15.8 g
Al mass in cladding	25.6 g
Total Al mass	41.3 g
Total plate mass	50.4 g
Volume specifications of TP	
Volume of TP	15.85 cm^3
Volume of meat	6.48 cm^3

Volume of cladding	9.37 cm^3
Volume of end pieces	1.585 cm^3
Volume of TP without end pieces	14.27 cm^3
Ratio of end piece to Al cladding	0.16916
Mass of U and Al in TP	
U in meat	9 g
Al in meat	16.1 g
Al in cladding	25.3 g
Al in end pieces	4.28 g
Al without end pieces	37.12 g
If TP without end pieces is divided into equal quarters	
Al in each piece	5.26 g
U in each piece	2.25 g
Total mass of each piece	7.51 g
Ratio of Al to total mass in each piece	0.7002

Table 3.3: TP pieces and end pieces showing calculated Al and U content.

	Piece 1 (g)	**Piece 2 (g)**	**Piece 3 (g)**	**Piece 4 (g)**	**Total (g)**
Al content	9.71	9.43	8.73	9.25	37.12
U content	2.35	2.29	2.12	2.24	9.00
Total mass of piece	12.07	11.72	10.84	11.49	46.12
Actual mass of piece	11.82	11.38	10.63	11.38	45.66
End piece masses (g)					
Piece 1	2.475				
Piece 2	2.104				

Calculations were made to compute the volume of NaOH solution needed to dissolve each U/Al piece. A volume of 119.9 ml of NaOH was poured into a four-necked flask, and when the solution reached 80°C, the first piece was dissolved. The second piece was dissolved with 73 ml of NaOH and 44 ml of 3.0 M $NaNO_3$ concentration were added to the reaction. After dissolving the TP, 20 ml samples of each solution were diluted to 100 ml, and these samples were taken to Pelindaba Analytical Laboratories (PAL) to analyse the solution using Inductive Coupled Plasma Optical Emission Spectrometry (ICP-OES) to detect how much aluminium had dissolved in each piece.

After dissolution, an attempt to filter the solution was made but the residues were too fine and would get lodged into the 541 and 1001-125 Whatman filter papers. Residue from previous

dissolutions that had been stored on site at Necsa was collected to conduct the rest of the experiments.

3.5 U residue dissolution

The residue from the dissolved U/Al TP was packaged and weighed to about 1.04 g for each vial (total of 4 vials) that were further dissolved in 150 ml HNO_3 (ACS grade (65%), supplied by Merck). The nitric acid concentrations used for residue dissolution were 1.0 M, 3.0 M and 6.0 M. The parameters tested were (a) temperature of the solution before dissolution and (b) different concentrations of HNO_3, the stirring rate was kept constant at 1000 rpm. Four dissolution runs were conducted as followed,

Run 1: 1.0321 g of the U/Al residue was dissolved in 150 ml of 3.0 M HNO_3 at 25°C

Run 2: 1.0431 g of the U/Al residue was dissolved in 150 ml of 3.0 M HNO_3 at 50°C

Run 3: 1.0494 g of the U/Al residue was dissolved in 150 ml of 6.0 M HNO_3 at 25°C

Run 4: 1.0402 g of the U/Al residue was dissolved in 150 ml of 1.0 M HNO_3 at 25°C

Completeness of dissolution was determined visually when no uranium residue could be observed in the dissolution flask. After dissolving, the residue, the solutions were left to cool and later the volume of the solutions were measured and placed in Kartell bottles for further analysis. The dissolution rate was determined using equation (25).

3.6 Solvent extraction and effect of Al on extraction

For solvent extraction, the optimised conditions in terms of concentration of extractant (30% TBP in Kerosene), concentration of stripping solution (0.5 M $(NH_4)_2CO_3$), organic: aqueous phase ratio (1:1) and acid concentration of the feed solution (3.0 M HNO_3) as stated by (Dixit et al., 2012, Stas et al., 2005 & Fourie et al., 2016)., were followed.

Five experiments were conducted with 30 ml of the 3.0 M HNO_3 uranium solution obtained during dissolution Run 1. From each of the 30 ml solutions, a 20 ml aliquot was mixed with 20 ml of 30% TBP in kerosene (97% supplied by Sigma-Aldrich of ACS (analytical grade)) and transferred into 50 ml falcon tubes. Different amounts of $Al(NO_3)_3{\cdot}9H_2O$ (ACS reagent (>98%) supplied by Fluka) were added to the uranium solution to observe if Al had any influence on the recovery and purification of uranium. From each of the 30 ml solvent extraction (SX) solutions, 10 ml was kept for pre-extraction analysis to determine the concentration of uranium.

SX Run 1 was the control test where only 20 ml of uranium solution and 20 ml of 30% TBP in kerosene were contacted.

SX Run 2, was conducted using 20 ml of uranium solution with 1.25% m Al/ m U and 20 ml of 30% TBP in kerosene.

SX Run 3, was conducted using 20 ml of uranium solution with 6.02% m Al/ m U and 20 ml of 30% TBP in kerosene.
SX Run 4, was conducted using 20 ml of uranium solution with 12.38% m Al/ m U and 20 ml of 30% TBP in kerosene.
SX Run 5, was conducted using 20 ml of uranium solution with 18.09% m Al/ m U and 20 ml of 30% TBP in kerosene.

For each of the SX runs, the solutions were shaken with the aid of a rotating shaker for 15 minutes at 7 rpm. After the 15 minutes had elapsed, the solutions were transferred into separatory funnels (figure 3.4) and left to settle for about an hour.

Figure 3.4: Organic phase and aqueous (uranium solution) phase in separatory funnels settling after being contacted with one another.

After settling, the aqueous and the organic phases were separated and the organic phase kept separate for further use. 5 ml of the aqueous phase was pipetted out and kept aside for analysis.

3.6.1 Optimising $(NH_4)_2CO_3$ concentration for uranium stripping

The organic phases that were kept separate (20 ml) were further contacted with 20 ml of stripping agent, $(NH_4)_2CO_3$ (supplied by Sigma-Aldrich of ACS (analytical) grade) of 0.5 M concentration and shaken on the rotating shaker (figure 3.5) for 15 minutes at 7 rpm using a Stuart Rotator (model SB3).

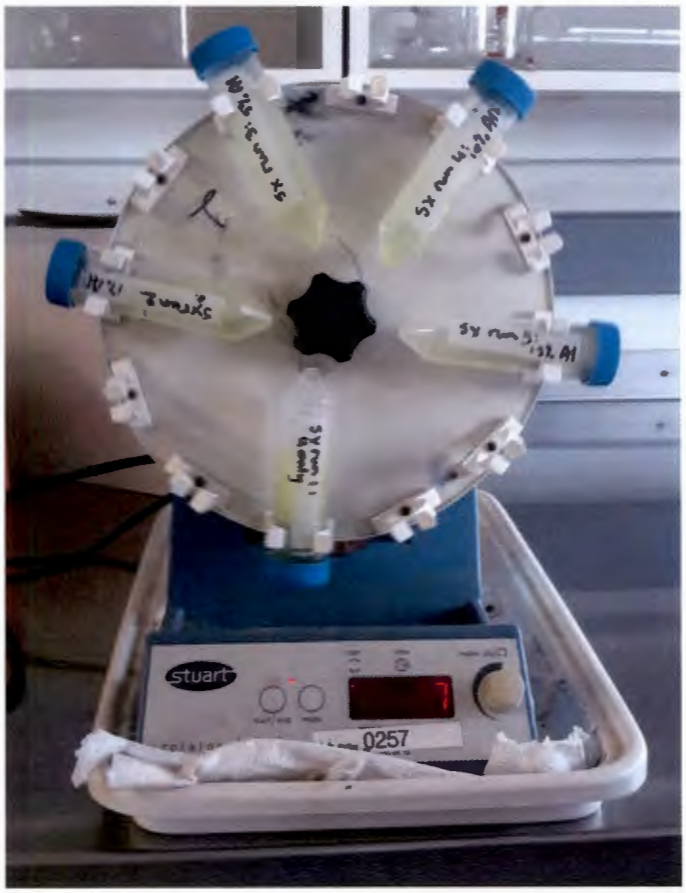

Figure 3.5: Process of stripping uranium from organic phase using 0.5 M $(NH_4)_2CO_3$.

After rotating them, the solutions were poured into separatory funnels and left to settle in order to fully separate the phases. The organic and aqueous phases were separated, with 15 ml (5 ml used for analysis) of the aqueous kept separate whilst the organic would be utilized for uranium strip using 1.0 M $(NH_4)_2CO_3$. The same procedure for stripping uranium with 0.5 M was used for stripping with 1.0 M ammonium carbonate.

To calculate the percentage extraction of uranium from the feed, equation (27) and (28) were used.

$$D_{extraction} = \frac{[U]_{organic}}{[U]_{aqueous\ feed}} \quad (27)$$

where $D_{extraction}$ is defined as the ratio of uranium concentration in organic phase over concentration in aqueous phase

$[U]_{organic}$ is the concentration of uranium in the organic phase (mol/L)

$[U]_{aqueous\ feed}$ is the concentration of uranium in the aqueous feed (mol/L)

Equation (27) was used to further calculate the percentage extraction,

$$\%E_U = \frac{D_{extraction}}{D_{extraction} + \frac{V_{aqueous}}{V_{organic}}} \quad (28)$$

where $\%E_u$ is the percentage extraction (indicating how much uranium was extracted from the organic phase)

$D_{extraction}$ is defined as the ratio of uranium concentration in organic phase over concentration in the aqueous phase

$V_{aqueous}$ is defined as volume of the aqueous feed (ml)

$V_{organic}$ is defined as volume of the organic phase (ml)

To determine the mass of uranium in the organic phase before conducting the second strip, calculated by using equation (29)

$$U_{org\ s2} = U_{org\ s1} - U_{aq\ s1} \quad (29)$$

Where $U_{org\ s2}$ is uranium mass in organic phase before the second strip (mg)

$U_{org\ s1}$ is uranium mass in organic phase before first strip (mg)

$U_{aq\ s1}$ is uranium mass in aqueous phase after first strip (mg)

3.7 Ion exchange as alternative method for U purification

3.7.1 Determination of distribution coefficients

This purpose of this experiment was to determine the distribution coefficient (K_D-values of uranium on various ion exchange resins identified as possible candidates for U purification in nitric acid solution. The three chosen resins were a cation exchange resin BioRad AG50W-X4, and two chelating resins, Amberlite IRC747, and Amberlite IRC 748. The distribution coefficient or K_D of a chemical species A on an ion exchanger describes the distribution of the species between the solution and the solid exchanger; therefore, $K_D = ([A]_{exchanger} / [A]_{solution})$; measured in ml/g, and calculated using equation (30):

$$K_D = \frac{concentration\ before - concentration\ after}{concentration\ after} \times \frac{solution\ volume\ (ml)}{dry\ mass\ of\ ion\ exchanger(g)} \quad (30)$$

It represents the theoretical volume of solution containing these species that can be processed per mass of exchanger under equilibrium conditions. It is very useful as a screening method to compare the capability of different ion exchangers to remove a specific species from a specific solution medium, since it describes in essence the affinity of an ion exchanger for a species under the particular experimental conditions such as pH, ionic strength and temperature.

The resins are stored moist in their containers, therefore, 1 g portions were weighed out in poly-top containers and left to dry in an oven overnight at 100°C, to determine the equivalent dry mass. Dry masses of resins Amberlite IRC747, Amberlite IRC748 and AG50W-X4, were 0.3783 g, 0.4173 g,

and 0.4477 g per g wet resin, respectively. To make up the feed solution for the distribution coefficient determination, 10 ml of the U solution from Run 5 (in 1.0 M HNO_3), were diluted 100 ml with demin water. This was done to increase the pH of the solution from 0 to 1. To obtain a solution with 5% Al(m/m U), 0.0172 g $Al(NO_3)_3 \cdot 9H_2O$ was added to 50 ml of the diluted solution, to determine the influence Al has on the K_D of U on the resins. Aliquots of 10 ml from the 50 ml solution were dispensed in centrifuge tubes that had weighed portions (0.1679 g AG50W-X4, 0.1855 g Amberlite IRC747 and 0.1575 g Amberlite IRC748 wet mass) of the ion exchangers. This is equivalent to 0.0752 g AG50W-X4, 0.0702 g Amberlite IRC747 and 0.0657 g Amberlite IRC748 dry mass. The mixtures were rotated (figure 3.6) for about 12 hours at 15 rpm. Calculations indicated that there would be 26 mg U in each 10ml solution.

Figure 3.6: Uranium solution contacted with three resins to determine the distribution efficiency of each.

From each vial, 9 ml aliquots of the supernatant were filtered through a 0.22 μm syringe filter that would be analysed. From the filtered solutions, the following aliquots were used for U analysis: 8

ml from each of the AG50W-X4 and Amberlite IRC747 solutions, and 7 ml from the Amberlite IRC748 solution. The distribution coefficient K_D, was calculated using equation (30).

From the obtained results from recovering uranium using two chelating resins and a cation exchanger, Amberlite IRC747 produced better results when compared to Amberlite748 and BioRad AG50W-X4. Amberlite IRC747 was further used to determine uranium recovery and purification from the feed solution.

3.7.2 Column experiment on Amberlite IRC747

A glass column with a plastic stopcock was used, with glass wool sandwiching the Amberlite IRC747 resin at the top and bottom to keep the resin bed stable (figure 3.7). The resin was poured into the column as a slurry in demineralized water and allowed to settle. The final column dimensions were a height of 70 mm and 20 mm diameter. The column was equilibrated with 0.1 M HNO_3 prior to doing the uranium run, to convert the resin from the supplied Na^+ form to the H^+ form.

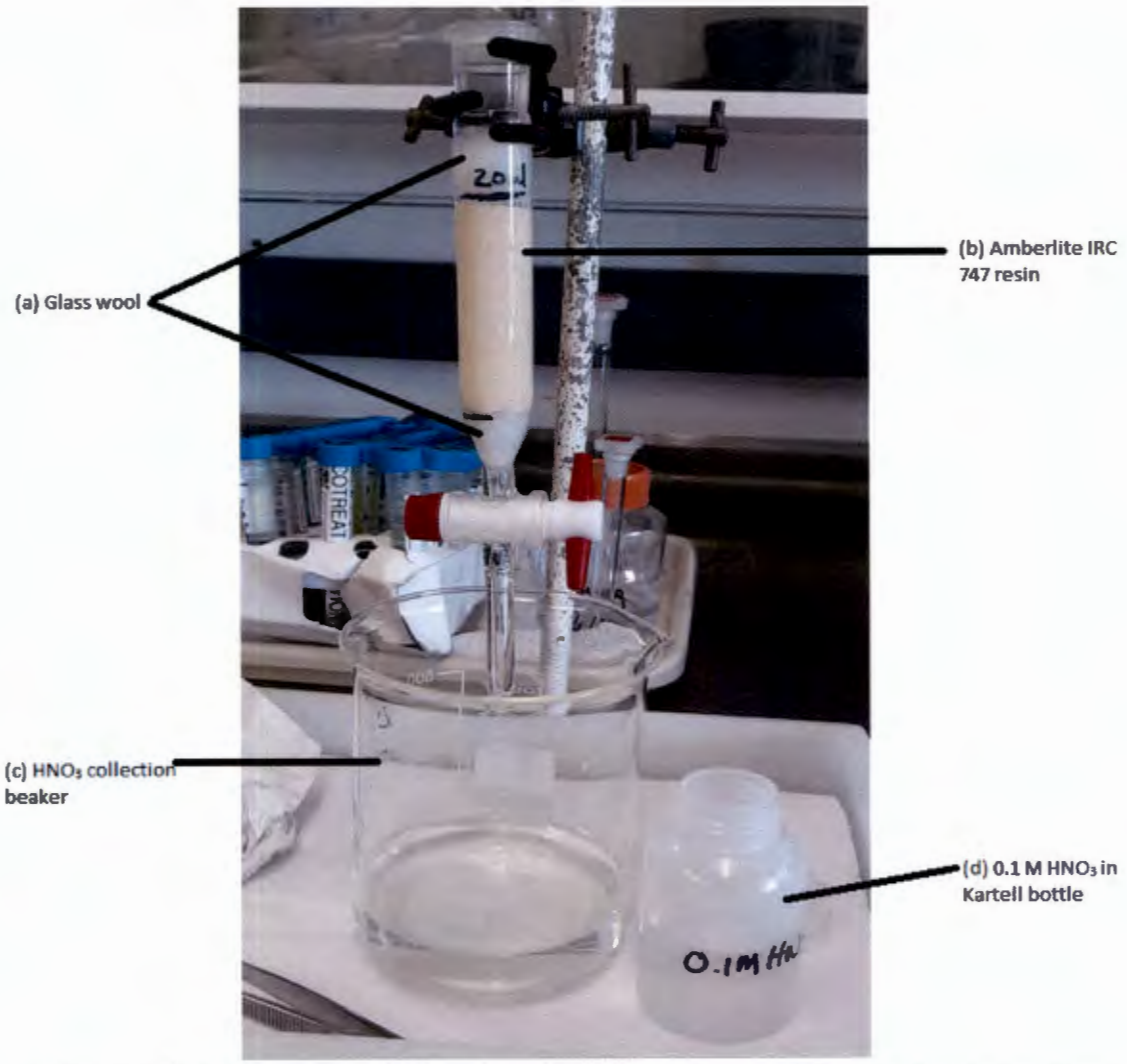

Figure 3.7: Amberlite IRC747 resin column setup prepared for uranium extraction.

To make up the feed solution for the column experiment, 130 ml of the U solution from Run 5 (in 1.0 M HNO_3), were diluted 1300 ml with demin water, to obtain a solution with 0.1 M HNO_3 (pH 1). To obtain a solution with 5% Al (m/m U), 0.045 g $Al(NO_3)_3 \cdot 9H_2O$ was added to the diluted solution, to determine if Al can be separated from U on the column. An aliquot of 20 ml was kept separate for U and Al analysis, and a total volume of 1252 ml of this solution was fed through the column, adding 20 ml of the feed as soon as the solution would just be above the top glass wool. The eluate from the column during the feed, was collected in 200 ml fractions in Kartell bottles. The beads changed from beige to a deep orange/rust colour, therefore confirming the sorption of uranium from the feed solution onto the resin beads (figure 3.8).

After the feed, the column was washed with 100 ml 2.0 M NaOH, and the uranium was thereafter eluted using 100 ml of a 1.0 M $(NH_4)_2CO_3$ solution with 30 % H_2O_2 in an 85:15 volume ratio. Each of these solutions was collected in separate 100 ml fractions in Kartell bottles. The reason for doing a NaOH wash before the carbonate elution, is to neutralize and wash the acid from the column before contacting with carbonate, to avoid formation of CO_2 gas during neutralization of HNO_3 with $(NH_4)_2CO_3$, which would cause gas bubbles to form and lead to break-up of the resin bed.

Figure 3.8: Uranyl ions adhering to the cation exchange beads.

3.8 Analysis of U solutions using UV/Vis carbonate method for U analysis

For analysis of U in solution, a UV/Vis spectrophotometric method was used. This method is based on the intensely coloured complex of uranium with peroxide in an alkaline carbonate medium. It is suitable for samples in the U concentration range 20–200 ppm, when diluted to 25 ml. The method has been investigated and utilized during the Manhattan project (Rodden, 1950), and also in the past at Necsa (Huyser et al., 1986). Prior to analyzing all the U solutions, a uranium standard of 1000 ppm (uranium atomic absorption standard solution, 1000 ppm in 1.2 wt% HNO_3) was used to prepare a calibration curve for the UV/Vis spectrometer. The linear curve (figure 3.9) was constructed with 50, 100, 150, and 200 ppm uranium standard. For 50, 100, 150, and 200 ppm, 1.25, 2.5, 3.75, and 5 ml of the standard was pipetted into 25 ml volumetric flasks respectively, 3 ml of 2.0 M Na_2CO_3 (chemically pure, anhydrous (>98%) supplied by Merck) and 1 ml of H_2O_2 (GR for analysis (30%) supplied by Merck) added, and further made up to the mark with demineralised water. The absorbance for each standard was measured against a reagent blank at 450 nm using a PerkinElmer Lambda 1050 UV/Vis spectrophotometer. The calibration curve is shown in figure 3.9. Aliquots of uranium solutions to be analysed, were mixed with 3 ml of 2.0 M Na_2CO_3 (with addition of a calculated volume of 2.0 M Na_2CO_3 required to neutralize acidic solutions) and 1 ml H_2O_2, and analysed at 450 nm.

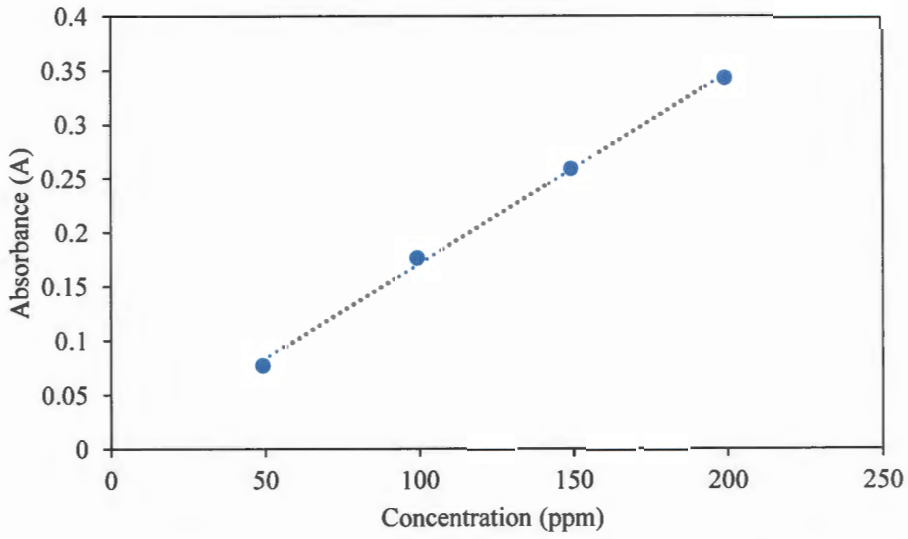

Figure 3.9: Calibration curve for uranium using 1000 ppm standard.

Chapter 4: Results and discussion

4.1 Alkali media

4.1.1 Optimising effective alkali media

In order to find the most effective alkaline solution to be used later in the dissolution process of UChem aluminium samples and thereafter a TP, optimisation of alkali media concentration to dissolve commercial aluminium using NaOH and KOH at stoichiometric 6.0 M solution, 1.5 M excess and 3.0 M excess alkali were conducted.

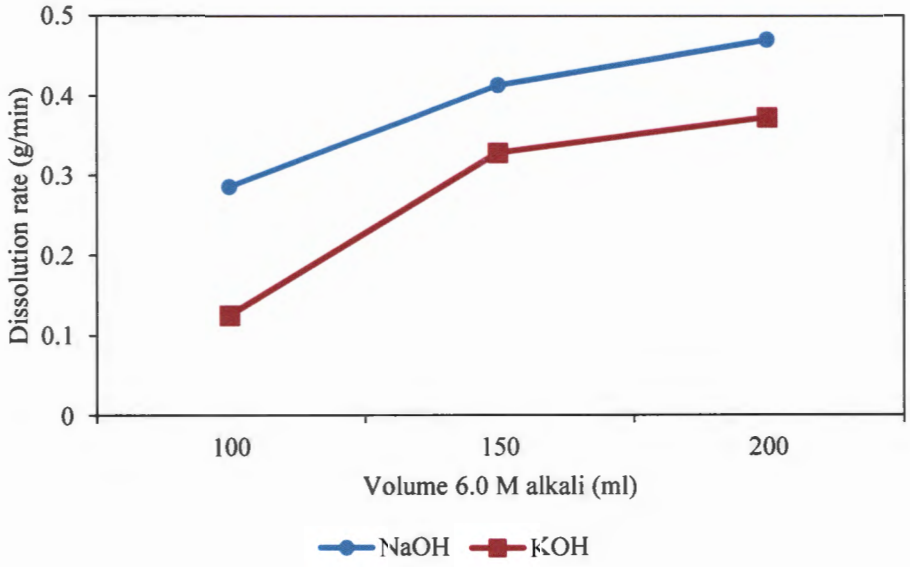

Figure 4.1: The dissolution rate of commercial Al at varying 6.0 M alkali volumes (100 ml = stoichiometric amount; 150 ml = 1.5 M excess; 200 ml = 3.0 M excess)

Figure 4.1 shows the dissolution rate of the commercial Al with a stoichiometric volume of 6.0 M alkali (100 ml), 50 ml excess volume representing 1.5 M excess, and 100 ml excess volume representing 3.0 M excess, at 80°C and stirred at a rate of 1000 rpm. For both alkali's, dissolution of commercial Al was fastest when 100 ml excess 6.0 M NaOH volume representing 3.0 M excess was used, with a dissolution rate of 0.470 and 0.373 g/min for NaOH and KOH, respectively. NaOH had consistently higher rates of dissolution than KOH.

The optimized volume of 6.0 M alkali, that is 200 ml per 16.2 g Al samples (representing a 3.0 M excess amount of alkali, above the stoichiometric amount required to dissolve the 16.2 g mass of Al), was thereafter used for optimization of the other dissolution parameters.

It was also observed in these experiments that during dissolution of commercial Al with the calculated stoichiometric volume, the reaction would reach super-saturation leading to re-precipitation of Al over time. Therefore, excess alkali was determined to be a requirement for both a

fast dissolution rate, and to avoid super-saturation leading to re-precipitation occurring soon after dissolution. This is supported by McFarlane et al. (2014), stating that factors that influence dissolution of aluminium include pH, Eh, solvated species in the aqueous phase, temperature and inadequate caustic solution (McFarlane et al., 2014). Wymer et al. (1955) have revealed that upon aging, solids will precipitate. Conversely, the sodium aluminate is a metastable compound and will therefore remain in solution for about 4.2 days in a 1.5 to two-fold excess of the caustic solution. After that period of time, the aluminate compound will ultimately convert to an insoluble aluminium oxide, that when examined by XRD it is revealed – depending on temperature of the solution and minor chemicals included in the aluminium - to be gibbsite, bohemite (Gong et al., 2003; Ruff et al., 2008) or bayerite (Taylor-Pashow & Hobbs, 2012).

4.2 Optimising dissolution parameters in NaOH and KOH

4.2.1 Stirring rate

4.2.1.1 Effect of stirring rate on dissolution rate

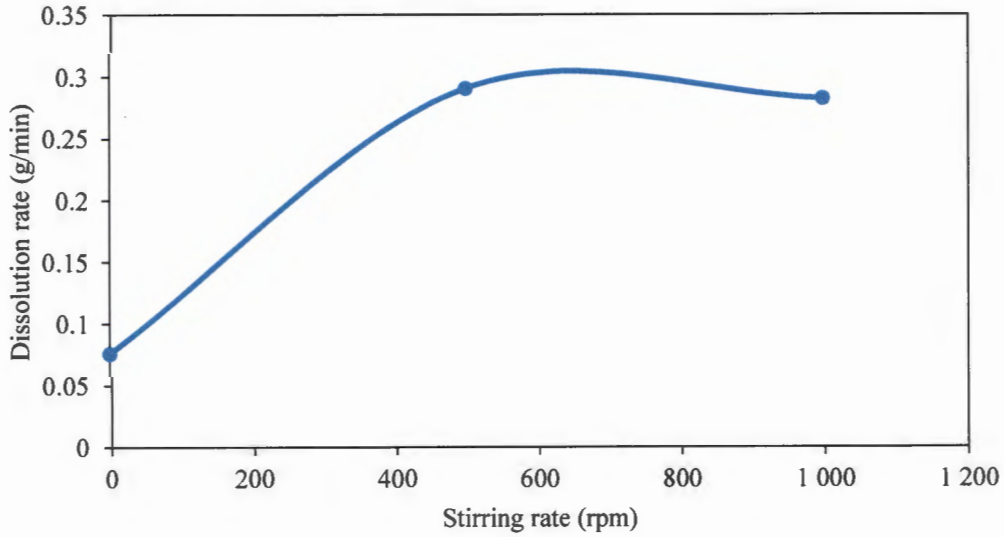

Figure 4.2: The effect of stirring rate on the dissolution rate of Al in NaOH with 3.0 M excess.

Stirring is one of the traditional methods of increasing the rate of the reaction. As shown in figure 4.2, there was an increase in the rate of dissolution as the solution was stirred at a rate of 500 rpm as compared to when there was no stirring. Increasing the stirring rate further has a faintly negative effect on the rate of dissolution, with a slight decrease in the dissolution rate. This decrease is minute enough to consider that a human error in recording the time to complete dissolution may have led to the results shown in figure 4.2. If KOH is used instead of NaOH, the same trend is observed (figure 4.3), with the only difference being sharper drop in dissolution rate as the stirring is increased from 500 to 1000 rpm.

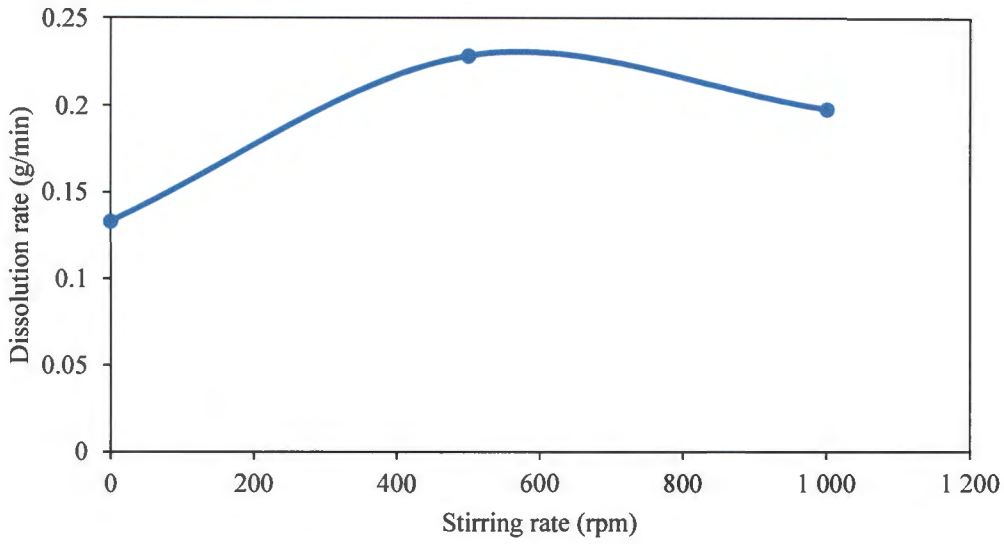

Figure 4.3: The effect of stirring rate on the dissolution rate of Al in KOH with 3.0 M excess.

4.2.1.2 Effect of stirring rate on re-precipitation

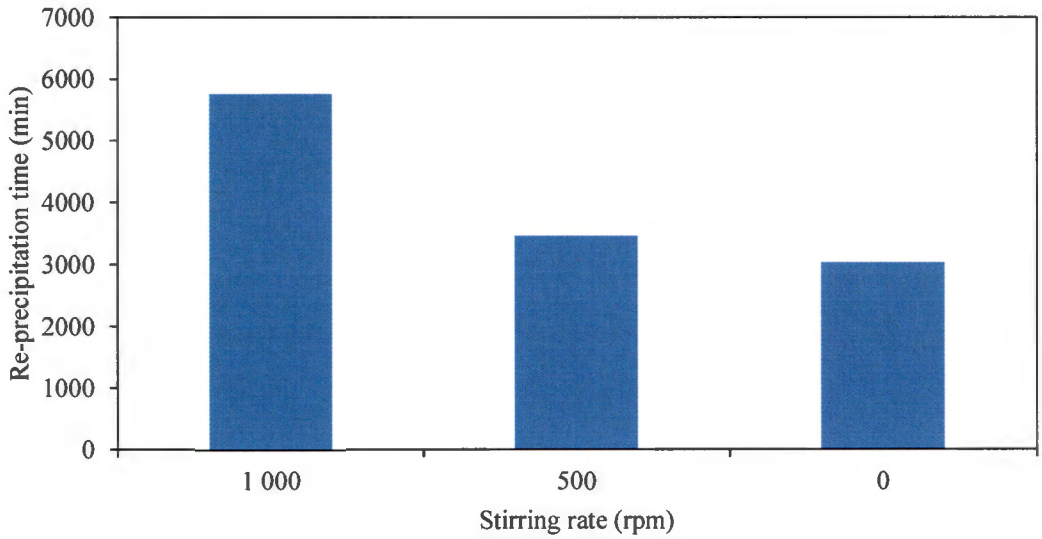

Figure 4.4: The effect of stirring rate on the time taken for NaOH solution with 3.0 M excess to start re-precipitation.

Another parameter tested in optimizing the dissolution of aluminium was the re-precipitation of the solution after implementing the stirring rate of both alkali solutions. The trend observed shows that re-precipitation time of NaOH solution (figure 4.4) increases with the increase of the stirring rate. The limiting factor to not increasing the stirring further was that there was a slight decrease in the dissolution rate when surpassing 1000 rpm. The contrast to NaOH, KOH (figure 4.5) experiences a slight decrease in the time it takes to re-precipitate when increasing the stirring rate from 500 rpm to 1000 rpm. The maximum time it took for KOH solution to re-precipitate was still less (5472 minutes) than that of NaOH (5760 minutes)

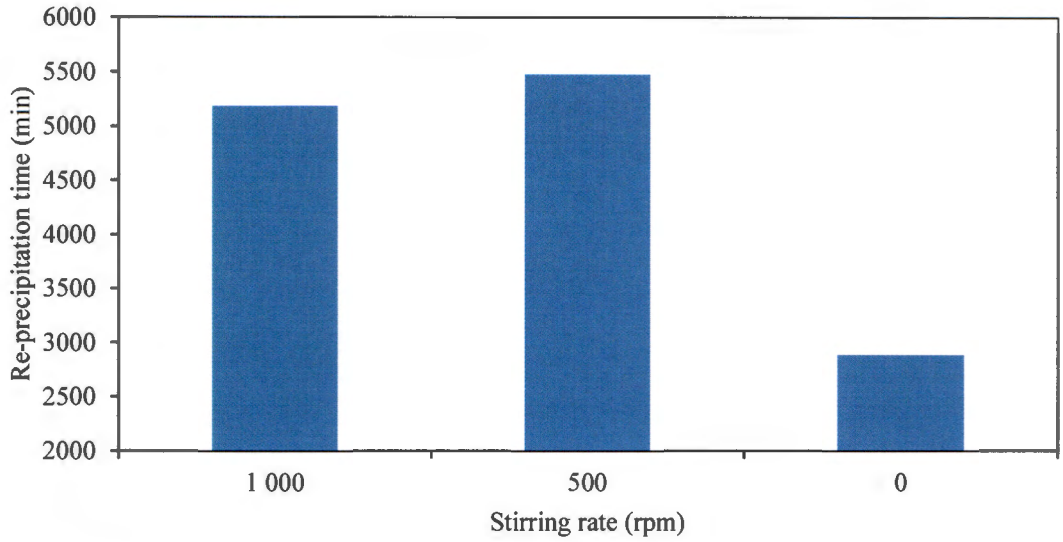

Figure 4.5: The effect of stirring rate on re-precipitation time of KOH solution with 3.0 M excess.

4.2.1.3 Summary

In terms of dissolution rate with NaOH, there is a 2% difference between using the stirring rate of 1000 rpm and 500 rpm. When looking at the time it takes for the solution to re-precipitate at 1000 rpm, it was 40% higher than that at 500 rpm. Therefore, the optimized stirring rate for NaOH was determined to be 1000 rpm. With KOH, a higher dissolution rate and re-precipitation time was observed when stirring the solution at 500 rpm, but even with that, when comparing the re-precipitation time of KOH with NaOH, KOH solution was still lagging behind.

4.2.2 Temperature

4.2.2.1 Effect of temperature of dissolution rate

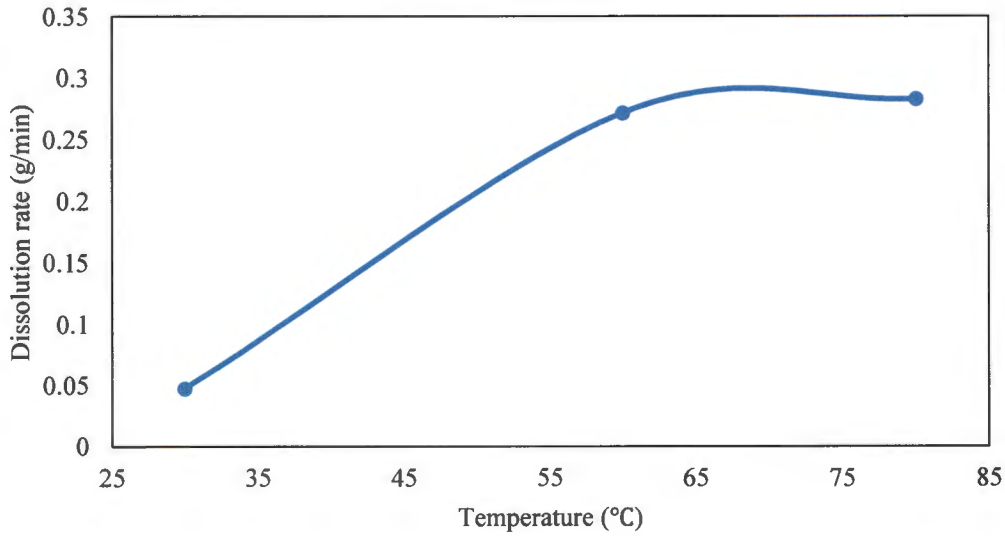

Figure 4.6: The effect of temperature on the dissolution rate of Al in NaOH solution with 3.0 M excess.

Figure 4.6 and figure 4.7 show the effect of temperature on the dissolution rate of Al in NaOH and KOH solutions, respectively. When the solvent is NaOH, the rate of increase in dissolution rate as the temperature is increased from 30 to 60°C is very dramatic, increasing more than five-fold. The increase in the dissolution rate is less pronounced as the temperature is increased from 60 to 80°C. However, with KOH, the increase in dissolution rate is less pronounced as the temperature is increased from 25 to 80°C, but it is more sustained compared to NaOH. Using NaOH, a higher dissolution rate is attainable, with a dissolution rate of about 0.27 g/min at 30°C while with KOH the rate is below 0.20 g/min even at temperatures above 80°C.

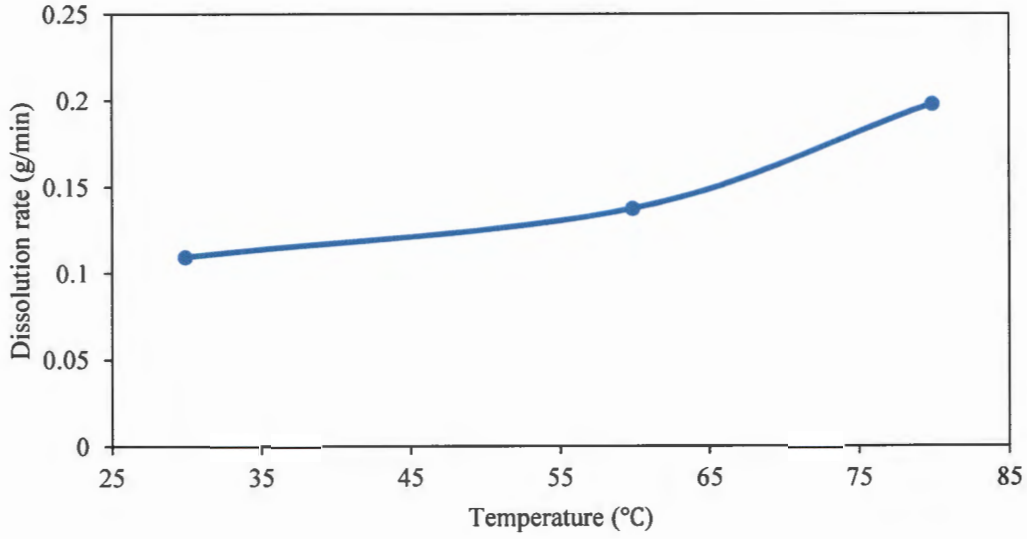

Figure 4.7: The effect of temperature on the dissolution rate of Al in KOH solution with 3.0 M excess.

4.2.2.2 Summary

When dissolving aluminium, the best temperature to conduct the experiment is at 80°C for both alkaline solutions, because at any temperature below 80°C there is a decrease in dissolution rate. Alternatively, dissolving aluminium in NaOH may be conducted at 60°C when considering the costs of increasing the temperature of the solution on an industrial scale because the difference in the dissolution rate between 60 and 80°C is negligible.

4.2.3 The effect of different concentrations of $NaNO_3$

4.2.3.1 Effect of $NaNO_3$ on dissolution rate

The reason for adding sodium nitrate to the reaction is that it reduces the production of hydrogen gas (Foster, 1955) that a flammable gas with the ability to cause explosive accidents when not properly handled. Hydrogen gas is also odourless and colourless, therefore detection would be problematic (Cadwallader & Herring, 2007).

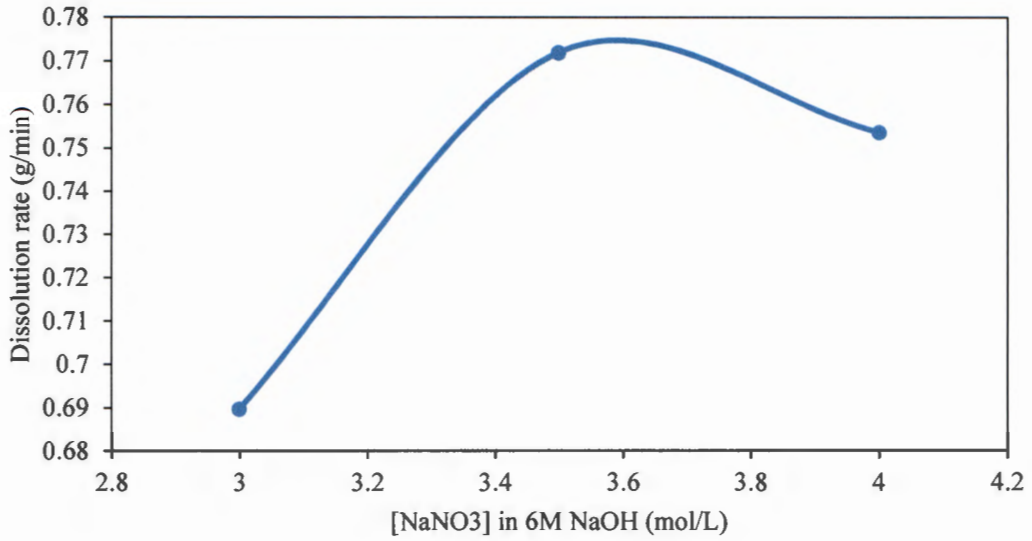

Figure 4.8: Effect of $NaNO_3$ concentration on Al dissolution rate using NaOH as a solvent.

The effect of adding $NaNO_3$ in the dissolution of Al using NaOH in 3.0 M excess was studied by adding three different concentrations of $NaNO_3$, 3.0, 3.5 and 4.0 M. As seen in figure 4.8 the rate of the dissolution increases as the concentration of $NaNO_3$ is increased from 3.0 M to 3.5 M. A further increase in concentration to 4.0 M leads to the dissolution rate decreasing. However, as observed in figure 4.9, with KOH in 3.0 M excess the dissolution rate increases as the amount of $NaNO_3$ added increases. The optimum $NaNO_3$ concentration to be used with KOH could not be determined in this study as the trend was a linear relationship between the KOH added and the dissolution rate.

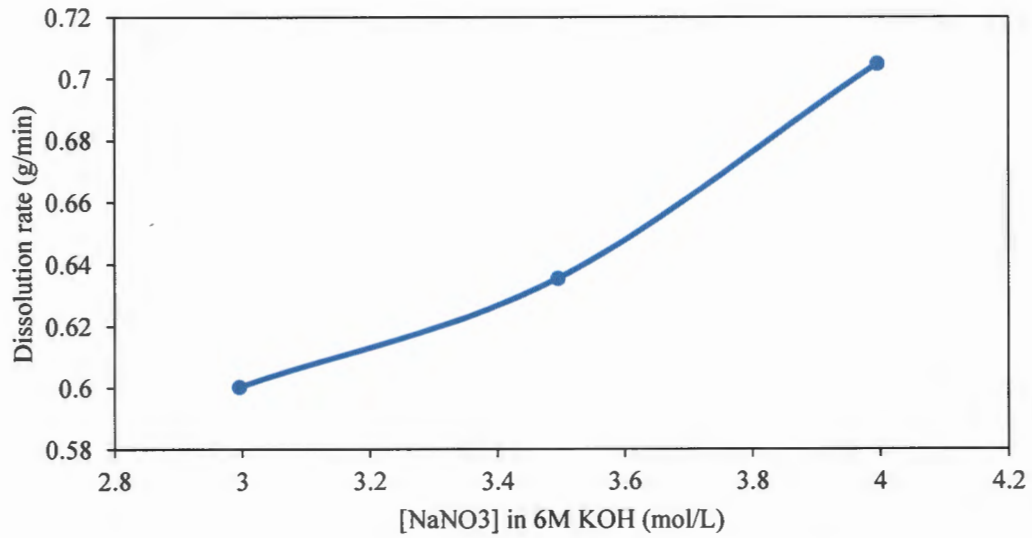

Figure 4.9: Effect of $NaNO_3$ concentration on Al dissolution rate using KOH in 3.0 M excess as a solvent.

4.2.3.2 Effect of $NaNO_3$ on re-precipitation rate

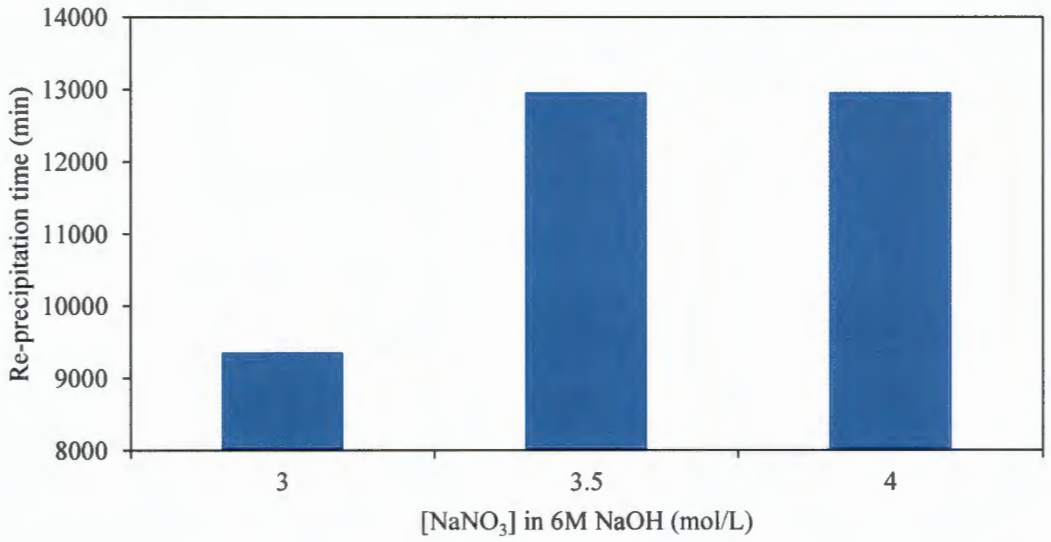

Figure 4.10: The effect of $NaNO_3$ at different concentrations on the re-precipitation rate of Al in NaOH in 3.0 M excess.

Figure 4.10 shows a dramatic increase in the re-precipitation time of Al in NaOH when increasing the concentration of sodium nitrate from 3.0 M to 3.5 M, but at concentrations higher than 3.5 M the trend stabilises. In figure 4.11, the results revealed that the addition of $NaNO_3$ significantly increases the re-precipitation time also in KOH, however showing a steady increase with the amount of sodium nitrate added to the solution. The optimum concentration of $NaNO_3$ with KOH could not be determined as it is an increasing linear trend. Therefore, the conclusion made for this parameter is that, although KOH showed an increasing trend, the highest re-precipitation time at a higher concentration of $NaNO_3$ being 10080 minutes, NaOH still has a higher re-precipitation time with both 3.5 M and 4.0 M $NaNO_3$.

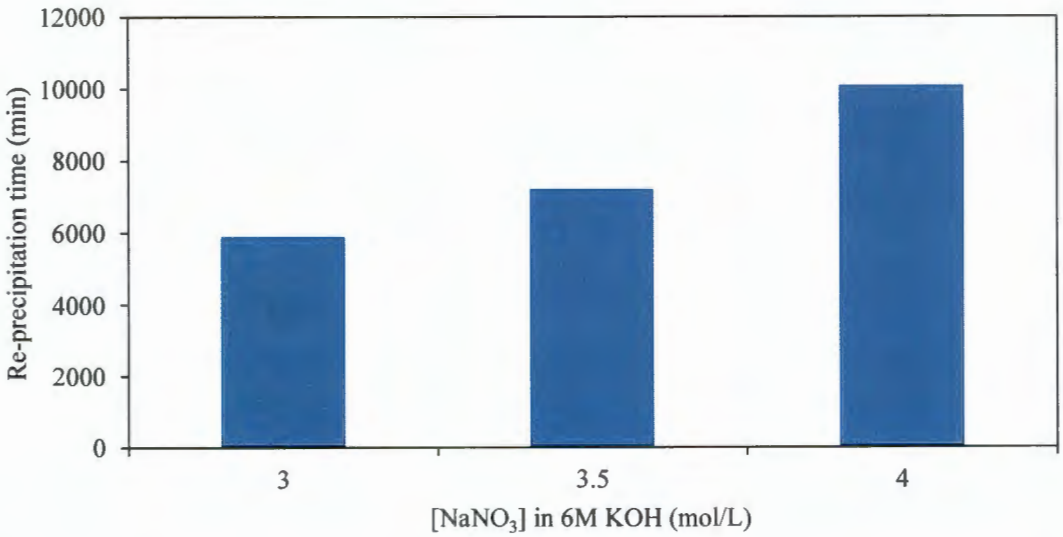

Figure 4.11: The effect of NaNO3 at different concentration on re-precipitation time.

4.2.3.3 Summary

Not only was the addition of sodium nitrate to the dissolution of aluminium in both alkali media beneficial in terms of reducing the production of hydrogen gas, it also increased the dissolution rate. Dissolving aluminium in sodium hydroxide in the presence of $NaNO_3$ increased the dissolution rate by over five-fold, with the dissolution rate of KOH increasing by over seven-fold. This method saves time on dissolving aluminium targets in an industrial setting. Another advantage of adding $NaNO_3$ in both alkali media is that it increases the time it takes for the solutions to re-precipitate to insoluble aluminum oxides.

4.2.4 Conclusion

From section 4.1, it was determined, that NaOH was the best alkali solution for the dissolution of aluminium. After conducting experiments to optimise parameters for the dissolution of aluminium, sodium hydroxide by addition of 6.0 M with an excess of 3.0 M, with temperature set to 80°C, with stirring of the solution at 1000 rpm and adding sodium nitrate with concentration of 3.5 M produced the best results. By implementing the aforementioned parameters, aluminium took a longer period to re-precipitate, therefore ensuring sufficient time for further processing of the solution.

4.3 UChem aluminium dissolution

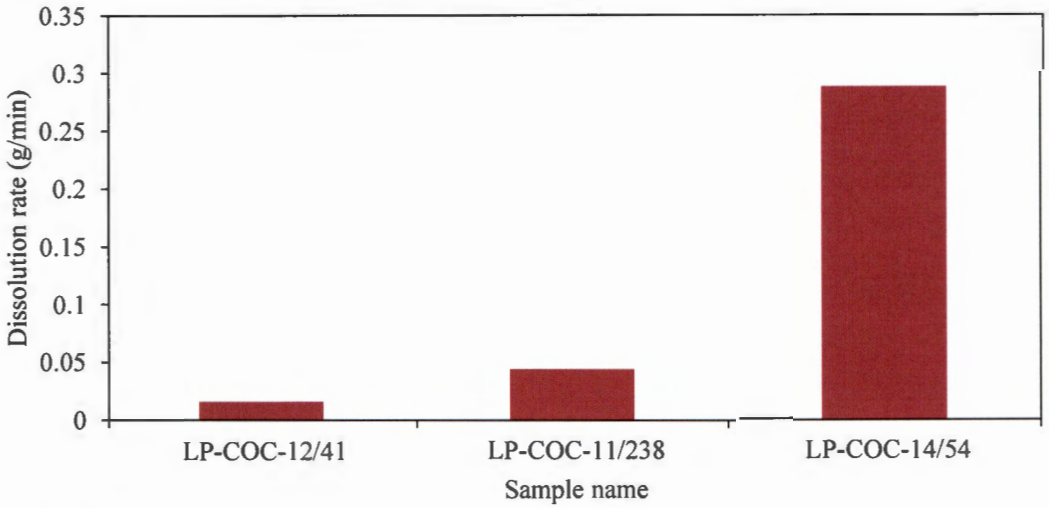

Figure 4.12: The effect of dissolving UChem aluminium in 6.0 M NaOH plus 3.0 M excess with 3.5 M $NaNO_3$ and without $NaNO_3$.

After optimising all the relevant parameters to be implemented on UChem aluminium samples, figure 4.12 evidently shows that the optimum factors were not matched for samples LP-COC-12/41 and LP-COC-11/238 in terms of the dissolution rate. The aforementioned samples experience dissolution rate of 0.0159 and 0.0443 g/min, respectively. However, LP-COC-14/54 did perform

just over the expected dissolution rate of 0.2822 g/min that was observed when dissolving pure aluminium in the optimised parameters, the dissolution rate was recorded at 0.2889 g/min. Therefore, aluminium sample LP-COC-14/54 confirmed the optimised dissolution parameters. The reason why the LP-COC-12/41 and LP-COC-11/238 samples dissolved so much faster, cannot be ascertained without further investigations, but unfortunately, only a very limited amount of this material was available.

The method followed at UChem is the KOH dissolution route, and it has not been optimised in terms of alkali dissolution of the TP for the recovery of uranium in them. UChem also does not use sodium nitrate to facilitate the dissolution. When comparing the method implemented by UChem to the optimised parameters that follow $NaOH/NaNO_3$ in this study, the results show an improvement to the existing dissolution process.

4.4 Testing optimized parameters on dissolution of aluminium containing DU

After demonstrating the effectiveness of the optimized parameters from sections 4.1 and 4.2, dissolution studies were conducted on a TP that had been sheared into rectangular pieces. Two tests were conducted with NaOH + 3.0 M excess only and another with NaOH plus 3.0 M and 3.0 M $NaNO_3$. The TP pieces weighed 11.5963 and 11.1596 g, respectively.

Table4.1: Target plate aluminium content and dissolution percentages in NaOH.

Mass of TP (g)	$[NaNO_3]$	Total Al in piece (mg)	Concentration of Al in solution (mg/L)	Mass of Al in solution (mg)	Percentage Al dissolved (%)
11.5963	0	9710	16064	9638.4	99.26
11.1596	3.0	9430	5367	3139.695	33.29

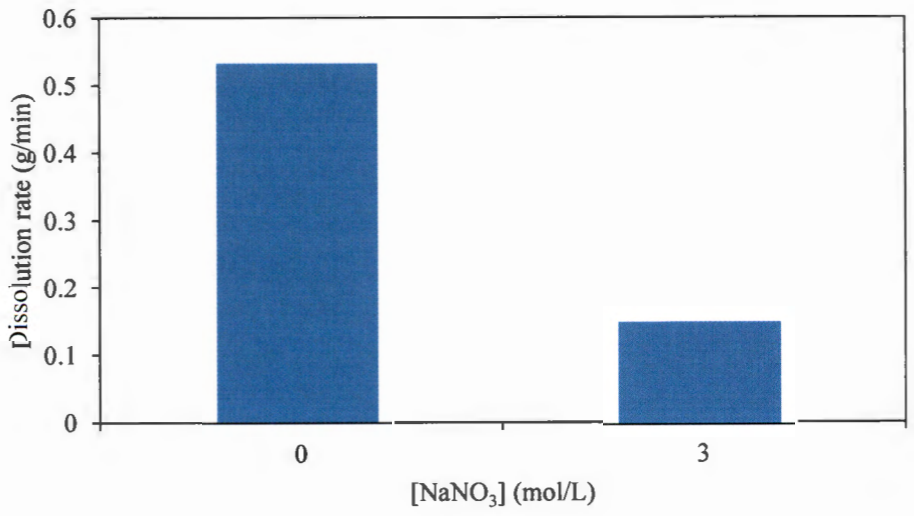

Figure 4.13: Effect of sodium nitrate on the dissolution rate of TP pieces.

Figure 4.13 shows that there is a huge difference in the reaction rate between the solution without sodium nitrate and that with sodium nitrate. The decrease in dissolution rate from only using NaOH (0.5328 g/min) and using NaOH/$NaNO_3$ (0.1488 g/min) is evident.

4.4.1 Summary

ICP-OES obtained results showed that the dissolution of the first piece of the TP was successful. A concentration of 16064 mg/L was detected in the solution, which amounted to 99.26% dissolution of aluminium. This substantiates that NaOH is a good dissolving agent for aluminium. The second piece was dissolved in the optimum concentration of sodium hydroxide with the addition of sodium nitrate. When dissolving the TP with sodium hydroxide coupled with 3.0 M sodium nitrate, the dissolution rate drastically decreased by over three-fold. Only 33.29% of the total 9430 mg Al in the piece dissolved, this method is not as efficient as using sodium hydroxide on its own as a solvent.

The revelation in figure 4.13 is in conflict with the results previously reported from sections 4.1 and 4.2 that the addition of sodium nitrate to the reaction had a positive impact on the dissolution rate. These results can be explained by the fact the target plate is made from alloyed aluminium that contains uranium. The uranium may be a factor in the decrease in dissolution rate. Another possible explanation is that re-precipitation of aluminium has started in the solutions prior to analysis at PAL, due to the long waiting times for these analyses, even though the samples were diluted with a factor of five in an attempt to prevent this re-precipitation over time. If that is the reason, although the dissolution efficiency of aluminium in the TP dissolved with addition of $NaNO_3$ may not have been as low as indicated by the analysis result, extensive re-precipitation is still a negative for dissolution with addition of $NaNO_3$. Nevertheless, the use of sodium nitrate in caustic dissolution of aluminium does prevent the production of hydrogen gas.

4.5 Uranium dissolution and analysis

The residue used in these experiments was obtained by dissolving the unirradiated U/Al target plates using an alkaline based method.

Due to the inefficiency of filtering the residue after dissolution, the residues from TPs that were previously dissolved in NaOH (from 10/04/2014) were further dissolved in nitric acid. The results to the dissolution reactions in nitric acid are tabulated in table 4.2.

4.5.1 Effect of HNO_3 concentration on U dissolution

Lacher et al. (1961) stated that it is apparent that the reaction of uranium and nitric acid is autocatalytic. This statement was confirmed by Carrott et al. (2012).

4.5.1.1 Effect on dissolution rate

Table 4.2: Dissolution results of U residue in nitric acid of different concentrations, at 25°C and stirring rate of 1000 rpm.

Residue mass (g)	[HNO_3] (M)	Dissolution time (min)
1.0402	1	27
1.0321	3	20
1.0494	6	8

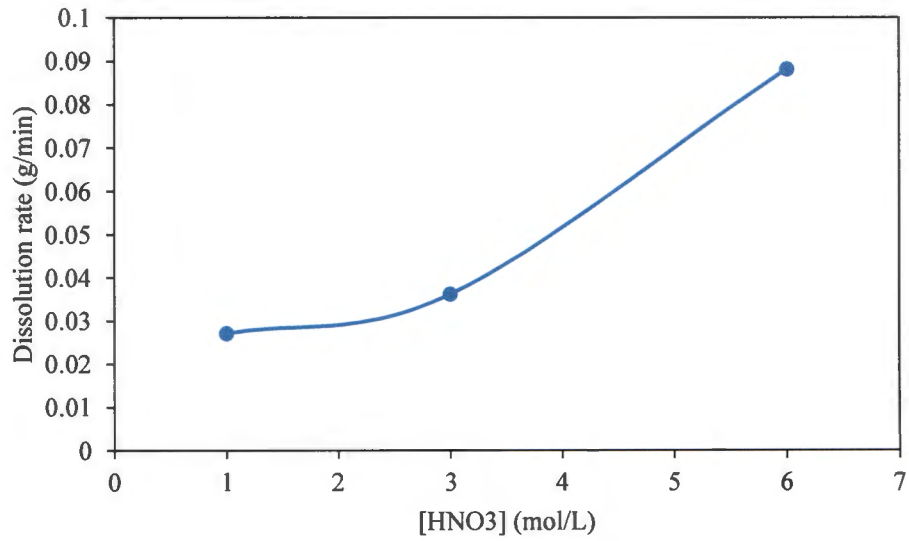

Figure 4.14: The effect of HNO_3 concentration on the dissolution of U dissolution at 80°C at 1000 rpm.

Dissolving uranium residue in nitric acid showed an increase in dissolution rate when the concentration of the acid increased. Figure 4.14 shows that increasing the concentration of the acid does have a positive effect on the dissolution rate. The reaction rate increased sharply from using 3.0 M acid to 6.0 M acid.

Studies (Hermann, 1984; Marc et al., 2017) have determined and reported that the increase of nitric acid concentration for the dissolution of uranium does increase the dissolution rate. The use of nitric acid to dissolve uranium has been widely reported and investigated by Hermann (1984). Marc et al. (2017) state that the increase of nitric acid concentrations results in the increase of dissolution kinetics (Marc et al., 2017). This statement is supported by (Taylor, 1962; Nishimura et al., 1995 Delegard et al., 2008; Zhao and Chen, 2008)

4.5.1.2 Effect on dissolution efficiency

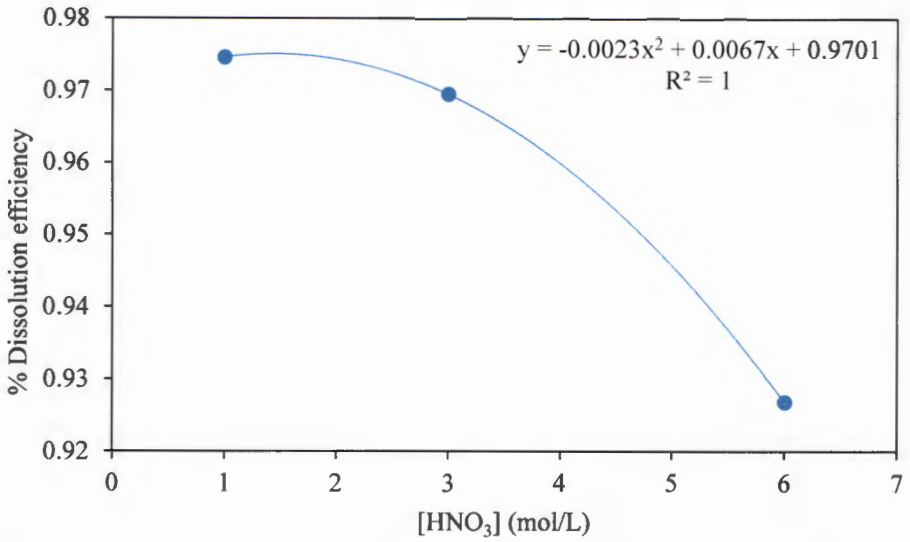

Figure 4.15: The effect of HNO_3 concentration on dissolution efficiency of uranium in the residue.

The trend observed in figure 4.15 shows that when the concentration of nitric acid was increased, there was a decrease in uranium dissolution efficiency. Dissolution efficiency decreased with increasing nitric acid concentration following a second order polynomial ($R^2 = 1$). Although at 6.0 M nitric acid concentration, the dissolution rate (figure 4.14) was at its peak, the efficiency of dissolution was at the lowest compared to the other concentrations of nitric acid. In the case of dissolution efficiency for uranium, a high concentration of nitric acid is not good.

4.5.2 Effect of temperature on U dissolution

4.5.2.1 Effect on dissolution rate

Table 4.3: Dissolution results of U residue in nitric acid at different temperatures keeping the stirring rate at 1000 rpm and HNO_3 concentration constant.

Residue mass	Temperature (°C)	Dissolution time (min)
1.0321	25	20
1.0431	50	8

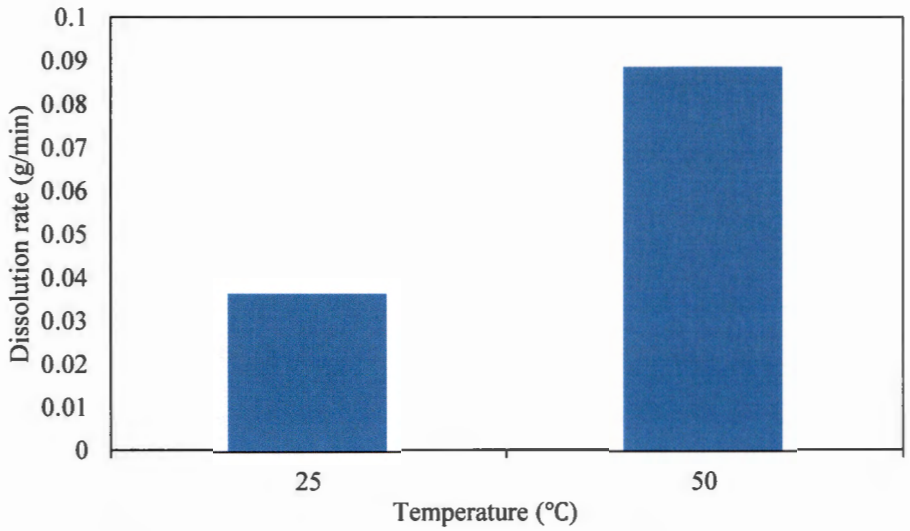

Figure 4.16: The effect of temperature on the dissolution rate of U residue with 3.0 M HNO_3.

A test on how temperature affects the dissolution rate of uranium was conducted where the results showed that at higher temperatures the dissolution rate increased.

When increasing the temperature of the solution/acid for dissolving uranium residue, an increase of the dissolution rate was observed. Another factor that has been stated is that the increase of uranium dissolution rate is influenced by the total nitrate concentration when the temperature is increased (Delegard et al., 2008).

In the investigation of dissolving uranium at different temperatures, it is reported that there is a significant increase in the dissolution rate with increase in temperature. (Broczkowski et al., 2007) reported their findings that were conducted at 22°C and 60°C. Srinivasan et al. (2004) also mentioned that by increasing the solvent's temperature, it enabled the decrease of dissolution time the uranium would undergo. Delegard et al. (2008) further elaborated that by dissolving uranium metal in nitric acid solution, the rate of dissolution increased with the increase of temperature.

4.5.2.2 Effect on dissolution efficiency

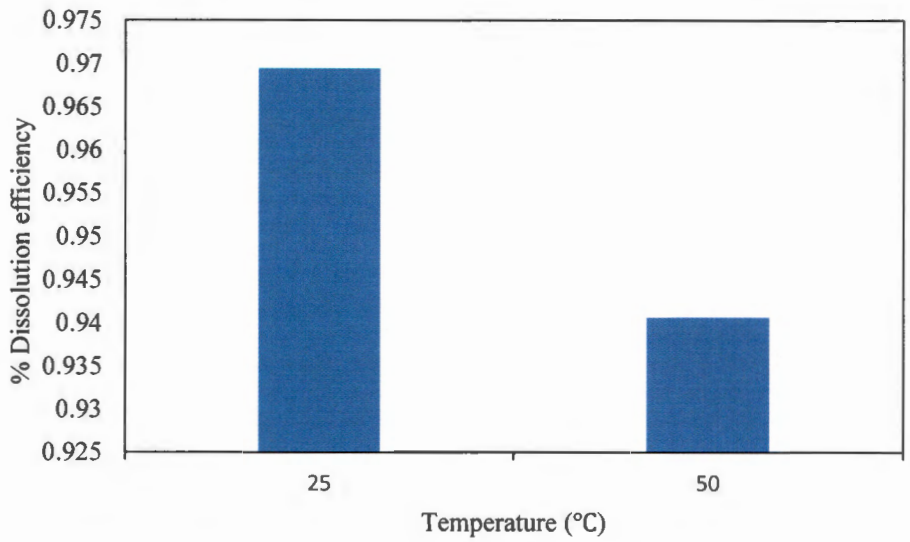

Figure 4.17: The effect of temperature on the dissolution efficiency of uranium residue at 3.0 M HNO_3.

A higher temperature of 50°C for dissolving uranium had a slightly negative effect on the dissolution efficiency compared to the temperature of 25°C (figure 4.17). When the temperature was increased from 25°C to 50°C, the difference in dissolution efficiency was only 2.8%. Higher temperatures were beneficial when relating to the dissolution rate (figure 4.16), however, not the dissolution efficiency when using nitric acid.

4.5.1.3 Summary

Dissolution of uranium residue in either a high concentration of nitric acid solution or at a high temperature, resulted in high dissolution rates. Therefore, the best possible results in terms of dissolution rates may be obtained by using a high nitric acid concentration (6.0 M) and a high temperature (50°C). However, these combinations will most likely produce comparatively lower uranium dissolution efficiency.

4.5.3 Conclusion

In conclusion, the highest dissolution efficiency could be obtained be dissolving uranium residue at a temperature of 25°C in 3.0 M nitric acid. In this study, the dissolution rate was highest when temperature was set to 50°C in 6.0 M nitric acid. According to this study, dissolution rate can be optimised by dissolving uranium residue at a high temperature with high nitric acid concentration. Dissolving the uranium residue at a low temperature coupled with a low nitric acid concentration, may result in a higher dissolution efficiency. A compromise can be made by either dissolving uranium residue at a high temperature with a low nitric acid concentration or at a low temperature with a high nitric acid concentration.

For the next stage in this study, a compromise was made between optimising for either a high dissolution rate or high dissolution efficiency by using 3.0 M nitric acid concentration. It was decided that a high dissolution efficiency was more important than a high dissolution rate and therefore, the uranium residue was dissolved at 25°C. An advantage of using nitric acid as a solvent is stated by Germain & Plout (1980) that the distribution value ratios of TBP increases with the increase in nitric acid concentration. The results from the study conducted by Germain & Plout (1980) showed a maximum distribution ratio at 3.0 M HNO_3 with the minimum at 0.3 M HNO_3. Germain & Plout (1980) also reported that the cause of TBP being soluble in nitric acid is due to the complex formation by hydrogen bonds along with the distribution ratio values increasing with nitric acid concentration are due to a lower solubility of TBP in the concentrated range of HNO_3 (Germain & Pluot, 1980)

4.6 Solvent extraction

The reason for analysing the influence that aluminium has on uranium extraction was due to the fact that during target plate fabrication, aluminium powder was added to the uranium fuel powder. This is practised due to uranium being pyrophoric and that during fission, the fuel plate gets heated. Therefore, the use of aluminium powder alleviates from potential risks of the fuel overheating and cracking causing leaching of fuel and inevitable contamination. Aluminium therefore aids as it has good neutron economy and good heat transfer properties (Gibson, 1966). The target plates therefore consist of a U/Al alloy "meat", with aluminium cladding surrounding the "meat". A lot of aluminium therefore needs to be dissolved during alkaline target plate dissolution, and the possibility is high that undissolved aluminium remain in the uranium residue after dissolution of the TP that may hinder the solvent extraction of uranium, and also needs to be separated from uranium during the extraction process.

To determine the effect of aluminium on uranium extraction, various amounts of $Al(NO_3)_3 \cdot 9H_2O$ were added to each solution except Run 1. Run 2, 3, 4 and 5 had 1.25%, 6.02%, 12.38% and 18.09% Al (m/m U), respectively.

4.6.1 Effect of aluminium on uranium extraction

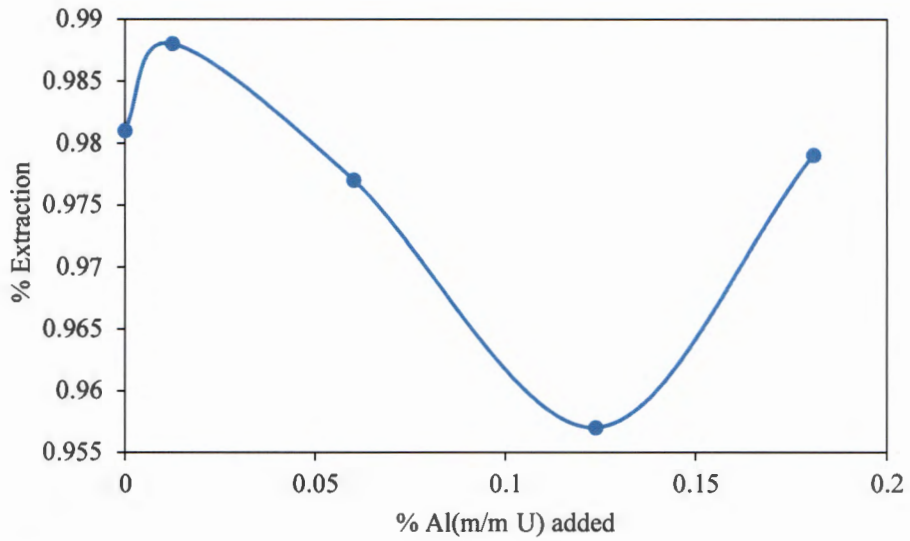

Figure 4.18: The effect of Al concentration on uranium extraction.

Figure 4.18 shows the percentage of uranium that was extracted with different amounts of aluminium added. A slight increase in extraction was observed from the solution that had 1.25% Al compared to the solution that had no Al in it. Adding 1.25% Al resulted in maximum uranium extraction. Increasing Al beyond 1.25% to 12.38% led to a decrease in uranium extraction. A further increase of the Al from 12.38% to 18.09% had a positive effect on the extraction. The range in extraction percentage is 3.08%, which on an industrial scale may be the difference between 7 and 10 g uranium recovery. Since no obvious reasons exist for the drop in U extraction % at 12.38% and thereafter increasing again at 18.09%, the low value at 12.38% could just be due to an analysis error and is an outlier. In this case, the % U extraction stays in a narrow band and no significant effect of Al on U extraction is observed.

4.6.2 Effect of $(NH_4)_2CO_3$ concentration on stripping

In this study, the effect of ammonium carbonate on stripping of uranium was investigated. Two concentrations were considered; 0.5 M $(NH_4)_2CO_3$ adopted from (Fourie et al., 2016) and a higher concentration of 1.0 M $(NH_4)_2CO_3$. Each of these concentrations were tested on the five solutions prepared with different concentrations of Al in the feed

Table 4.4: Stripping efficiency at 0.5 M $(NH_4)_2CO_3$ and 1.0 M $(NH_4)_2CO_3$

%Al (m/m U) present in feed	% U stripped (0.5 M $(NH_4)_2CO_3$)	% U stripped (1.0 M $(NH_4)_2CO_3$)
0.0	24.45	81.83
1.25	24.25	73.29
6.02	24.07	85.82
12.38	23.44	91.74
18.09	23.24	86.82

At a concentration of 0.5 M $(NH_4)_2CO_3$ uranium stripping ranged from 23.24% to 24.25% which were low values in terms of the desired stripping percentage. When a concentration of 1.0 M $(NH_4)_2CO_3$ was used, uranium stripping efficiency ranged from 73.29% to 91.74%. These values were much higher compared to those obtained when 0.5 M $(NH_4)_2CO_3$ was used.

The reason why ammonium carbonate can act as an effective stripping agent for U from TBP, is due the strong coordination and complexation of the uranyl ion with the carbonate ions in solution according to equation (31).

$$UO_2^{2+} + 3CO_3^{2-} \rightarrow [UO_2(CO_3)_3]^{4-} \quad (31)$$

An overall stability constant calculated according to equation (31) has been determined as log β = 21.54 at 0.1 M $NaHCO_3$ (Cinnéide et al., 1975). This corresponds well with stability constants reported from literature in the seminal overview of uranium thermodynamics (Guillaumont & Mompean, 2003), where log β values varied between 21.6 and 21.9.

$$\beta = \frac{[UO_2(CO_3)_3^{4-}]}{[UO_2^{2+}][CO_3^{2-}]^3} \quad (32)$$

A negative effect which was observed during uranium stripping, was due to the formation of a third phase between the aqueous phase and organic phase after they had been rotated and allowed to rest and settle in a separatory funnel for an hour (figure 4.19). Fortunately, this did not have a detrimental effect on the efficiency of U stripping observed, but will have to be further investigated if this method of stripping should be implemented at UChem (note that UChem currently use dilute HNO_3 for stripping, which is much less effective and requires far larger stripping volumes).

Whenever liquid-liquid extraction systems are utilised, the development of a third phase normally denotes the occurrence whereby the original organic phase separates into two immiscible organic phases that jointly coincide with the immiscible aqueous phase. Many different liquid-liquid extraction systems generally experience the formation of a third phase (Jassim, 2011). After studying the extraction of hydrochloric acid with TBP-kerosene system, (Irving and Edgington, 1959) found out that above 5.0 M hydrochloric acid concentration, three phases were observed to be separated. The upper phase (containing most of the kerosene which had very little amounts of water or acid), a middle phase of TBP that had been saturated with water and HCl but with little kerosene in it. Suresh et al. (2009) explored the formation of third phases in the extraction of Th(IV) using TBP/n-dodecane, while Plaue et al. (2006) investigated with Pu(IV) nitrate using 30% TBP and Jensen et al. (2002) conducted the experiment with U(IV) nitrate-TBP. In the process of extracting uranium nitrate, Poczynailo et al. (1973) discovered, by means of spectroscopy, the occurrence of disolvate and trisolvate of $UO_2(NO_3)_2$ by TBP, whereas with the aid of infrared studies of $UO_2(NO_3)_2$ – 20% TBP in dodecane system, a disolvate of $UO_2(NO_3)_2$ was stated (Alibrahim &

Shlewit, 2007). Boukis & Kanellakopulos (1983) explained that in a system that contained $UO_2(NO_3)_2 - HNO_3 - 30\%$ TBP in dodecane, the critical temperature in order for the third phase to be formed has been studied as a function of the uranyl-concentration and/or the aqueous phase acidic nature (Boukis & Kanellakopulos, 1983). Boukis & Kanellakopulos (1983) further explained that the quantity of the third phase either increased with the decrease in temperature or with the increase of acidity in the aqueous phase.

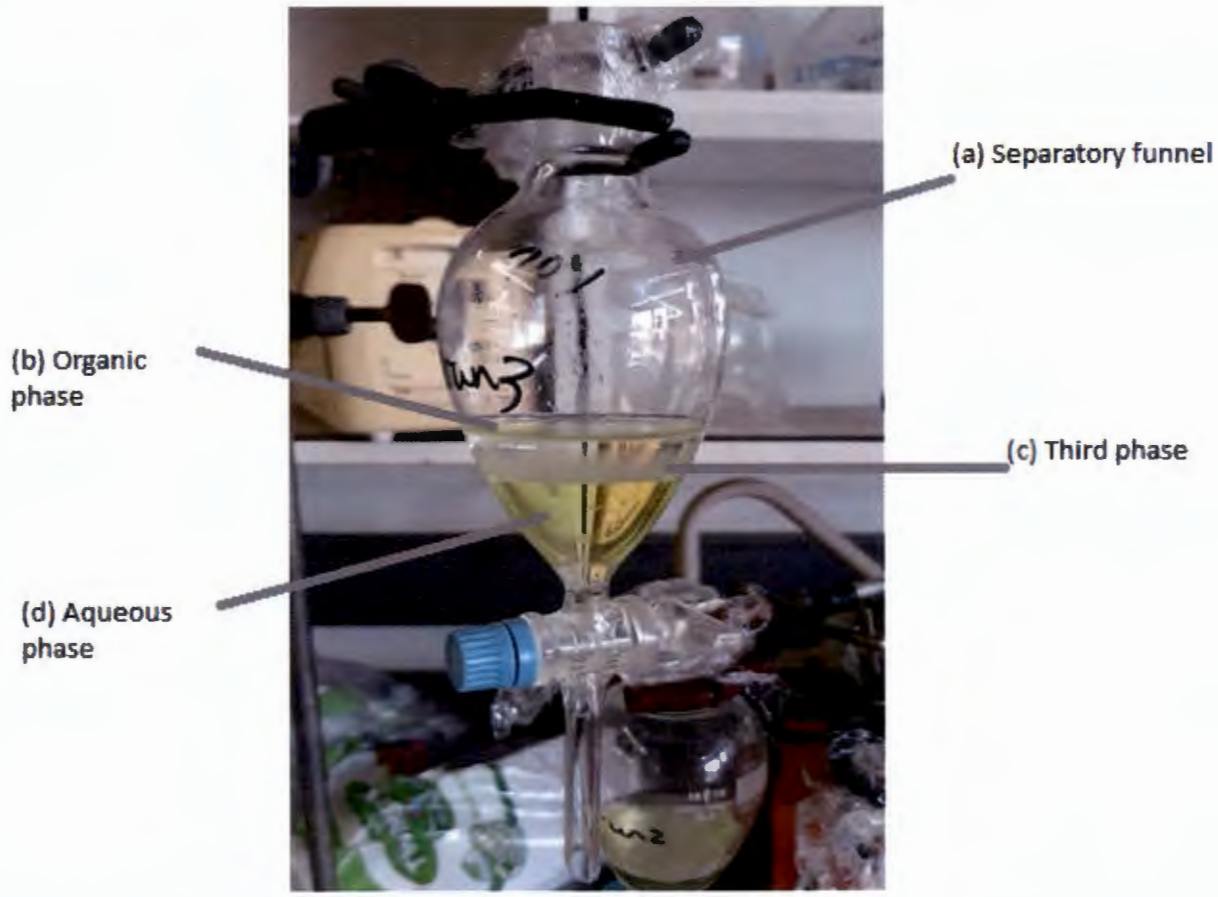

Figure 4.19: Separatory funnel with the organic phase (b), third phase (c), and aqueous phase (d) after the settling period.

4.6.3 Aluminium decontamination factor

The aluminium decontamination factor was calculated to evaluate the level of aluminium/uranium co-extraction and the purification of uranium from aluminium that can be obtained using solvent extraction. Table 4.5 shows the decontamination factors calculated for different amounts of aluminium added to uranium solutions. It should be noted that the decontamination factors presented in table 4.4 were underestimated due to the analytical instrument used, which had a detection limit of 1 ppm for Al.

Table 4.5: Decontamination factors of different amounts of aluminium in uranium solutions.

Al added (% m/m U)	Al concentration before extraction (mg/L)	Al concentration after extraction (mg/L)	Decontamination factor
0	21.5	< 1	>21.5
1.25	89.1	< 1	>89.1
6.02	447	< 1	>447
12.38	720	< 1	>720
18.09	983	< 1	>983

The results obtained for the decontamination of aluminium from uranium ore supported by Stas et al. (2005), who reported that TBP is highly selective for uranium and also offers exceptional decontamination from most contaminants. During a typical separation process of uranium, a step that entails scrubbing is included in the process to separate all contaminants from uranium, this ensures the purity of uranium before being stripped and further precipitated (Awwad, 2004).

4.6.4 Conclusion

The addition of Al to the uranium solution has an almost negligible effect on uranium extraction. The percentage extraction range as the amount of aluminium added is increased from 1.25% to 12.38% is only 3.08%. During uranium stripping, a third phase was formed in this study, which fortunately had no detrimental effect on the stripping efficiency. This hypothesis was proposed by Germain & Pluot, (1980). Stripping using 1.0 M $(NH_4)_2CO_3$ was seen to be the optimum concentration to use compared to the use of a 0.5 M $(NH_4)_2CO_3$ for stripping uranium from TBP. The amount of Al in the final U strip was in all cases below the detection limit of the analytical instrument (1 mg/l), indicating no extraction of Al occurred and very efficient separation from U, for even the highest amount of Al added. This shows that solvent extraction of U from 3.0 M HNO_3 into 30% TBP, is an effective method for purifying U from Al.

4.7 Ion exchange as an alternative purification method

Solvent extraction has generally been the most common method of recovery for uranium, particularly with the aid of TBP. In this study, an alternative method was suggested to recover uranium by using ion exchange technology. Reynier et al. (2016) mentioned that the process of ion exchange has been regarded as the favoured method for separating uranium from accompanying impurities in order to produce a purified and concentrated uranium solution that will qualify for producing a uranium product (Reynier et al., 2016). This technology was investigated in this study to show the effectiveness of recovering uranium using ion exchange technique.

4.7.1 Distribution coefficient determination

The distribution coefficient is characterized by the capability of an ion exchange resin to absorb ions from a solution. In this study, the ion of interest was uranyl ion from a uranium solution. The distribution coefficient can be used to calculate the theoretical maximum capacity of the ion exchange bed to purify a volume of waste solution (Ojovan & Lee, 2013).

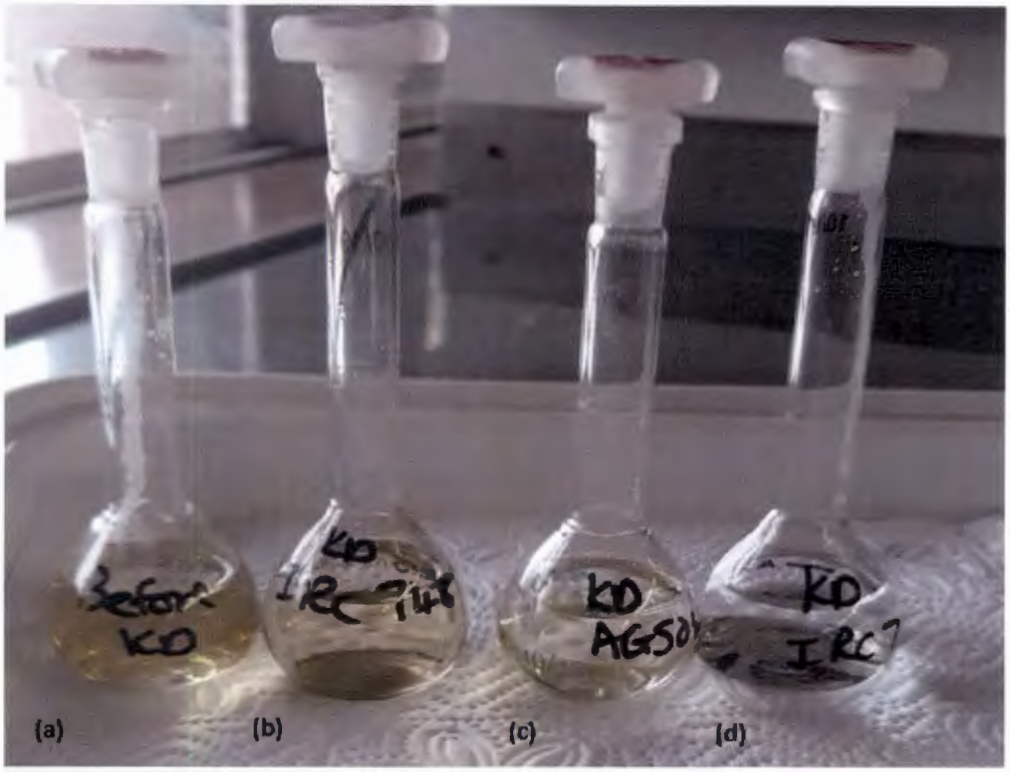

Figure 4.20: (a) Solution before using resin, (b) solution after using Amberlite IRC748, (c) solution after using AG50W-X4, and (d) solution after using Amberlite IRC747.

The feed solutions for ion exchange testing were diluted to 0.1 M HNO_3, due to the declining distribution coefficients of U on cation exchange resins at increased acidity (Strelow et al., 1965). Another factor that was considered was that a high concentration of acid may have an influence on the elution of uranium from the chelating resin. This experiment was conducted to test the sorption of uranium on Amberlite IRC748, AG50W-X4 and Amberlite IRC747 resins using 10 ml of solution that contained 5 mg of U. After contacting the uranium solution with the resin, the distribution coefficients were calculated using equation (30).

The results showed that Amberlite IRC747 had the highest uranium distribution coefficient of 4461.9 ml/dry g while Amberlite IRC748 and BioRad AG50W-X4 performed poorly, with only 167.0 ml/dry g and 433.1 ml/dry g, respectively (figures 4.20 and 4.21). The Amberlite IRC747 resin was therefore chosen to test further for U recovery and purification from Al, in a column experiment.

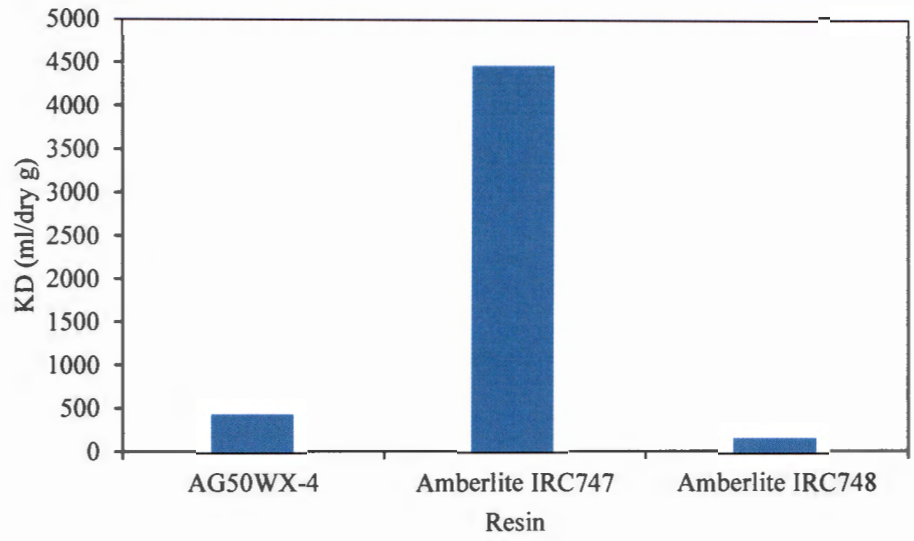

Figure 4.21: Distribution coefficient of uranium on three different resins in 0.1 M HNO_3.

4.7.2 Column sorption of uranium from nitric acid solution by Amberlite IRC747

Amberlite IRC747 is a macro-porous resin that has a styrene di-vinyl-benzene copolymer matrix that is crosslinked with DVB, containing amino-phosphonic groups ($-CH_2-NH-CH_2-PO_3Na_2$). The main reason for possessing such amino-phosphonic groups is so that it is able to form complexes with desired metal ions. The resin, according to Rohm and Haas – a chemical manufacturing company - has a capacity of ≥1.75 eq/L of ions in the form of Na^+. The resin is supplied in Na^+ form where it is washed with water and subsequently equilibrated with 0.1 M HNO_3 in order to convert it to H^+ form.

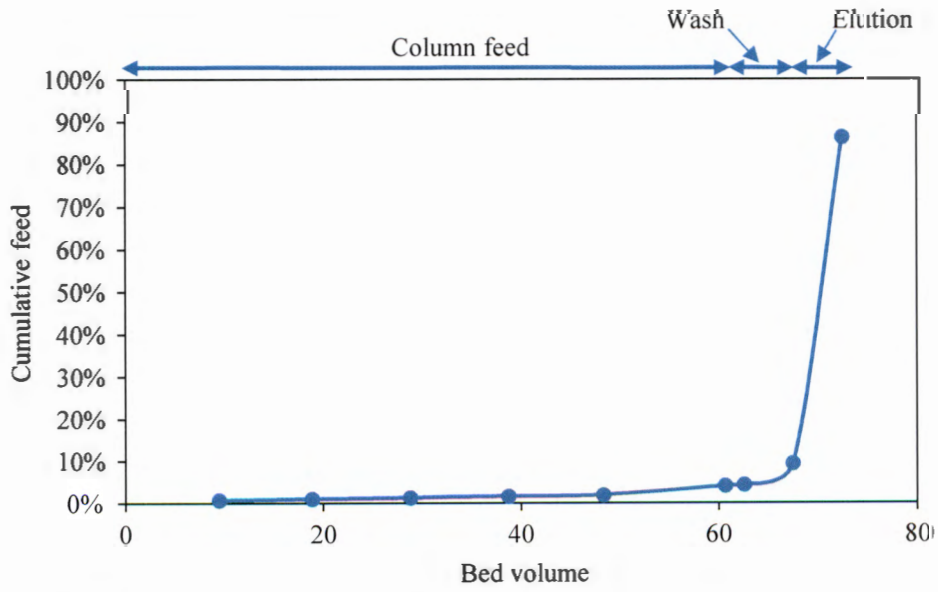

Figure 4.22: The breakthrough of uranium feed using Amberlite IRC747 resin.

The total amount of feed was 1252 ml or 60.69 bed volumes (BV), followed by a NaOH wash of 100 ml between 62.60 and 67.51 BV, with the elution taking place after 67.51 BV (figure 4.22).
The breakthrough point is defined as the volume fed to the column until the effluent reaches a uranium concentration equal to 2% of the concentration in the feed (Merritt, 1971b). In this study, the breakthrough point was observed at 60.69 BV, with the flow rate set at 1.65 ml/min and a uranium feed concentration of 480 ppm. Uranium was eluted from the resin using 85 ml ammonium carbonate mixed with 15 ml of 30% hydrogen peroxide. Figure 4.23(a) shows a yellow colour on the resin which is due to the uranium loaded. In figure 4.23(b), the yellow colour has disappeared showing that most of the uranium has been eluted from the resin.

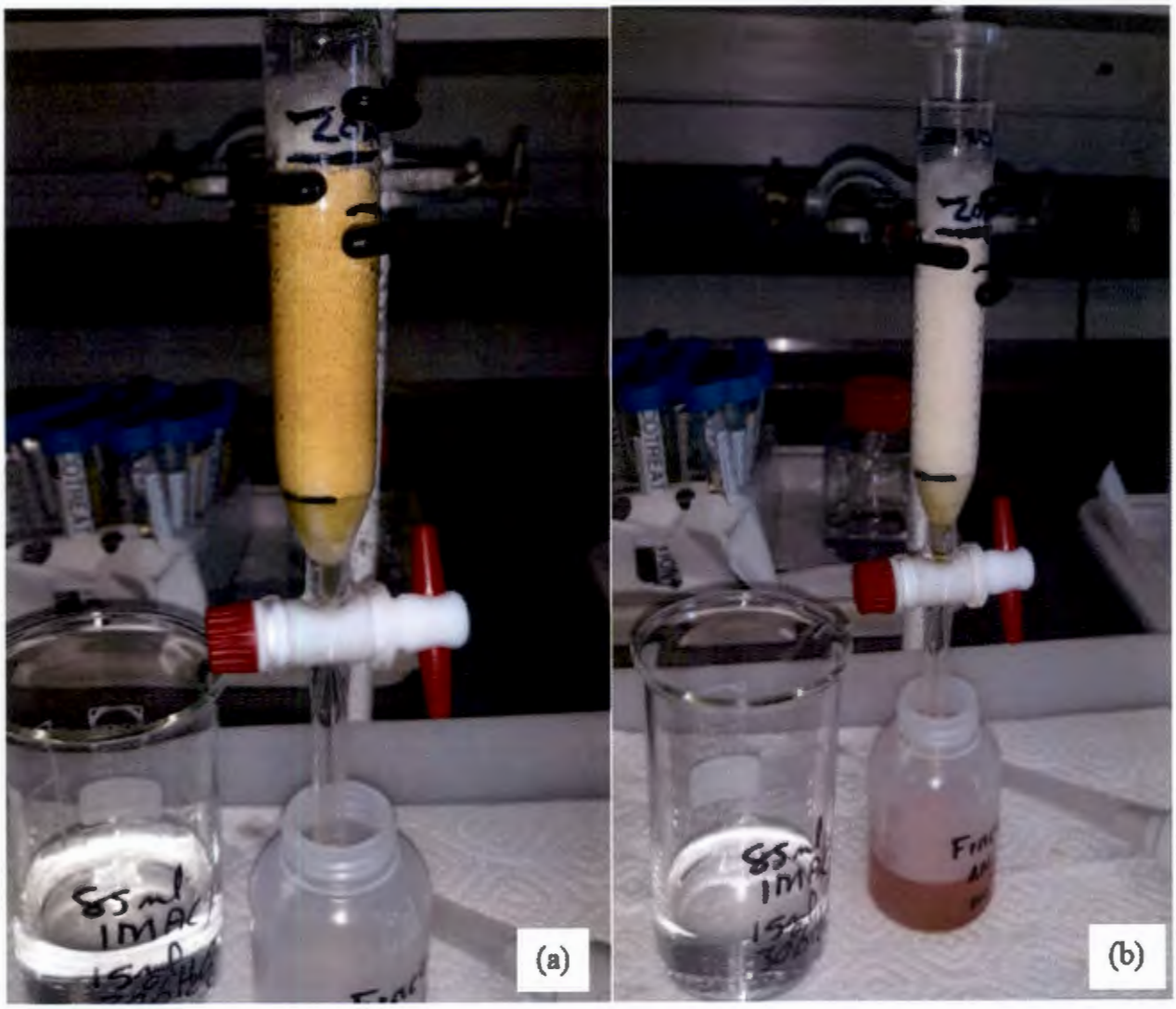

Figure 4.23: Elution of uranium from the resin using ammonium carbonate and hydrogen peroxide.

Breakthrough of uranium occurred when the resin was loaded with 577.65 mg. The breakthrough capacity was 29.11 g U/L resin. The breakthrough occurred at 13.98% (0.245 eq UO_2^{2+}/L resin) of the theoretical capacity of Amberlite IRC747 which is 1.7 eq/L resin.

4.7.3 Separation of aluminium from uranium on Amberlite IRC747

An amount of 5% Al (m/m U) was added to the feed solution of the column, to study the behaviour of Al on Amberlite IRC747, and determine if it can be successfully separated from U using this resin.

Due to the high cost of aluminium analyses at PAL, it was not possible to analyse each fraction of the column to determine the breakthrough point of Al, and therefore only the feed solution and the last two fractions (the NaOH wash and the carbonate/peroxide eluate) were analysed for Al, since the real matter of importance is only whether it is eluted from the column with U or not, which will indicate the possible extent of separation from U. The results are given in table 4.5:

Table 4.6: Aluminium analysis results for the Amberlite IRC747 column experiment

Solution	Volume (ml)	Al Conc. (mg/l)	Al mass (mg)
Column feed	1230	2.1	2.58
Fraction 8	98.07	48.6	4.77
Fraction 9	100.62	14.7	1.48
=> %Al eluted:			241.8%

The Al mass balance in the three solutions analysed do not tally with each other (amount of Al recovered in the wash and eluate fractions is 242% of that in the feed), and this is probably due to the very low Al concentration in this solution, leading to a relatively large analysis error. However, the results do indicate that most or all of the aluminium in the feed solution was eluted in the same fractions where U was recovered, signifying that no separation between U and Al is possible using ion exchange on Amberlite IRC747.

Chapter 5: Conclusion and recommendations

5.2 Conclusion

During the production of U/Al target plates, a lot of scrap is generated that contains high valued uranium that need to be recovered, purified and recycled into the target plate manufacturing process. The use of alkaline (KOH) medium for target plate dissolution has been followed by Necsa but is not optimised.

The aim of this study was to determine the optimum dissolution medium for the U/Al scrap material in either NaOH and KOH, optimise conditions for dissolving uranium from the residue generated during alkaline dissolution of the target plate scrap, test the separation of U and Al using solvent extraction into TBP, and evaluate ion exchange as an alternative purification technology. The objectives of this study included finding the most effective alkaline solution to dissolve aluminium and its requirement for excess solution in order to keep Al stable in solution, by comparing kinetics of dissolution in NaOH and KOH. We optimised all dissolution parameters in the chosen alkali, that is temperature, stirring rate, NaOH or KOH concentration, $NaNO_3$ on dissolution rate and solution stability. More tests were on the validity of the optimised parameters on aluminium samples provided by UChem. Other tests were on the optimized parameters on aluminium containing depleted uranium (DU); determining the optimum dissolution parameters (optimum HNO_3 concentration and temperature) for U residues in nitric acid. The effects of the various amounts of Al added to the dissolved uranyl nitrate were determined. This was executed based on the efficacy of uranium extraction with TBP and further used to determine the viability of using ion exchange technology to recover and purify U from the generated solution with added Al on chelating ion exchange resins (Amberlite IRC747 and Amberlite IRC748). The cationic exchange resins (BioRad AG50W-X4) was also used as an alternative for uranium purification.

To determine the best dissolution medium between NaOH and KOH, a series of tests were conducted to optimise the volume of alkali to dissolve the standardised 16.2 g of Al. The effectiveness of these parameters was evaluated based on the dissolution rate and re-precipitation time. Once concentration was optimised for both hydroxides, the effects of temperature, stirring rate and $NaNO_3$ were assessed. Temperature was varied from 30 to 80°C, stirring rate varied from 0 to 1000 rpm and $NaNO_3$ concentration was optimised using 3.0, 3.5, and 4.0 M concentrations. Once all the parameters were optimised along with the best dissolution medium, they were implemented on aluminium alloy samples that are used for ^{99}Mo production. The optimum parameters were compared to the current method of dissolution utilised by UChem.

The optimum parameters were further applied to dissolve a non-irradiated target plate containing depleted uranium. Subsequently, the residue recovered after caustic dissolution of the target plate was dissolved in HNO_3 at different concentrations and temperatures. The effects of nitric acid concentration and temperature were assessed using the dissolution rate and dissolution efficiency. Uranium was separated and recovered using solvent extraction, with 30% TBP in kerosene as an extractant and $(NH_4)_2CO_3$ as a stripping agent. A purification method of ion exchange was explored as an alternative. Three different resins, Amberlite IRC747, Amberlite IRC748 and BioRad AG50W-X4, were tested. The partition coefficient of uranium in each resin was determined and the resin with the highest sorption was further used to purify and recover uranium from the solution in a column experiment.

NaOH was found to be the optimum medium at the concentration of 6.0 M with 3.0 M excess above the stoichiometric amount required for complete dissolution of Al. This conclusion was reached based on the results that dissolving aluminium with sodium hydroxide at a 3.0 M excess resulted in the fastest dissolution rate of 0.470 g/min, whereas KOH with a 3.0 M excess had a dissolution rate of 0.373 g/min.

Dissolution parameters tested showed that dissolution of 16.2 g Al at 80°C, stirred at 1000 rpm with 3.5 M $NaNO_3$ yielded the highest dissolution rate and the longest re-precipitation time. NaOH with 3.0 M excess with 3.5 M $NaNO_3$ had a higher dissolution rate of 0.7718 g/min and a rep-precipitation time of 12960 minutes, whereas with KOH plus 3.0 M excess and 4.0 M $NaNO_3$ the dissolution rate was 0.7048 g/min and a re-precipitation of 10800 minutes (KOH plus 3.0 M excess with 3.5 M $NaNO_3$ were even lower).

The two determining factors (dissolution rate and time to re-precipitation) were considered as the industry is constantly looking for a method to dissolve target plates in less time also assuring that solutions remain stable over a longer period to allow for complete workability and analysis of the solution.

The optimised parameters worked for all aluminium samples as they were all able to dissolve completely. Judging from the dissolution rate results, LP-COC-14/54 performed better than LP-COC-12/41 and LP-COC-11/238. The optimisation from this study led to an improvement in the dissolution parameters compared to the method employed at that time.

The optimum dissolution parameters were further applied to a target plate that contained depleted uranium. The rate of dissolving the TP in only sodium hydroxide was higher (0.5328 g/min) than with the inclusion of sodium nitrate at concentrations of 3.0 M (0.1488 g/min). This was a contradiction of the results reported when optimising the dissolution parameters for pure

aluminium. This could be due to the impurities amalgamated in the alloying of Al to form the specified target plate.

The effects of varied nitric acid concentrations and temperatures were optimised for the dissolution of uranium residue. The results showed that increasing the temperature and nitric acid concentration leads to an increase in dissolution rate. However, when increasing both parameters this also led to a poor uranium dissolution efficiency. Reducing the temperature and nitric acid concentration, led to a lower dissolution rate but ensured a higher uranium dissolution efficiency.

When using solvent extraction to recover uranium, adding aluminium to the solution affected uranium recovery only minimally. It was observed that the difference between the highest and the lowest extraction was 3.08%. The optimisation of uranium stripping from TBP was executed with different concentrations of ammonium carbonate. Concentrations of 0.5 M and 1.0 M $(NH_4)_2CO_3$ were used to check the percentage strip from uranium solutions. The results showed that at a concentration of 0.5 M only an average of 23.89% uranium was stripped from all five solutions. Using 1.0 M $(NH_4)_2CO_3$ increased the uranium stripping to an average of 83.90%. After stripping, decontamination of uranium from aluminium was determined. TBP had a high selectivity for uranium therefore decontaminating it from impurities. Due to the sensitivity of the analytical equipment used (with an Al detection limit of 1 ppm), only a lower limit of the decontamination factors for different amounts of aluminium added could be determined.

Three ion exchange resins were compared using their uranium distribution coefficients. Amberlite IRC747 had the highest distribution coefficient of 4461.9 ml/dry g with AG50W-X4 and Amberlite IRC748 having 433.1 ml/dry g and 167.0 ml/dry g, respectively. Amberlite IRC747 was further used to recover uranium in a column experiment. The breakthrough point was observed at 60.69 BV, with the flow rate set to 1.65 ml/min and a uranium feed concentration of 480 ppm. The breakthrough capacity was 29.11 g U/L resin. Breakthrough occurred at 13.98% (0.245 eq UO_2^{2+}/L resin) of the theoretical capacity of Amberlite IRC747 which is 1.7 eq/L resin.

In this study, solvent extraction and an alternative uranium recovery method, ion exchange, were used to recover uranium from a solution. Solvent extraction recovered 86.27% in a single stripping step of 20 ml volume, but this could be improved by using a number of sequential stripping steps, as is routinely practiced in industry. With the ion exchange column, U recovery of 82.08% was achieved with a 200 ml wash and eluate volume. The difference in recovery between the two methods is 4.19%. Solvent extraction method performed better not only in the percentage recovery of uranium, but also with the time it took to conduct recovery, and in terms of the volume in which U was recovered. Furthermore, complete separation of Al was achieved using SX, while with the

ion exchange column, all of the Al was eluted with uranium, indicating no possibility of separation. Using SX, several extractions can be performed in parallel with little training required. For this specific application, the solvent extraction process already implemented at UChem Necsa, therefore seems to be superior to ion exchange technology

5.2 Limitations

1. When the optimized dissolution parameters for pure aluminium were tested on aluminium samples from UChem, a large variation in dissolution rates between the three available samples was observed. Due to a lack of enough material to experiment with, the reasons for this difference could not be further investigated.
2. When the optimized dissolution parameters for pure aluminium were tested on pieces of target plate containing U/Al alloy, a discrepancy was observed in that the addition of $NaNO_3$ had a severely negative effect on the dissolution efficiency of aluminium, while when dissolving pure aluminium it had a positive effect. Due to a lack of enough target plate material, this discrepancy could not be further investigated. Because the addition of $NaNO_3$ has such a huge beneficial effect on eliminating evolution of dangerous quantities of flammable hydrogen gas, this should be further investigated.
3. Another limitation that was met during this study was during the process of dissolving uranium residue. Due to a limited amount of the residue available, the study of dissolving the residue at a wider range of temperature was not conducted.

5.3 Recommendations for future work

For future work in optimising parameters for TP dissolution studies the following are recommended:

- When dissolving aluminium in sodium hydroxide, it is recommended that the stirring rate be tested at 1000, 1500 and 2000 rpm. This would provide a broader spectrum of rpms that would be deemed optimal. The aforementioned rpms were not tested due to the time constraint.
- Dissolving aluminium in potassium hydroxide, higher temperatures should be explored to optimise dissolution temperature.

The above recommendations have been made because they could not be implemented in the study due to time constraints.

- While dissolving aluminium in potassium hydroxide and sodium nitrate, it is recommended that the concentration of sodium nitrate be increased to 4.0 M, 4.5 M and 5.0 M to determine the optimum concentration.

- A wider range of samples of the aluminium used for actual target plate manufacture should be tested with the optimized Al dissolution parameters.
- Further investigations should be done with U/AL target plate material, to investigate the effect of $NaNO_3$ on the dissolution process
- During the dissolution of uranium residue, only two temperatures were tested. A wider range of temperature (30, 45, 60 and 70°C) is recommended to determine the optimum temperature.
- Two $(NH_4)_2CO_3$ concentrations were tested for uranium stripping. Although a higher concentration of 1.0 M stripped a higher percentage of uranium, increasing the stripping agent concentration to 1.5 M and 2.0 M is recommended in order to evaluate their stripping percentages.

The above recommendations have been made due to unavailability of resources during the study.

References

A Abbasi, W., Streat, M., 1998. Sorption of uranium from nitric acid solution using TBP-impregnated activated carbons. Solvent Extr. ion Exch. 16, 1303–1320.

Adams, T.M., Peacock, H.B., Rhode, F.C., 1999. The melt-dilute treatment of Al-base highly enriched DOE spent nuclear fuels: Principles and practices. MRS Online Proc. Libr. Arch. 556.

Addai-Mensah, J., Li, J., Rosencrance, S., Wilmarth, W., 2004. Solubility of amorphous sodium aluminosilicate and zeolite A crystals in caustic and nitrate/nitrite-rich caustic aluminate liquors. J. Chem. Eng. Data 49, 1682–1687.

Adhikari, S., 2008. Alkaline dissolution of aluminum: surface chemistry and subsurface interfacial phenomena. Retrospective Theses and Dissertations. 15828 . https://doi.org/https://doi.org/10.31274/rtd-180813-17031

Alcock, K., Grimley, S.S., Healy, T. V, Kennedy, J., McKay, H.A.C., 1956. The extraction of nitrates by tri-n-butyl phosphate (TBP). Part 1.—The system TBP+ Diluent+ H_2O+ HNO_3. Trans. Faraday Soc. 52, 39–47.

Aleksandrov, Y.A., Tsyganova, E.I., Pisarev, A.L., 2003. Reaction of aluminum with dilute aqueous NaOH solutions. Russ. J. Gen. Chem. 73, 689–694.

Alexandratos, S.D., 2008. Ion-exchange resins: a retrospective from industrial and engineering chemistry research. Ind. Eng. Chem. Res. 48, 388–398.

Ali, K.L., Khan, A.A., Mushtaq, A., Imtiaz, F., Ziai, M.A., Gulzar, A., Farooq, M., Hussain, N., Ahmed, N., Pervez, S., 2013. Development of low enriched uranium target plates by thermo-mechanical processing of UAl_2–Al matrix for production of ^{99}Mo in Pakistan. Nucl. Eng. Des. 255, 77–85.

Alibrahim, M., Shlewit, H., 2007. Solvent extraction of uranium (VI) by tributyl phosphate/dodecane from nitric acid medium. Period. Polytech. Chem. Eng. 51, 57–60.

Almond, P.M., Daniel, W.E., Rudisill, T.S., 2018. Process for dissolving aluminum for recovering nuclear fuel. U.S. Patent 9,896,738.

Alwitt, R.S. in: Diggle, J.S. Vijh, A.K., 1974. The Anodic Behavior of Metals and Semiconductors 4, 169.

Armstrong, R.D., Braham, V.J., 1996. The mechanism of aluminium corrosion in alkaline solutions. Corros. Sci. 38, 1463–1471.

Awwad, N.S., 2004. Equilibrium and kinetic studies on the extraction and stripping of uranium (VI) from nitric acid medium into tri-phenylphosphine oxide using a single drop column technique. Chem. Eng. Process. Process Intensif. 43, 1503–1509.

Ball, G., Pond, R., Hanan, N., Matos, J., 1995. Neutronic study on conversion of SAFARI-1 to LEU

silicide fuel. Argonne National Lab. (No. ANL/TD/CP-85126; CONF-9409107-12).

Basson, I.J., Greenway, G., 2004. The Rössing uranium deposit: a product of late-kinematic localization of uraniferous granites in the Central Zone of the Damara Orogen, Namibia. J. African Earth Sci. 38, 413–435.

Böck, H., Villa, M., 2001. Survey of research reactors. Prep. IAEA Course Safety, Manag. Util. Res. React.

Boukerche, I., Djerad, S., Benmansour, L., Tifouti, L., Saleh, K., 2014. Degradability of aluminum in acidic and alkaline solutions. Corros. Sci. 78, 343–352.

Boukis, N., Kanellakopulos, B., 1983. Extractive phase distribution of the uranyl nitrate with tri-n-butyl phosphate. Pt. 2. Kernforschungszentrum Karlsruhe GmbH (Germany). (No. KFK--3352).

Bourgeois, M., 2000. Retraitement du combustible. principales opérations. Tech. l'ingénieur. Génie nucléaire BN3650-1.

Broczkowski, M.E., Noel, J.J., Shoesmith, D.W., 2007. The influence of temperature on the anodic oxidation/dissolution of uranium dioxide. Electrochim. Acta 52, 7386–7395.

Bronsted, J.N., Kane, N.L.R., 1931. On the Dissolution of Metals in Acids. J. Am. Chem. Soc. 53, 3624–3644.

Burns, R.E., Holm, C.H., 1952. Nitric Acid Dissolution of Uranium-Aluminum Alloy. Hanford Works, Richland, Wash. (No. HW-18414).

Burrill, K.A., Harrison, R.J., 1987. Development of the Mo-99 Process at CRNL. Atomic Energy of Canada Ltd. (No. AECL--9621).

Cadwallader, L.C., Herring, J.S., 2007. Hydrogen and Gaseous Fuel Safety and Toxicity. Idaho National Laboratory (INL). (No. INL/CON-07-12095).

Carrott, M. J., Cook, P. M. A., Fox, O. D., Maher, C. J., Schroeder, S. L. M., 2012. The chemistry of (U, Pu) O_2 dissolution in nitric acid. Procedia Chemistry, 7, 92–97.

Cestau, D., Novello, A., Cristini, P., Bronca, M., Centurión, R., Bavaro, R., Cestau, J., Carranza, E., 2008. HEU and LEU comparison in the production of molybdenum-99. Argonne National Laboratory, Nuclear Engineering Division, RERTR Department, Argonne, IL (United States); Czech Technical University, Prague (Czech Republic).

Cinnéide, S.Ó., Scanlan, J.P., Hynes, M.J., 1975. Equilibria in uranyl carbonate systems—I: The overall stability constant of $UO_2(CO_3)_3^{4-}$. J. Inorg. Nucl. Chem. 37, 1013–1018.

Cols, H., Cristini, P., Marques, R., 1997. Preliminary investigations on the use of uranium silicide targets for fission Mo-99 production. (No. ANL/RERTR/TM--20).

Compton, R.G., Harding, M.S., Pluck, M.R., Atherton, J.H., Brennan, C.M., 1993. Mechanism of solid/liquid interfacial reactions: the dissolution of benzoic acid in aqueous solution. J. Phys.

Chem. 97, 10416–10420.

Conner, C., Aase, S., Wygmans, D.G., Vandegrift, G.F., Wu, D., Landsberger, S., 1997. Dissolution of low-enriched UO_2/Al dispersion plates in alkaline peroxide solution. (No. INIS-XA-C--009).

Conturbia, G.R., Durazzo, M., 2017. Study of thermomechanical treatment for manufacturing UAlx/Al dispersion targets.

Cunningham, J.E., Boyle, E.J., 1955. MTR-Type fuel elements, in: United Nations. Peaceful Uses Atomic Energy: Proceedings of the International Conference on..., Held in Geneva. Vol. I. 203–207.

Davis, J.R., 2001. Alloying: understanding the basics. ASM international.

De, A.K., Khopkar, S.M., Chalmers, R.A., 1970. Solvent Extraction of Metals. Van Nostrand Reinhold Company. Reinhold Co., London.

Deepa, P., Padmalatha, R., 2017. Corrosion behaviour of 6063 aluminium alloy in acidic and in alkaline media. Arab. J. Chem. 10, S2234–S2244.

Delegard, C.H., Sinkov, S.I., Schmidt, A.J., Chenault, J.W., 2008. Uranium Metal Analysis via Selective Dissolution. Pacific Northwest National Lab.(PNNL), Richland, WA (United States).

Dixit, S., Mukhopadhyay, S., Govalkar, S., Shenoy, K.T., Rao, H., Ghosh, S.K., 2012. A mathematical model for pertraction of uranium in hollow fiber contactor using TBP. Desalin. Water Treat. 38, 204–215.

Durazzo, M., de Carvalho, E.F.U., Silva, A.M.S., Souza, J.A.B., Riella, H.G., 2007. Current status of U_3Si_2 fuel elements fabrication in Brazil, in: International Meeting on Reduced Enrichment for Research and Test Reactors–RERTR2007, Prague. 23–27.

Elseaidy, I.M., Ghoneim, M.M., 2010. Re–qualification of MTR-type fuel plates fabrication process. (No. INIS-BE--10K0001) http://www.iaea.org/inis/collection/NCLCollectionStore/_Public/41/064/41064180.pdf. (accessed 2.22.17).

Emregül, K.C., Aksüt, A.A., 2000. The behavior of aluminum in alkaline media. Corros. Sci. 42, 2051–2067.

EPA, 2004. Sample Dissolution, in: MARLAP Manual. EPA, 1–30.

Eremin, N.I., Volokhov, Y.A., Mironov, V.E., 1974. Structure and Behaviour of Aluminate ions in Solution. Russ. Chem. Rev. 43, 92–106.

Evans, U.R., 1981. An Introduction to Metallic Corrosion, 3rd ed. Edward Arnold Ltd., London: Metals Park, Ohio.

Fallais, C.J., Morel, de W., Heeren, L., Baugnet, J.M., Gandolfo, J.M., Boeykens, W., 1978. Production of radioisotopes with BR2 facilities. Belgium. (No. INIS-MF--4426).

Farrell, K., 2012. Performance of aluminum in research reactors. Compr. Nucl. Mater. 5, 143–175.

Foley, R.T., 1986. Localized corrosion of aluminum alloys—a review. Corrosion 42, 277–288.

Foster, D.L., 1955. The caustic dissolution of unirradiated uranium-aluminum alloy fuel in a trickle-type dissolver. Oak Ridge National Lab., Tenn. (No. CF-55-11-123)

Fourie, M., Meyer, W.C.M.H., van der Westhuizen, D.J., Krieg, H.M., 2016. Uranium recovery from simulated molybdenum-99 production residue using non-dispersive membrane based solvent extraction. Hydrometallurgy 164, 330–333.

Fournier, S., 2000. Study of the dissolution of mixed oxides (U, Pu) O2 with a high plutonium content.. (Doctoral dissertation, Montpellier 2).

Garcia-Garcia, F.J., Skeldon, P., Thompson, G. E., Smith, G. C., 2012. The effect of nickel on alloy microstructure and electrochemical behaviour of AA1050 aluminium alloy in acid and alkaline solutions. Electrochimica Acta,75, 229–238.

Germain, M., Pluot, P., 1980. Diluent washing of aqueous phase using centrifugal contactors. CEA Nuclear Research Center Fontenay-aux-Roses. (No. CEA-CONF--5427).

Gibson, G.W., 1966. The Use of Uranium Aluminide Powders in Nuclear Reactor Fuel Elements, in: Modern Developments in Powder Metallurgy. Springer, 26–35.

Gile, H.S., 1965. Separation and recovery of uranium from uranium-aluminum alloys. U.S. Patent 3,201,191.

Goldberg, S., Davis, J.A., Hem, J.D., 1996. The surface chemistry of aluminum oxides and hydroxides. Environ. Chem. Alum. 271–331.

Gong, X., Nie, Z., Qian, M., Liu, J., Pederson, L.A., Hobbs, D.T., McDuffie, N.G., 2003. Gibbsite to boehmite transformation in strongly caustic and nitrate environments. Ind. Eng. Chem. Res. 42, 2163–2170.

Guillaumont, R., Mompean, F.J., 2003. Update on the chemical thermodynamics of uranium, neptunium, plutonium, americium and technetium. Elsevier Amsterdam. 5, 64-70

Harland, C.E., 2007. Ion exchange: theory and practice. Royal Society of Chemistry.

Hermann, B., 1984. Dissolution of unirradiated UO_2-pellets in nitric acid.

Horng, J.S., 1984. Semiempirical model for liquid-liquid extraction equilibrium of uranyl nitrate-TBP-kerosene system in acid medium. Ind. Eng. Chem. Process Des. Dev. 23, 603–609.

Hough, N., 1997. Reprocessing of MTR fuel at Dounreay.

Huyser, D.J., Sandrock, T.L., Schaekers, J.M., Van Dyk, G.J., 1986. Uranium determination with peroxide in alkaline medium. South African J. Chem. 39, 119–124.

International Atomic Energy Agency, V. (Austria), 2000. Nuclear research reactors in the world September 2000 ed. IAEA, International Atomic Energy Agency (IAEA).

Iracane, D., 2006. The JHR, a new material testing reactor in Europe. Nucl. Eng. Technol. 38, 437–

442.

Irving, H., Edgington, D.N., 1959. The extraction of some metal chlorides into tri-n-butyl phosphate. J. Inorg. Nucl. Chem. 10, 306–318.

Jassim, T.N., 2011. A Study of the Third Phase Formation in the Extraction of U (IV) in TBP-HCl System Using Toluene and Kerosene as Diluents. Ibn Al-Haitham J. Pure Appl. Sci. 24, 183–192.

Jensen, M.P., Chiarizia, R., Ferraro, J.R., Borkowski, M., Nash, K.L., Thiyagarajan, P., Littrell, K.C., 2002. New insights in third phase formation in the U (VI)-HNO_3, TBP-alkane system, in: International Solvent Extraction Conference.

Jones, R.T., 1982. AEC-2 Experiments in Support of ^{99}Mo Production in NRU. AECL-7335.

Kaminski, M.D., Goldberg, M.M., 2002. Aqueous corrosion of aluminum-based nuclear fuel. J. Nucl. Mater. 304, 182–188.

Kammerer, J., Carle, R., Kammerer, D.R., 2010. Adsorption and ion exchange: basic principles and their application in food processing. J. Agric. Food Chem. 59, 22–42.

Kohut, C., Echenique, P., Podesta, D., Adelfang, P., 2000. Targets development of low enrichment for production of Mo-99 for fission. (No. INIS-XA-C--002).

Kopečni, M.M., Petković, D.M., 1994. A chemical model of the solvent extraction systen: water–uranyl nitrate–nitric acid–tri-n-butyl phosphate–diluent. J. Chem. Soc. Dalt. Trans. 2209–2212.

Kumar, J.R., Kim, J.-S., Lee, J.-Y., Yoon, H.-S., 2011. A brief review on solvent extraction of uranium from acidic solutions. Sep. Purif. Rev. 40, 77–125.

Kumar, S., Jain, S., 2013. History, introduction, and kinetics of ion exchange materials. J. Chem. 2013.

Lacher, J.R., Salzman, J.D., Park, J.D., 1961. Dissolving uranium in nitric acid. Ind. Eng. Chem. 53, 282–284.

Ladeira, A.C.Q., Morais, C.A., 2005. Effect of ammonium, carbonate and fluoride concentration on the uranium recovery by resins. Radiochim. Acta 93, 207–209.

Larsen, R.P., 1959. Dissolution of uranium metal and its alloys. Anal. Chem. 31, 545–549.

Lecomte, M., Bonin, B., 2008. Treatment and recycling of spent nuclear fuel: Actinides partitioning - Application to waste management. CEA Saclay; Groupe Moniteur

LibreTexts, 2019. Overview of Extraction. https://chem.libretexts.org/Bookshelves/Organic_Chemistry/Book%3A_Organic_Chemitry_Lab_Techniques_%28Nichols%29/4%3A_Extraction/4.1%3A_Overview_of_Extraction. Accessed on 15/05/2019

Mahbub Hasan, M., Hasan, E., Amin, A., 2014. Study on Water Treatment Plant. (Doctoral dissertation, Daffodil International University).

Maher, C.J., 2015. Current headend technologies and future developments in the reprocessing of spent nuclear fuels, in: Reprocessing and Recycling of Spent Nuclear Fuel. Elsevier, 93–124.

Marc, P., Magnaldo, A., Vaudano, A., Delahaye, T., Schaer, É., 2017. Dissolution of uranium dioxide in nitric acid media: what do we know? EPJ N-Nuclear Sci. Technol. 3, 1–13.

McFarlane, J., Benker, D., DePaoli, D.W., Felker, L.K., Mattus, C.H., 2015. Dissolution and separation of aluminum and aluminosilicates. Sep. Sci. Technol. 50, 2803–2818.

McFarlane, J., Benker, D., DePaoli, D.W., Felker, L.K., Mattus, C.H., 2014. Aluminum Target Dissolution in Support of the Pu-238 Program. Oak Ridge Natl. Lab. Oak Ridge, TN.

Merritt, R.C., 1971a. The extractive metallurgy of uranium. Colorado School of Mines Research Institute, in: Library of Congress Catalog Card.

Merritt, R.C., 1971b. Extractive metallurgy of uranium. Colorado School of Mines Research Institute, United States.

Mindrisz, A.C., Camilo, R.L., Araujo, I.C., Forbicini, C.A.L.G. de O., 2013. Evaluation of alkaline dissolution of Al 6061 and Al 1050 for the production of Mo-99 from LEU targets. IAEA.

Mushtaq, A., 2011. Specifications and qualification of uranium/aluminum alloy plate target for the production of fission molybdenum-99. Nucl. Eng. Des. 241, 163–167.

Naito, K., 1960. On the mechanism of the extraction of uranyl nitrate by TBP (partition study). Bull. Chem. Soc. Jpn. 33, 363–371.

Nampira, Y., 2000. Dissolution of uranium silicide fuel element using acid and base solution. Proceeding of the Fifth Scientific Presentation on Nuclear Fuel Cycle: Development of Nuclear Fuel Cycle Technology in Third Millennium. Indonesia: Nuclear Fuel Elements Development Centre, National Atomic Energy Agency. p. 322.

Nash, K.L., Nilsson, M., 2015. Introduction to the reprocessing and recycling of spent nuclear fuels, in: Reprocessing and Recycling of Spent Nuclear Fuel. Elsevier, 3–25.

National Academies of Sciences, Engineering, and Medicine, 2016. Reducing the use of highly enriched uranium in civilian research reactors. National Academies Press.

National Academies of Sciences, Engineering, and Medicine, 2016. Molybdenum-99 for medical imaging. National Academies Press. https://doi.org/10.17226/23563

National Research Council, 2009. Medical isotope production without highly enriched uranium. National Academies Press.

Nishimura, K., Chikazawa, T., Hasegawa, S., Tanaka, H., Ikeda, Y., Yasuike, Y., Takashima, Y., 1995. Effect of Nitrous Acid on Dissolution of UO_2 Powders in Nitric Acid. J. Nucl. Sci. Technol. 32, 157–159.

Noor, E.A., 2009. Potential of aqueous extract of Hibiscus sabdariffa leaves for inhibiting the corrosion of aluminum in alkaline solutions. J. Appl. Electrochem. 39, 1465–1475.

Norbash, K., Bakhitiar, S., Wachs, D., 2010. Reprocessing of research reactor nuclear fuel based fuel on pyrochemical separations technique. (No. INIS-BE--10K0001)

Nothnagel, G., 2015. A Tribute to SAFARI-1:Technology Excellence, in: Nuclear Africa 2015. Pelindaba (Necsa), South Africa, p. 7.

NTP Radioisotopes SOC, 2017. SAFARI-1 http://www.ntp.co.za/safari-1/ (accessed 3.3.17).

Oguzie, E.E., 2007. Corrosion inhibition of aluminium in acidic and alkaline media by Sansevieria trifasciata extract. Corros. Sci. 49, 1527–1539.

Ojovan, M.I., Lee, W.E., 2013. An introduction to nuclear waste immobilisation. 2nd ed.Elsevier Newnes.

Pashalidis, I., Tsertos, H., 2004. Radiometric determination of uranium in natural waters after enrichment and separation by cation-exchange and liquid-liquid extraction. J. Radioanal. Nucl. Chem. 260, 439–442.

Patel, J., 2016. ION EXCHANGE RESINS.

Peterson, R.A., Lumetta, G.J., Rapko, B.M., Poloski, A.P., 2007. Modeling of Boehmite Leaching from Actual Hanford High□Level Waste Samples. Sep. Sci. Technol. 42, 1719–1730.

Peterson, S., Wymer, R. G., 1963. Chemistry in nuclear technology. Addison-Wesley

Plaue, J., Gelis, A., Czerwinski, K., Thiyagarajan, P., Chiarizia, R., 2006. Small□Angle Neutron Scattering Study of Plutonium Third Phase Formation in 30% TBP/HNO_3/Alkane Diluent Systems. Solvent Extr. ion Exch. 24, 283–298.

Poczynailo, A., Danesi, P.R., Scibona, G., 1973. Solvation of uranyl nitrate by TBP in n-hexane by vapour pressure lowering measurements. J. Inorg. Nucl. Chem. 35, 3249–3255.

Pyun, S.-I., Moon, S.-M., 2000. Corrosion mechanism of pure aluminium in aqueous alkaline solution. J. Solid State Electrochem. 4, 267–272.

Reynier, N., Lastra, R., Laviolette, C., Fiset, J.-F., Bouzoubaâ, N., Chapman, M., 2016. Comparison of Uranium Recovery by Ion Exchange from Sulfuric Acid Liquor in Iodide and Chloride Media. Solvent Extr. Ion Exch. 34, 188–200. https://doi.org/10.1080/07366299.2016.1140431

Rodden, C.J., 1950. Analytical chemistry of the Manhattan project. Vol. I. McGraw-Hill.

Ruff, T.J., Toghiani, R.K., Smith, L.T., Lindner, J.S., 2008. Studies on the gibbsite to boehmite transition. Sep. Sci. Technol. 43, 2887–2899.

Saliba-Silva, A.M., de Carvalho, E.F.U., Riella, H.G., Durazzo, M., 2011. Research reactor fuel fabrication to produce radioisotopes, in: Radioisotopes-Applications in Physical Sciences. InTech.

Schulz, W.W., Navratil, J.D., 1984. Science and technology of tributyl phosphate. Vol. I: Synthesis, properties, reactions and analysis.

Shabbir, M., Robins, R.G., 1968. Kinetics of the dissolution of uranium dioxide in nitric acid. I. J.

Appl. Chem. 18, 129–134.

Siddall III, T.H., Parker, S.G., Prout, W.E., 1957. Equilibrium distribution data for Purex and similar extraction processes. Du Pont de Nemours (EI) & Co. Savannah River Lab., Augusta, Ga. (No. DP-53).

Sim, M., Ryu, H.J., Lee, Y.S., Park, J.-M., Lee, J.H., 2013. Fabrication of Uranium Dispersion Targets for Mo-99 Production, in: Proceedings of the 8th Pacific Rim International Congress on Advanced Materials and Processing. Springer, 3417–3425.

Snyder, M.D., Davis, M.W., 1956. Caustic dissolution Of Uranium-Aluminium Alloy. Savannah River Site (SRS), Aiken, SC (United States). (No. DP-67).

Sole, K.C., Feather, A.M., Cole, P.M., 2005. Solvent extraction in southern Africa: An update of some recent hydrometallurgical developments. Hydrometallurgy 78, 52–78.

Sposito, G., 1984. The surface chemistry of soils. Oxford university press. New York, USA. 234

Srinivasan, B., Leonard, R.A., Aase, S., Vandegrift, G.F., Moeridun, A., Rauf, A., Lubis, H., Hardi, A., Amini, S., Nampira, Y., 2004. Processing of LEU targets for ^{99}Mo production-Dissolution of metal foils by nitric-acid/sulfuric-acid mixtures.

Stary, J., Irving, H., 1964. The solvent extraction of metal chelates. Vol. I

Stas, J., Dahdouh, A., Shlewit, H., 2005. Extraction of uranium (VI) from nitric acid and nitrate solutions by tributylphosphate/kerosene. Period. Polytech. Chem. Eng. 49, 3–18.

Stassen, L., Suthiram, J., 2015. Initial development of an alkaline process for recovery of uranium from ^{99}Mo production process waste residue. J. Radioanal. Nucl. Chem. 305, 41–50.

Strelow, F.W.E., Rethemeyer, R., Bothma, C.J.C., 1965. Ion Exchange Selectivity Scales for Cations in Nitric Acid and Sulfuric Acid Media with a Sulfonated Polystyrene Resin. Anal. Chem. 37, 106–111.

Suresh, A., Srinivasan, T. G., Rao, P. V., 2009. Parameters influencing third-phase formation in the extraction of $Th(NO_3)_4$ by some trialkyl phosphates. Solvent Extraction and Ion Exchange, 27 2nd Ed, 132–158

Taylor-Pashow, K., Hobbs, D., 2012. Effect of cations on aluminum speciation under alkaline conditions. SRS. (No. SRNL-STI-2012-00136).

Taylor, R.F., 1962. Processing in Limited Geometry. Part 3. The Dissolution of Uranium Dioxide Sintered Pellets in Nitric Acid. Atomic Energy Research Establishment.

Thompson, H.S., 1850. On the absorbent power of soils. J.R. Agric. Soc. Engl. 11, 68–74.

Tóth, J., 2002. Adsorption: theory, modeling, and analysis. Surfactant Sci. Ser. Marcel Dekker, Sci. Ser, 107, 50, 971-983.

Way, J.T., 1850. On the power of soils to absorb manure. Part 1. Journal of the Royal Agricultural Society of England, Vol XI.

Wesolowski, D.J., 1992. Aluminum speciation and equilibria in aqueous solution: I. The solubility of gibbsite in the system Na-K-Cl-OH-$Al(OH)_4$ from 0 to 100 C. Geochim. Cosmochim. Acta 56, 1065–1091.

World Nuclear Association, n.d. Research Reactors. http://www.world-nuclear.org/information-library/non-power-nuclear-applications/radioisotopes-research/research-reactors.aspx (accessed 19/05/17).

Wymer, R.G., Helton, D.M., Kibbey, A.H., Land, J.L., 1955. Caustic dissolution: preliminary studies. Oak Ridge, TN Oak Ridge Natl. Lab.

Ye, X., Cui, S., de Almeida, V.F., Hay, B.P., Khomami, B., 2010. Uranyl nitrate complex extraction into TBP/dodecane organic solutions: a molecular dynamics study. Phys. Chem. Chem. Phys. 12, 15406–15409.

Zhang, J., Klasky, M., Letellier, B.C., 2009. The aluminum chemistry and corrosion in alkaline solutions. J. Nucl. Mater. 384, 175–189.

Zhao, Y., Chen, J., 2008. Studies on the dissolution kinetics of ceramic uranium dioxide particles in nitric acid by microwave heating. J. Nucl. Mater. 373, 53–58.